Phosphoinositide Regulation of Intracellular Nucleic Acid Sensors

PHOSPHOINOSITIDE REGULATION OF INTRACELLULAR NUCLEIC ACID SENSORS

A dissertation presented

by

Katherine Camille Barnett

to

The Division of Medical Sciences

in partial fulfillment of the requirements

for the degree of

Doctor of Philosophy

in the subject of

Virology

Harvard University

Cambridge, Massachusetts

July 2019

Abstract

Phosphoinositide Regulation of Intracellular Nucleic Acid Sensors

Innate immune sensing relies on pattern recognition receptors (PRRs) to bind molecular motifs unique to pathogens to initiate inflammation and the adaptive immune response. These PRRs are tightly regulated, particularly in regard to their localization and access to ligands. This spatial regulation of PRRs is well characterized for transmembrane proteins, such as those of the Toll-like receptor (TLR) family. However, little is known about the subcellular positioning of intracellular PRRs that lack transmembrane domains, which generally are assumed to be residents of the cytosol. To determine if these receptors, like their transmembrane counterparts, had specific subcellular positioning, we interrogated the localization of the intracellular nucleic acid sensors cyclic GMP-AMP synthase (cGAS) and Retinoic acid inducible gene I (RIG-I) and the role of this localization in regulating their sensory capacity.

Our studies revealed that cGAS, an integral sensor of cytosolic DNA, localizes to the plasma membrane in the absence of stimuli in human and murine monocytes. This subcellular positioning occurs through an electrostatic interaction between the cGAS N terminus and the plasma membrane lipid phosphatidylinositol-4,5-bisphosphate ($PI(4,5)P_2$). Loss of the cGAS N terminus led to a loss of membrane localization and heightened interferon (IFN) signaling in the absence of infection. Mislocalized cGAS also generated heightened responses to genotoxic stress, but not viral infection. These data reveal that the subcellular positioning of this receptor serves as a mechanism of self-nonself discrimination by specifically inhibiting sensing of self-DNA. Similar to cGAS, we found that RIG-I, a key sensor of viral RNA, interacts with the membrane lipid $PI(3,5)P_2$ *in vitro* and that this interaction inhibited RIG-I RNA binding and ATPase activity. Together, these data suggest that subcellular positioning through electrostatic interactions with phosphatidylinositol phosphates (PIPs) may be a common mechanism of localization and regulation for intracellular PRRs lacking transmembrane domains.

Table of Contents

Acknowledgements

First and foremost, I want to thank my advisor, Dr. Jonathan Kagan, whose guidance was integral to both this project and my growth as a scientist. His passion for discovery encouraged mine to flourish. Discussing new data or ideas with him was always positive and constructive, and his attention to both detail and logic fostered my development as an experimentalist. His enthusiasm and excitement were a support that kept me grounded, even when mine were lacking. I am truly grateful that I had the opportunity to work with him and learn from him.

With that, I also want to thank all of the members of the Kagan lab. A family of sorts, we discussed science openly, honestly, and with a critical eye—always striving to make experiments better and each other stronger. Though people came and went during my tenure, all of the lab members were a fundamental support, answering innumerable questions, commiserating or celebrating every loss or victory, and getting into a fair amount of antics.

Outside of the lab, I want to thank my collaborators, my committee, and the Virology Program. Throughout this project, I received excellent advice, reagents, and training from many collaborators, including Dr. Philip Kranszuch, Dr. Wen Zhou, Dr. Victor Cid, Dr. Michael Anderson, Dr. Sun Hur, and Dr. Sadeem Ahmad. In addition, my dissertation advisory committee provided excellent feedback and support throughout my graduate studies, and for that, I want to thank Dr. Sun Hur, Dr. Lee Gehrke, and Dr. Nir Hacohen. Furthermore, I am thankful to be a part of the Virology Program at Harvard, a community of scientists whose encouragement and sensibilities were invaluable to me as a scientist.

I also want to thank the people who mentored me and let me dabble in their labs in high school and college. These experiences directly informed my decision to pursue a Ph.D. and opened my eyes to the world of scientific research. I am forever grateful to have worked in the labs of Dr. Zafer Hatahet, Dr. Marcelo Kuroda, and Dr. Erica Ollman-Saphire. Furthermore, I would like Dr. Allison Landry, Dr. Benjamin Lassater, and Dr. Robert Dotson, a group of professors

who introduced me to cell biology and biochemistry and encouraged me to pursue a career in science.

Finally, I would like to thank my fiancé, family, and friends for their support throughout this process. Foremost, my fiancé, Ben, whose unwavering support in this endeavor kept me moving forward. He was always willing to listen to me fret about data, asking great questions and even suggesting experiments. I also truly appreciate that he never thought I was insane for talking about one protein almost 24/7. In addition, I want to thank my family for their support in my semi-crazy decision to become a scientist. Many calls home gave me strength and insight that grounded me throughout my time in graduate school, and with that, I would like to thank my parents, Barry and Amanda, and my siblings, Lee, Marc, and Lily. I would also like to thank the many friends who gave me reasons to get out of the lab and have some non-scientific fun.

Dedication

I dedicate this thesis to my mother, Amanda.

Her diligence in the face of the threat of infectious disease sparked my passion for the molecular world.

Chapter 1: Introduction

The Spatial Regulation of Innate Immunity

Portions of this chapter were published elsewhere:

Barnett, K. C., & Kagan, J. C. Lipids that directly regulate innate immune signal transduction. *Innate Immun.* 1–11 (2019).

Author Contributions:

K.C.B. and J.C.K. conceptualized, wrote, and edited this review article. K.C.B. designed and generated all illustrations.

1.1 Innate Immune Sensing Pathways and Pattern Recognition

Clearance of infection through adaptive immunity is a fundamental function of the human immune system, resolving infection and creating immune memory. To activate the adaptive immune response, the body must first recognize that an infection is underway. This is achieved through innate immune sensing pathways, which recognize hallmarks of infection to initiate inflammation. Through inflammation, the adaptive immune response is activated to generate pathogen-specific mechanisms to fight the nascent infection.

Therefore, innate immune signaling pathways act as gatekeepers to the overall immune response. At the apex of these pathways are germline-encoded protein receptors, known as pattern recognition receptors (PRRs), that recognize molecular motifs present in pathogens (Pathogen-Associated Molecular Patterns or PAMPs) or that are generated as a result of cellular damage (Damage-Associated Molecular Patterns or DAMPs)[1]. Upon interaction with target ligands, PRRs initiate signal transduction cascades to produce pro-inflammatory cytokines and/or interferons (IFN). These secreted molecules recruit immune cells to the site of infection and generate an antiviral state in the cell[1]. Genetic deletion of PRRs prevents the activation of inflammation and therefore the clearance of pathogens, frequently causing the host to succumb to infection[1-3], while activating mutations in these receptors commonly lead to autoimmune disease[1,4].

1.1.1 Innate Immune Sensing of Viruses

Viruses are obligate intracellular pathogens that utilize the machinery of a host cell to replicate. Because of this, viral molecules bear striking resemblance to those of the host. Other microbial pathogens, like bacteria, produce PAMPs that are completely foreign to the host, such as *E. coli* lipopolysaccharide (LPS)[1]. However, the best characterized viral PAMPs are viral DNA (vDNA) or viral RNA (vRNA)[5], and cognate molecules of these nucleic acids are always present in the host. However, viral nucleic acids are chemically distinct and/or mislocalized as compared to host DNA or RNA, allowing for pattern recognition to occur[5].

Several different classes of PRRs recognize viral nucleic acids to initiate an immune response. First, the Toll-Like Receptors (TLRs) 3, 7/8, and 9 reside within the acidified late endosome, where viral entry into the host cell cytosol frequently occurs. TLR3 and TLR7/8 recognize forms of vRNA. TLR3 specifically engages double stranded RNA (dsRNA), while TLR7/8 recognizes single stranded RNA (ssRNA)[5]. Similarly, TLR9, binds double stranded DNA (dsDNA) containing CpG motifs to activate an immune response[5]. In addition, several nucleic acid-specific PRRs detect vRNA or vDNA within the intracellular space. For vRNA, these sensors include 2'5'-oligoadenlyate synthetases (OAS)[6] and the Rig-I-Like Receptors (RLRs) Retinoic Acid Inducible Gene I (RIG-I) and Melanoma Differentiation Associated Protein 5 (MDA5)[6]. While in the case of vDNA, the sensors Absent in Melanoma-2 (AIM2)[7], Interferon-Inducible Protein 16 (IFI16)[7], and Cyclic GMP-AMP Synthase (cGAS)[7,8] all detect this common PAMP. Because of their near universal requirement for detecting intracellular DNA or RNA viruses, respectively, the cGAS and RIG-I sensing pathways are discussed in detail below. As a group, these nucleic acid sensing PRRs serve as sentinels of viral infection to produce an antiviral response, inflammation, and ultimately, adaptive immunity.

1.1.2 The RIG-I-MAVS Signaling Pathway

The RLRs are a family of widely expressed DExD box RNA helicases required for the control of many RNA virus infections[9,10]. Members of this family include RIG-I and MDA5, which both induce potent antiviral responses to vRNA[2,5]. The third member of the RLR family, Laboratory of Genetics and Physiology 2 (LGP2), has an unclear role in antiviral control and does not produce an inflammatory response vRNA on its own[5]. Of these helicases, RIG-I is the most well characterized and is necessary to restrict a broad range of RNA virus infections, including Influenza A Virus, Respiratory Syncytial Virus, and Hepatitis C Virus[9,10]. However, gain-of-function mutations in RIG-I are associated with autoinflammatory diseases, including Aicardi–Goutières syndrome (AGS) and Singleton-Merten syndrome (SMS)[11,12]. Study of this intracellular PRR is

vital to understanding the control of RNA virus infection and developing therapeutics for both infection and autoinflammatory disease.

Human RIG-I is a 925 amino acid (aa) protein encoded by the *ddx58* gene. RIG-I interacts with vRNA through its helicase domains and a C-Terminal Domain (CTD), while its downstream antiviral activity is propagated by its two N-Terminal Caspase Activation and Recruitment Domains (CARDs)[13]. RIG-I specifically recognizes 5' di- and tri-phosphorylated RNA with some amount of double stranded character, enabling discrimination between self- and nonself RNA[14,15]. Binding vRNA releases the CARDs from an autoinhibitory conformation[16] and promotes RIG-I oligomerization along vRNA[17]. Additionally, RIG-I is ubiquitinated by the E3 ubiquitin ligase Riplet[18,19]. These activities activate RIG-I and allow the oligomerized CARDs of RIG-I interact with the CARD domain of the Mitochondrial Antiviral Signaling protein (MAVS)[20-23], a transmembrane protein present not only on the mitochondrial but also the peroxisomes and the mitochondria-associated membranes (MAM) of the endoplasmic reticulum (ER)[24,25]. Upon interaction with RIG-I, MAVS forms prion-like aggregates that act as a supramolecular organizing center (SMOC) to promote the activation of the transcription factors nuclear factor kappa-light-chain-enhancer of activated B cells (NF-κB), Interferon Regulatory Factors 3/7 (IRF3/7), and Activator Protein-1 (AP-1)[13,26]. Together, these transcription factors upregulation the production of IFNs and proinflammatory cytokines[1]. In turn, these secreted proteins activate the transcription of antiviral genes in the infected and nearby cells and promote the recruitment of immune cells to the site of infection.

1.1.3 The cGAS-STING Signaling Pathway

In parallel, enzyme cGAS is a ubiquitously expressed sensor of dsDNA in the intracellular space that is essential for the control of many infections, including both DNA virus and retrovirus infection[3,27-29]. Upon encountering its ligand, cGAS interacts with the sugar-phosphate backbone of dsDNA through a basic spine helix and a zinc thumb motif[30]. This interaction promotes the rearrangement of the enzyme's active site, the dimerization of cGAS, and the formation of large

cGAS-DNA phase-separated liquid droplets, which ultimately leads to the production of the secondary messenger 2'3'-cyclic GMP-AMP (cGAMP) [30-33]. This cyclic dinucleotide is recognized by the transmembrane protein Stimulator of Interferon Genes (STING) on the ER[8,34,35]. Activation of STING through cGAMP binding leads to STING multimerization[36,37], palmitoylation[36,38], phosphorylation[39], and translocation through the ERGIC compartment[34]. These activities lead to the activation of tank binding kinase 1 (TBK1) and IRF3 to upregulate IFN production to fight the nascent infection[35,39].

Because cGAS is capable of recognizing dsDNA in a sequence-independent manner, cGAS recognition of pathogens is not limited to viruses, as cGAS detects bacterial and protozoan infections[40-43], as well as endogenous DNA[44-51]. Given this activity, cGAS is an important sensor of cellular stress by binding mitochondrial DNA released due to mitochondrial stress[52,53] and nuclear DNA released during DNA damage[44,45,47,54]. Because of this, cGAS activity is implicated in both cancer progression and cellular senescence[46,48,50]. Understanding this PRR, its pathway, and the wide range of processes it regulates is an active area of research.

1.2 Role of Subcellular Positioning and Protein-Lipid Interactions in Innate Immune Signaling

Membrane lipids orchestrate innate immune sensing through interactions with PRRs and their downstream signaling components. Cellular membranes are not simply barriers that serve a singular function in compartmentalization, but are also important platforms for signal transduction, protein synthesis, and other cellular activities. Both transmembrane proteins and peripheral membrane proteins are regulated by their resident membranes, and PRRs and the pathways they initiate are not exempt from such regulation. These interactions not only dictate protein localization but also substantially influence their function, which are discussed in detail below.

1.2.1 Spatial Regulation of PRR Activation and Signal Transduction

PRRs are positioned within cells to maximize rapid responses to microbial encounters. Such positioning places the host cell at a kinetic advantage by enabling detection of infection at its onset. For example, TLRs that detect bacterial or fungal cell surface components, such as TLR2, 4 and 5, are present at the cell surface[55]. This positioning ensures microbial detection in the extracellular space. Microbial nucleic acids, in contrast, are rarely displayed on the surface of a potential pathogen. Consequently, the nucleic acid sensing PRRs, which includes TLR3, 7-9 and murine TLR13, the RLRs and cGAS, are most commonly found within the cell, either in endosomes or the cytosol[55]. These receptors are therefore poised to detect nucleic acids after microbial degradation in lysosomes or after viral uncoating in the cytosol. Furthermore, PRRs linked to inflammasome activation are located within the host cytosol to rapidly detect infection and initiate pyroptotic cell death.

The loss of proper PRR localization can have catastrophic consequences for the host organism. For example, TLR9 transits through the secretory pathway in an inactive form to early and late endosomes, where proteolytic cleavage enables its ability to sense unmethylated CpG containing DNA and initiate an inflammatory response[56,57]. Altering the localization of TLR9 such that this protein is directed to the cell surface causes an autoinflammatory response in mice,

through the detection of extracellular self-DNA[58]. Therefore, the specific location of these receptors is fundamental to self-nonself discrimination.

Cell biological analysis of PRR activities has revealed an increasing number of examples of receptors whose subcellular sites of microbial detection are distinct from the sites of signal transduction. Indeed, it is now recognized that a necessary step in inflammatory signaling pathway activation by PRRs is the movement of ligand-bound receptors to a signaling-permissive subcellular location. Examples of this principle came first from the studies of TLR4. Upon binding lipopolysaccharide (LPS), TLR4 must first move into plasma membrane subdomains known as lipid rafts in order to drive inflammatory responses[59-61] (Figure 1A). Subsequent movement of TLR4 into endosomes is necessary to maximize expression of these inflammatory genes and to induce the additional expression of IFNs[62], which drive NK cell activation and T cell mediated adaptive immunity[55]. Similarly, plasma membrane localized TLR2 must move into endosomes after microbial detection to promote maximal inflammatory gene expression[63], while TLR7 and 9 must move between endosomes after nucleic acid detection to stimulate inflammatory cytokine and IFN expression[64,65]. In the cytosol, the RLRs RIG-I and MDA5 can presumably bind viral RNA in any location, but inflammatory and IFN responses only occur after their transport to MAVS at the mitochondria, peroxisomes or MAM of the ER[20,24,25]. Finally, cGAS, which detects cytosolic DNA, produces cGAMP upon DNA detection, and this secondary messenger must translocate to the ER, where it is detected by the protein STING[35]. Only through activation of STING and its subsequent translocation from the ER can inflammatory and antiviral transcriptional responses be induced[34,66]. Therefore, a common feature of these diverse pathways is the spatial dissociation of microbial sensing and initiation of proinflammatory signaling cascades, which could aid in the prevention of aberrant immune activation.

1.1A

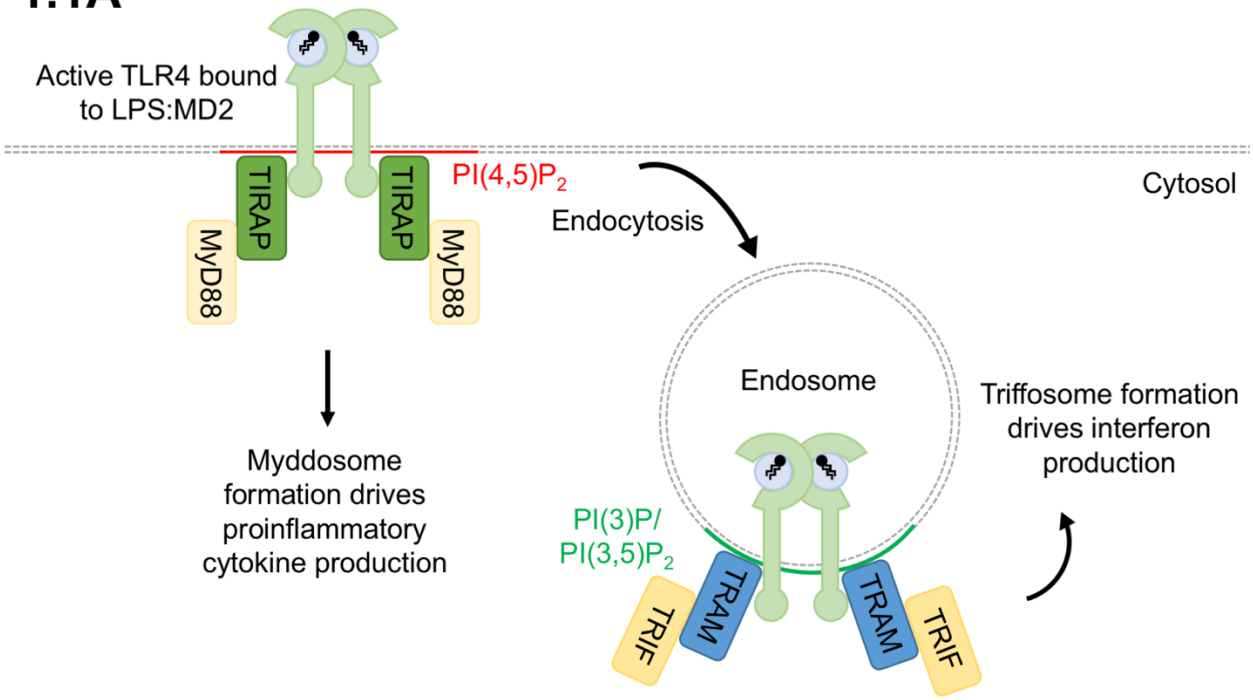
Active TLR4 bound
to LPS:MD2
PI(4,5)P2
Cytosol
TIRAP
TIRAP
MyD88
MyD88
Endocytosis
Endosome
Myddosome
formation drives
proinflammatory
cytokine production
Triffosome formation
drives interferon
production
PI(3)P/
PI(3,5)P2
TRAM
TRAM
TRIF
TRIF

1.1B

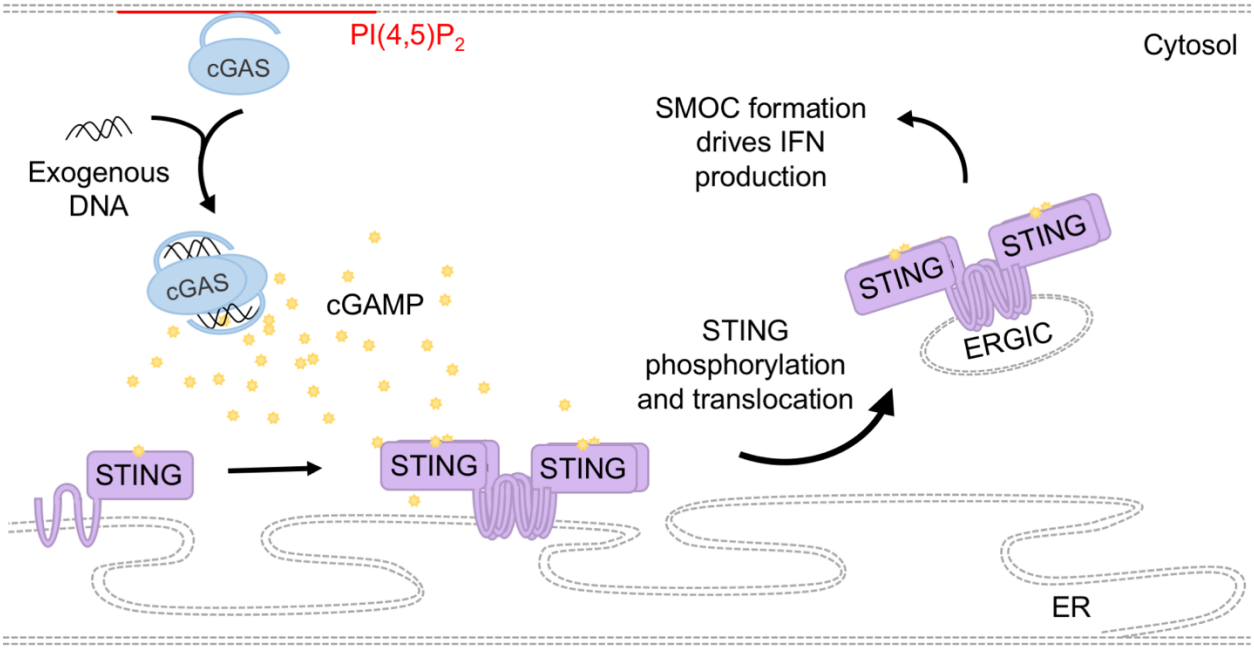
PI(4,5)P2
Cytosol
cGAS
Exogenous
DNA
SMOC formation
drives IFN
production
cGAS
cGAMP
STING
STING
STING
STING
STING
phosphorylation
and translocation
ERGIC
ER

Figure 1.1: Subcellular Localization Directs SMOC Assembly and the Response to Innate Immune Stimuli

1.1A) TLR4 signaling outcomes are determined by its positioning and interaction with localization-dependent sorting adaptors. Active, dimerized TLR4 localizes to $PI(4,5)P_2$ enriched plasma membrane lipid rafts to interact with TIRAP form the Myddosome. Upon endocytosis, TLR4 interacts with TRAM on the endosome to form the Triffosome. **1.1B)** At steady state, cGAS rests on the plasma membrane (discussed in detail in Chapter 2). Sensing of DNA by cGAS stimulates the production of cGAMP, which is bound by the ER resident protein STING. STING-cGAMP interactions leads to STING SMOC formation through its oligomerization, phosphorylation, and translocation to the ERGIC to stimulate the synthesis of IFN.

At the precise subcellular site of PRR signal transduction are proteins known as sorting adaptors, which are the only known factors that are present at the sites of signaling before any microbial encounter has occurred[67]. As such, these proteins serve as landmarks of where in the cell signal transduction will eventually occur. The sorting adaptors TIR domain containing adaptor protein (TIRAP) and translocating chain-associated membrane protein (TRAM) operate in the TLR pathways, while the transmembrane proteins MAVS and STING operate in this manner in the RLR and cGAS pathways, respectively (Figure 1.1). These proteins must be engaged, either directly or indirectly, by upstream receptors to stimulate inflammatory and defensive gene expression.

Mechanistically, sorting adaptors function as intracellular sensors of ligand-bound receptors. When ligand-bound receptors or the secondary messenger cGAMP enter the subcellular site of sorting adaptor residence, these adaptors stimulate the assembly of large multiprotein complexes known as SMOCs[68]. SMOCs operate as the principal subcellular site from which defensive signals emanate. Each sorting adaptor operates to seed the assembly of a different SMOC. For example, the sorting adaptor TIRAP, present on plasma membrane lipid rafts and endosomal membranes, links most TLRs to the assembly of a SMOC known as the myddosome, which drives inflammatory gene expression[69,70] (Figure 1.1A). The endosome-localized sorting adaptor TRAM serves an analogous function for TLR4 specifically, where it links ligand-bound receptors to an inflammation-inducing SMOC known as the triffosome[62] (Figure 1.1A). In a similar manner, activated RLRs stimulate SMOC assembly by the MAVS adaptor on mitochondria, peroxisomes and the MAM to drive inflammatory and antiviral responses[20,24,25] (Figure 1.1B). Furthermore, MAVS aggregation and SMOC assembly is also implicated in the induction of pyroptosis[71]. Similarly, upon cGAMP binding, the adaptor protein STING forms a multimeric complex to activate antiviral and inflammatory gene expression[34,36,37] (Figure 1.1B).

The identification of sorting adaptors as molecular links between activated receptors and SMOC assembly explains the precise means by which PRR signaling is activated from discrete

locations in the cell. Indeed, studies of the adaptors TIRAP, TRAM, and MAVS demonstrated that elimination of a sorting adaptor from its native subcellular position prevents proper signal transduction and inflammatory gene expression[24,62,69]. In the next section, we will discuss recent studies of sorting adaptor regulation with particular focus on electrostatic protein-lipid interactions. This discussion will then be expanded to include other regulators of innate immunity that also use protein-lipid interactions for subcellular positioning with functional consequences for the host.

1.2.2 Protein-Lipid Interactions as a Mechanism of Sorting Adaptor Positioning

Because SMOC assembly occurs at discrete locations in the cell, understanding the mechanisms that direct sorting adaptor localization to seed these complexes is an active area of research. Some of these mechanisms are self-evident, as the transmembrane proteins STING and MAVS are physically inserted into the membranes of eventual SMOC assembly. However, other sorting adaptors, which lack transmembrane domains, do not have a readily apparent mechanism of membrane association. In this section, mechanisms of membrane association that do not rely on transmembrane domains will be discussed along with the specific mechanisms of membrane association by the sorting adaptors TIRAP, TRAM, and the *Drosophila* protein MyD88 (dMyD88).

Cell membranes are lipid bilayers comprised of amphiphilic phospholipids with hydrophobic lipid tails facing the inside of the membrane and hydrophilic head groups facing the extracellular space or the cytosol. Many proteins are able to interact electrostatically with the hydrophilic head groups that make up the membrane surface. Of the phospholipids that comprise cell membranes, the phosphoinositide phosphates (PIPs) play an important role defining membrane spaces and in directing proteins to specific locations within the cell[72]. PIPs are a dynamic group of membrane component lipids that are defined by specific phosphorylation modifications on the 3', 4', or 5' carbons of a phosphatidylinositol head group[72]. Several kinases and phosphatases regulate the phosphorylation patterns of these lipids, and they are rapidly converted as organelles change identity, such an early endosome transitioning to late

endosome[72]. A well characterized example of these lipids is phosphatidylinositol-4,5-bisphosphate ($PI(4,5)P_2$), which is enriched on the plasma membrane[72]. $PI(4,5)P_2$ recruits several peripheral membrane proteins to the cytosolic face of the plasma membrane, such as phospholipase Cδ1 (PLCδ1), adaptor protein complex 2 (AP-2), and several actin-binding proteins[73-75]. Interactions of these proteins with $PI(4,5)P_2$ influences cell activities, such as endocytosis and phagocytosis[74-77]. Other PIPs play similar roles on different organelles, such as PI(3)P on the cytosolic face of early endosomes[78,79] or $PI(3,5)P_2$ on late endosomes[72,80]. Together, these lipids orchestrate many activities of peripheral membrane proteins through electrostatic interactions, and their activities and regulation are the subject of several recent reviews[72,81-83]. In addition to PIPs, other membrane component lipid head groups can serve as binding partners for peripheral membrane proteins, such as phosphatidylserine (PS)[84]. Another mechanism of peripheral membrane association is through the post-translational addition of a lipid anchor, such as myristoylation, palmitoylation, or prenylation[85]. These small lipid anchors insert into membranes and interact with hydrophobic center of the cell membrane. Both of these mechanisms of membrane association are important for directing innate immune sorting adaptors and play essential roles in SMOC formation, which will be discussed in detail below.

The sorting adaptor TIRAP acts as a sensor of activated TLRs to form the myddosome, eliciting the expression of proinflammatory genes (Figure 1.1 A). Prior to TLR activation, TIRAP is positioned on lipid raft microdomains within the plasma membrane through an interaction with $PI(4,5)P_2$[69]. TIRAP interacts with $PI(4,5)P_2$ through a basic, N-terminal phosphoinositide binding domain[69]. Deletion of this domain leads to a loss of proinflammatory cytokine expression upon LPS treatment, preventing TLR4-mediated signaling, while reconstitution of TIRAP membrane association with another $PI(4,5)P_2$ binding domain rescues this activity[69]. However, although at steady state TIRAP is most concentrated at the plasma membrane, it is also capable of localizing to the endosomal compartments through interactions with other membrane lipids, namely PI(3)P, PS, and $PI(3,5)P_2$[70]. Like many PIP binding domains, the N terminus of TIRAP is a promiscuous

and intrinsically disordered PIP binding domain. A recent study demonstrated that TIRAP interacts with multiple PIPs through a similar mechanism[86]. This promiscuity of localization is key to TIRAP's ability to serve as a sorting adaptor for both plasma membrane and endosomal TLRs. Indeed, TIRAP mediates myddosome formation upon LPS (TLR4-mediated) and CpG DNA (TLR9-mediated) stimulation[70]. The promiscuity of TIRAP for multiple PIPs is important for its function, as mutant TIRAP alleles that display specificity for plasma membrane lipids are unable to mediate myddosome formation downstream from endosomal TLRs[70]. Likewise, TIRAP alleles that display specificity for endosomal PIPs are unable to stimulate myddosome formation downstream from plasma membrane localized TLRs[69].

The protein TRAM serves as another sorting adaptor for TLR signaling, mediating triffosome formation and the expression of type I interferons upon TLR4 activation[87] (Figure 1.1A). At steady state, TRAM localizes to the plasma membrane and endosomal compartments[88]. The significance of plasma membrane localization is unclear, but its endosomal localization is necessary and sufficient to mediate interferon expression upon TLR4 activation by LPS[62]. Unlike TIRAP, TRAM contains a bipartite membrane localization motif found in many different peripheral membrane proteins[62]. The first 7 amino acids of TRAM contain a myristoylation sequence, placing a lipid anchor on the protein's N terminus[88]. Directly adjacent to this motif is a short polybasic region that interacts promiscuously with PIPs and other acidic lipids[62]. Together, these lipidation and lipid binding motifs direct TRAM localization and function in the TLR4 pathway.

Similar to the TLR pathways found in mammals, the Toll pathway in insects is a critical regulator of anti-microbial immunity[89]. The cell surface receptor Toll serves as a sensor of gram-positive bacterial and fungal infections, with the sorting adaptor dMyD88 serving to initiate formation of a SMOC consisting of the adaptor Tube and the kinase Pelle[90]. This SMOC induces the upregulation numerous NF-κB dependent genes, most notably antimicrobial peptides (AMPs) that curtail infection[89]. Similar to TIRAP in mammalian cells, dMyD88 localizes to the plasma membrane through an interaction with $PI(4,5)P_2$[91], and this interaction is required for Toll

stimulated AMP production and survival of gram-positive bacterial infection[91]. Based on the similarities to mammalian TIRAP and TRAM, PIP-mediated membrane binding can be considered a conserved mechanism of TLR sorting adaptor activity in multicellular eukaryotes.

While PIPs position several TLR-associated sorting adaptors at sites of eventual signal transduction, there are also examples of PIP-mediated localization that dictate function after signaling initiation. These examples will be discussed below.

1.2.3 Membrane Lipids as Mediators of Innate Immune Effector Activity

Innate immune signaling pathways follow a common sequence—pattern recognition nucleates SMOC formation, which activates inflammatory and defensive responses. Whereas many PRR pathways induce host defense via the upregulation of cytokines, chemokines and interferons, other pathways induce inflammation by processes of lytic cell death, namely pyroptosis and necroptosis[92,93]. Like the transcription-inducing PRR pathways, specific localization of key signaling proteins within cells is essential for pyroptosis or necroptosis execution, and these activities are directed through protein-lipid interactions.

Recent studies have revealed an important role of the protein Gasdermin D (GSDMD) in pyroptotic cell death[94]. GSDMD exists in an autoinhibited state in the cell cytosol and is cleaved by cellular caspases upon inflammasome activation[94]. Once cleaved, the N terminus of GSDMD interacts with membrane lipids to form pores in the plasma membrane, enabling the release of the inflammatory cytokine interleukin-1β (IL-1β) and disrupting cellular ion gradients to facilitate cell death[95-99]. *In vitro* binding assays demonstrated that GSDMD interacts with several lipids found on the inner leaflet of the plasma membrane, including PI(4)P, PI(4,5)P_2, PS, and phosphatidylinositol (PI)[96,100]. Mutation of residues implicated in interactions with these membrane lipids prevented the GSDMD N terminus from associating with cell membranes and prevented GSDMD-mediated cell death[96]. In addition, GSDMD also has a high affinity for cardiolipin (CL), a lipid found in the inner mitochondrial and bacterial membranes[101,102]. This binding activity for CL may allow GSDMD to kill *E. coli* and *S. aureus*, as they display CL on their cell wall[96,100].

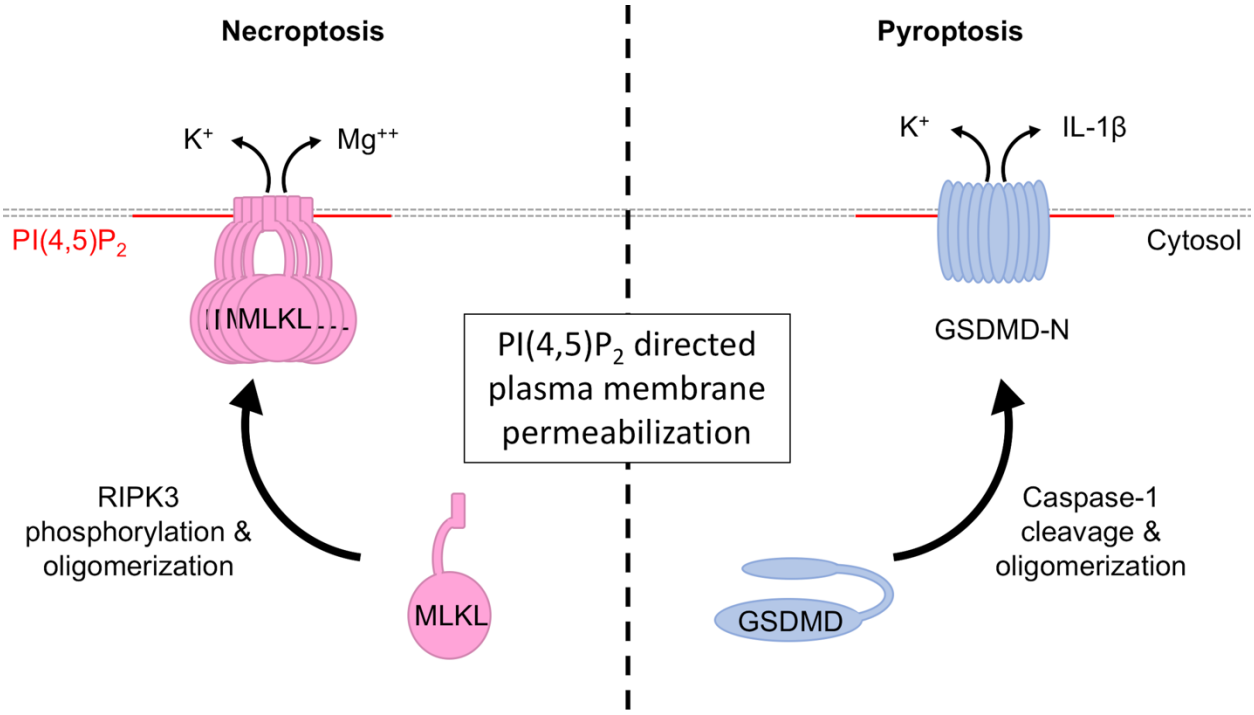

Figure 1.2: Phosphoinositide-Directed Membrane Disruption Is a Common Attribute of Inflammatory Cell Death Pathways

Both necroptosis and pyroptosis rely on plasma membrane pore formation to facilitate cell death. While the mechanisms of activation and the proteins mediating pore formation are unrelated, $PI(4,5)P_2$ binding directs these pore-forming proteins to the plasma membrane.

GSDMD is a member of a larger protein family collectively referred to as Gasdermins (GSDMs)[103]. Like GSDMD, the N termini of almost all GSDM family members mediate cell death when overexpressed and are also capable of killing bacterial cells, and this includes GSDMA (murine GSDMA3), GSDMB, GSDMC, GSDMD, and GSDME (also known as Dfna5)[100]. Many of these family members bind PIPs *in vitro* and are implicated in pathologies linked to immune function, such as asthma and inflammatory bowel disease[100,104]. Further research into this family of pore forming proteins is necessary to understand the specifics of their activity and better characterize their interactions with membrane lipids in health and disease.

In addition to the GSDM family, other pore forming proteins mediate innate immune signaling through interactions with PIPs. For example, the protein Mixed Lineage Kinase Domain Like Protein (MLKL) forms pores to facilitate necroptosis[105,106]. Upon phosphorylation by the necrotic executioner kinase RIPK3, MLKL oligomerizes and inserts into the plasma membrane to form a pore that disrupts ion gradients and leads to cell death[105-107]. *In vitro* binding analysis of recombinant MLKL demonstrated that MLKL binds directly to PIPs, including PI(4)P and $PI(4,5)P_2$[108,109]. This activity is mediated by an N-terminal helical bundle that contains several basic amino acids, which mutagenesis studies implicated in plasma membrane recruitment of MLKL[109]. Considering the similarities between MLKL and GSDMD, PIP-directed plasma membrane pore formation can be considered a common strategy of inflammatory cell death (Figure 1.2). Other examples of pore-mediated cell death in immunity include the extracellular proteins perforin and the complement membrane attack complex[110,111]. However, these pore-forming proteins do not rely on specific phospholipids for their localization, and their mechanisms of targeting membranes and pore formation have been reviewed elsewhere[110,111].

Membrane-directed innate immune effector activity is not limited to pore-forming proteins, as a recent study proposed that cytokine egress from the cytosol is mediated by membrane association[112]. In this report, the proinflammatory cytokine IL-1β localizes to the plasma membrane upon its cleavage by caspase-1[112]. Mutation of a polybasic motif in IL-1β led to a significant decrease in its secretion from cells, and colocalization studies with the PLCδ1-pleckstrin homology (PH) domain suggest its membrane association may be mediated by $PI(4,5)P_2$[112]. However, direct interactions between $PI(4,5)P_2$ and IL-1β have not been demonstrated. With these data, the authors proposed a model in which IL-1β maturation poises the cytokine for secretion through GSDMD pores and membrane blebbing. When considered with GSDMD and MLKL, these instances suggest that membrane positioning by PIPs is utilized for activities downstream of innate immune pathway activation and mediates further activation of the immune system after pathogen detection.

1.2.4 Protein-Lipid Interactions as a Mechanism of PRR Activation

Some of the best characterized activators of innate immunity are lipids, such as the gram-negative bacterial cell wall component LPS. However, recent research has detailed that endogenous lipids also serve as stimulators of innate immune signaling. Upon tissue injury and cell death, membrane phospholipids are oxidized spontaneously and are capable of mediating inflammation in the absence of infection[113,114]. As such, these oxidized lipid molecules are DAMPs that are implicated in various disease states, including atherosclerosis and acute lung injury[114-116].

Oxidized derivatives of 1-palmitoyl-2-arachidonoyl-*sn*-glycero-3-phosphorylcholine (PAPC), collectively referred to as oxPAPC, are one class of DAMPs generated through oxidation of membrane component phospholipids, and upon tissue injury, can reach concentrations as high as 100μM in the blood[115,116]. oxPAPC binds the LPS receptor CD14, and CD14-mediated capture of oxPAPC allows for the internalization of these ligands and transport to the cell cytosol, where oxPAPC activates the inflammasome regulator caspase-11[117,118]. Indeed, following priming with various TLR ligands, oxPAPC treatment of DCs led to the secretion of IL-1β and IL-18, cytokines only released from the cell upon inflammasome activation[117]. *In vitro* binding assays and intracellular immunoprecipitation assays revealed that oxPAPC interacts directly with caspase-11 and caspase-1 to form the inflammasome[117,118]. However, unlike other activators of inflammasome activity, such as intracellular LPS, ATP, or nigericin, oxPAPC-mediated inflammasome activation did not lead to pyroptotic cell death in addition to IL-1β release in DCs[117]. Study of components of oxPAPC indicate that different oxidation products may have differential stimulatory capacity in various cell types[118-121]. For instance, the oxPAPC component molecules 1-pamitoyl-2-glutaryl-*sn*-glycero-3-phosphocholine (PGPC) and 1-palmitoyl-2-(5'-oxo-valeroyl)-*sn*-glycero-3-phosphocholine (POVPC) induce inflammasome activation and IL-1β secretion from living (hyperactive) DCs and macrophages[118-120].

While oxPAPC acts in the aforementioned manner as an inducer of inflammation, its actions are context dependent. For example, oxPAPC pretreatment of naïve cells has long been known to prevent subsequent responses to LPS[122], probably due to the fact that both of these lipids interact with the same amino acids in CD14, a TLR4 co-receptor for LPS[118]. These conditions may represent sterile tissue injury, where oxPAPC serves to prevent detection of potential endogenous TLR4 ligands. In contrast, the pro-inflammatory activities of oxPAPC and LPS co-detection may represent events that occur at sites of pathogen interactions, where both PAMPs and DAMPs are commonly found. In these ways, membrane-derived oxPAPC serves as either an activator or inhibitor of innate immune signaling, depending on the context in which this lipid is encountered.

Finally, recent work suggests that lipid interactions play an important role in regulating PRR activity within the cytosol. A recent study of the nucleotide-binding domain and leucine rich repeat family (NLR) family member NLRP3, a regulator of inflammasome activation, determined that this protein localizes to the trans Golgi network (TGN) upon various stimuli[123]. Binding to PI(4)P was proposed as the mechanism of TGN association by NLRP3, and amino acid residues implicated in PI(4)P binding were required for NLRP3-mediated inflammasome assembly and activation[123]. However, these findings stand in contrast with previous work that described NLRP3 association with the mitochondria through an interaction with cardiolipin[124,125]. Further research will clarify these discrepancies and pinpoint the specific localization of NLRP3, but these studies demonstrate how intracellular PRRs can interact with membrane lipids to direct the initiation of innate immune signaling.

1.3 Subcellular Positioning as a Regulator of Intracellular Nucleic Acid Sensors

Membranes are fundamental to the cell itself, defining its periphery and compartments, serving as platforms for pathway activation, and directing the downstream activity of cellular receptors. Cellular membranes are even capable of activating the immune system, as cell death leads to the production of oxPAPC[118]. Through this and the examples discussed above, it is clear that cell membranes and their component lipids are organizers and regulators of innate immune signal transduction. Therefore, to better understand innate immunity is to better understand the cell biology that serves as its context.

Given this, we propose that many PRRs defined as being purely cytosolic may indeed be regulated through subcellular positioning through electrostatic interactions with PIPs or other membrane component lipids. In particular, we were curious to understand the positioning of the critical intracellular nucleic acid sensors cGAS and RIG-I. Lacking transmembrane domains, these sensors are considered purely cytosolic proteins, and with such an assumption, their specific subcellular localization has yet to be thoroughly interrogated.

In particular, the sensor cGAS was of interest due to the nature of its ligand: dsDNA. DNA is fundamental to all cellular life. While cGAS sensing of DNA protects the cell during damage or viral infection, this ligand is constantly present in the environment that cGAS surveys. Inappropriate sensing of this ligand will generate an autoimmune response, requiring interaction between cellular DNA and cGAS to be minimized at steady state. Therefore, we hypothesized that cGAS may interact with a cellular membrane to prevent aberrant activation of the enzyme, sequestered from interactions with nuclear or mitochondrial DNA.

Unlike cGAS, RIG-I ligands are not present in the cell at steady state. However, RIG-I expression is extremely low at the onset of infection[126] and the assumed diffusion-mediated model of ligand encounter does not allow for optimal detection of vRNA at the early steps of viral infection. Given that a rapid immune response is essential for the clearance of infection, we

hypothesized that this PRR may be poised at sites of viral entry to allow for rapid detection of vRNA.

In the following chapters, we present the results of interrogation of these hypotheses and redefine the activity of these PRRs with emphasis on the intracellular dsDNA sensor cGAS. The activity of these PRRs, and perhaps all intracellular PRRs, are defined by interactions with and positioning by membrane lipids. These interactions shape the sensitivity of PRRs to their ligands and provide a threshold for activation that is essential for optimal innate immune sensing and the prevention of autoimmunity.

Chapter 2: cGAS

Self/Nonself Discrimination through Localization:

cGAS Association with the Plasma Membrane

A version of this chapter was published elsewhere:

Barnett, K. C., Coronas-Serna, J. M., Zhou, W., Ernandes, M.J., Cao, A., Kranzusch, P. J. & Kagan, J. C. Phosphoinositide Interactions Position cGAS at the Plasma Membrane to Ensure Efficient Distinction between Self- and Viral DNA. *Cell.* 1–15 (2019).

Author Contributions:

K.C.B. and J.C.K. conceptualized the study. K.C.B. conceived, designed, and performed most experiments, with assistance from J.M.C.-S., M.J.E., and A.C. W.Z. and P.J.K. provided reagents. J.C.K. supervised all research. K.C.B. and J.C.K. discussed the results and wrote the manuscript.

2.1 Abstract

The presence of DNA in the cytosol of mammalian cells is an unusual event, which is often associated with genotoxic stress or viral infection. The enzyme cGAS is a sensor of cytosolic DNA, which induces interferon and inflammatory responses that can be protective or pathologic, depending on the context. Along with other cytosolic innate immune receptors, cGAS is thought to diffuse throughout the cytosol in search of its DNA ligand. Herein, we report that cGAS is not a cytosolic protein, but rather localizes to the plasma membrane via the actions of an N-terminal phosphoinositide-binding domain. This domain interacts selectively with $PI(4,5)P_2$, and cGAS mutants defective for lipid-binding are mislocalized to the cytosolic and nuclear compartments. Mislocalized cGAS induces potent interferon responses to genotoxic stress, but weaker responses to viral infection. These data establish the subcellular positioning of a cytosolic innate immune receptor as a mechanism that governs self-nonself discrimination.

2.2 Introduction

The ability to discriminate between self and nonself is critical for recognition and response to pathogens, and ultimately, survival. In mammals, numerous proteins serve as sensors of PAMPs[1]. Some PAMPs, such as bacterial lipopolysaccharide, are exclusively nonself, in which no cognate molecule exists in the host organism[1]. However, other PAMPs, such as viral nucleic acids, bear strong similarities to molecules found in the host cell. In the case of RNA, structural differences between host and viral RNA allow for discrimination between self and non-self[2,14,127]. Yet with DNA, the distinction between host-derived and pathogen-derived molecules is less clear. Despite this, several DNA sensors are encoded in the germline and are essential for clearance of many infections, including TLR9, the AIM2-like receptors (ALRs), and cGAS[7].

Of these receptors, cGAS has emerged as a PRR that is functionally implicated in the detection of both self- and nonself-DNA. cGAS surveys the intracellular space for DNA, and generates IFN and inflammatory responses upon detection [8]. cGAS recognizes double stranded, B form DNA independent of its sequence through contact with the sugar-phosphate backbone[30]. Upon DNA binding, cGAS dimerizes, self-assembles into large liquid droplets, and produces the secondary messenger cGAMP[31,128,129]. This molecule binds to a pocket in the ER resident protein STING, leading to its activation and the subsequent expression of IFNs and other inflammatory mediators[8,34]. Because cGAS does not recognize specific DNA sequences, it is essential for the detection and control of many bacterial[40-42], viral[3,29,52,130,131], and parasitic[43] infections. Notably, cGAS also regulates immune responses in the absence of infection through the detection of endogenous (self) DNA. For instance, cGAS promotes IFN responses to genotoxic stress induced by DNA damaging agents[47,51], the formation of micronuclei[44,45], and cellular senescence[48-50]. Additionally, cGAS is activated by mitochondrial DNA released into the cytosol as a result of mitochondrial stress[52,53]. cGAS is therefore not only a sensor of pathogens but also a sensor of cellular stress and genomic integrity.

While the ability of cGAS to detect pathogen-derived DNA promotes beneficial responses during infection, its ability to detect self-DNA is associated with immunopathology. Indeed, the cGAS-STING signaling pathway is a driver of pathologies associated with autoinflammatory diseases[27,132,133]. Genetic analysis of human patients suffering from various interferonopathies revealed loss of function mutations in cytosolic nucleases that hydrolyze DNA or RNA-DNA hybrids, both of which are cGAS ligands[134-137]. These observations support the current view that the maintenance of low cytosolic DNA concentrations is critical to prevent inappropriate cGAS pathway activation. Whether additional mechanisms exist to prevent inappropriate activation of cGAS remains unknown.

Studies over the last several years have demonstrated that other nucleic acid-sensing PRRs are regulated by the positioning of receptors and ligands in distinct subcellular locations. An example of this principle derives from studies of TLR7 and TLR9, which respectively detect RNA and DNA[1]. These transmembrane receptors are synthetized as signaling-incompetent pro-proteins and are transported via the secretory pathway to endolysosomes[57]. Only upon delivery to these terminal compartments are TLR7 and TLR9 cleaved into receptors capable of inducing inflammation[56]. This mechanism of subcellular positioning ensures TLRs do not detect self-encoded extracellular nucleic acids[58].

Though some have noted nuclear localization[29,48], the subcellular positioning of cGAS at steady state is loosely defined as within the cell cytosol, where it encounters its ligands through diffusion[8]. Since cGAS lacks a transmembrane domain, the possibility of its specific positioning within the cytoplasm is unexplored. However, work over the last decade identified several innate immune regulators that were first considered to be cytosolic but are now recognized to associate with membranes through electrostatic interactions. These proteins include the mammalian proteins TIRAP and TRAM, and the *Drosophila* protein dMyD88, which regulate TLR and Toll pathway signaling, respectively[62,69,70,91]. Each of these proteins contain phosphoinositide phosphate (PIP) binding domains, enabling their positioning at the cell surface. Mutant alleles

lacking these domains are mislocalized to the cytosol and are consequently defective for TLR or Toll signaling. To date, the use of PIP binding proteins to regulate PRR activation is best characterized in the TLR family, and how this aspect of regulation extends to other pathways is unknown.

In this study, we report that cGAS is not a soluble, cytosolic protein, but is rather a peripheral membrane protein that primarily resides on the plasma membrane of human and mouse macrophages. We find this membrane association is mediated by an N-terminal phosphoinositide-binding domain within cGAS that interacts selectively with phosphatidylinositol 4,5-bisphosphate ($PI(4,5)P_2$), a plasma membrane resident lipid. A mutant allele of cGAS lacking its $PI(4,5)P_2$ binding domain is mislocalized to the cytosol and nucleus and is hyper-responsive to genotoxic stress, inducing an IFN response and consequently cell death. However, this mislocalized allele of cGAS does not generate a similarly potent response to viral infection. These findings identify a novel strategy of self-nonself discrimination, whereby positioning of cGAS at the plasma membrane prevents the recognition of self-DNA. These findings also establish subcellular positioning through PIP binding as a common feature of the TLR and cGAS signaling pathways to optimize signaling potential.

2.3 Materials and Methods

2.3.1 Cell Culture and Recombinant Cell Lines

Immortalized bone marrow derived macrophages (iBMDMs), Hela cells, HEK 293Ts, and L929 fibroblasts were cultured in DMEM supplemented with 10% FBS, Penicillin and Streptomycin (Pen+Strep), L-glutamine, and sodium pyruvate, referred to as complete DMEM, at 37°C in 5% CO_2. For passage, iBMDMs were lifted using PBS supplemented with 2.5mM EDTA and plated at dilution 1:10. HEK293T, L929, and Hela cells were grown under the same conditions as iBMDMs but were passaged by washing with PBS and lifting with 0.25% trypsin with a 1:10 dilution factor. THP1 cells were grown in suspension culture using RPMI-1640 media supplemented with 10% FBS, Pen+Strep, L-glutamine, and sodium pyruvate, referred to as complete RPMI-1640, at 37°C in 5% CO_2. For passage, cells were washed in PBS and plated at a dilution of 1:4. For intracellular DNA stimulation, iBMDMs were transfected with 1:1 Lipofectamine 2000:CT-DNA at the specified concentrations.

To generate lentiviral particles for the stable expression of transgenes, HEK293T cells were transfected with the packaging plasmids psPAX2 and pCMV-VSV-G along with the transgene in pLenti-CMV-GFP-Puro. All genes of interest were subcloned into the GFP site, and all mutant variants of cGAS were generated by overlap-extension PCR. For the production of TIRAP-GFP retroviral particles for stable expression, the packaging plasmids pCL-Eco and pCMV-VSV-G were used in addition to the target construct pMSCV2.2-TIRAP-GFP-IRES-hCD2tm. Plasmids were transfected into 10cm^2 dishes of HEK293Ts at 50%-80% confluency using polyethyleneimine (PEI) at a ratio of 3:1 PEI:DNA. Media was changed on transfected 293Ts 16 hours after transfection, and virus-containing supernatants were harvested 24 hours following the media change. Viral supernatants were passed through a 0.45μm filter to remove any cellular debris. Filtered viral supernatants were placed directly onto target cells for 24 hours and then replaced with the appropriate complete media. Cells expressing the transgenes were

selected using puromycin (5μg/mL for THP1; 10μg/mL for iBMDM) treatment for 3 days or until all cells in control wells were dead. Transgene expression was assessed by western analysis and confocal microscopy.

2.3.2 Primary Macrophage Culture and Manipulation

For the production of primary bone marrow derived macrophages, the leg bones of dead, female C57BL/6 mice were cleaned, cut with scissors, and flushed with sterile PBS using a syringe. The resultant isolated marrow was passed through a 70μm cell strainer to remove debris. Cells were plated into non-cell culture treated dishes in macrophage differentiation media, complete DMEM containing 30% L929 conditioned media containing MCSF. Three days after isolation, cells were fed additional macrophage differentiation media. On day 7, cells were lifted using PBS containing 2.5mM EDTA and plated for further experiments. Primary mouse macrophages were transfected using the Amaxa™ Nucleofector II (Lonza) in coordination with the Mouse Macrophage Nucleofector® Kit (Lonza) and were used according to the manufacturer's instructions.

For the production of immortalized *Cgas*-/- cells, primary macrophages were differentiated from isolated bone marrow, as described above, and immortalized using J2 retrovirus from supernatants collected from CREJ2 cell lines. *Cgas*-/- C57BL/6 leg bones were kindly provided by Dr. D. Stetson. Following differentiation, *Cgas*-/- primary macrophages were incubated with macrophage differentiation media containing 50% CREJ2 supernatant for seven days with a media replacement after the first three days of culture. Following viral transduction, cells were cultured until confluent in complete DMEM containing 30% L929 supernatant, split 1:2 into complete DMEM containing 25% L929 supernatant, and then slowly weaned from L929 supernatant with each passage into fresh complete DMEM with 5% less L929 supernatant than the previous. Once cells were able to grow in complete DMEM lacking any L929 supernatant, the immortalization process was complete.

For the production of CRISPR/Cas9 mediated generation of THP1 cGAS-/- cells, an cGAS-specific guide RNA was cloned into the previously described the pRRL-Cas9-Puro vector, kindly provided by Dr. D. Stetson, and transduced into THP1 cells, as described above. Cells were then single cell cloned, tested for cGAS expression by western blot, and tested for loss of intracellular DNA sensing by transfection of 1µg/mL CT-DNA.

2.3.3 Viral Infections

The MVA-Ova strain was generously provided Dr. N. Chevrier. For infection, viral stocks were diluted to a MOI of 3 in serum-free DMEM and incubated with cells for 1 hour at 37°C in 5% CO_2 with frequent agitation. After the period of infection, viral media was aspirated and replaced with complete DMEM and incubated at 37°C in 5% CO_2. At the indicated time points, cells were lysed with 1x Laemmli Buffer for western analysis or lysed for RNA isolation for RT-qPCR analysis.

2.3.4 H_2O_2, Doxorubicin, and PMA Treatments

THP1 monocytic cells were incubated with either 500µM H_2O_2, 50ng/mL PMA, or 500nM Doxorubicin in complete DMEM and incubated at 37°C in 5% CO_2. At the indicated time points, cells were lysed with 1x Laemmli Buffer for western analysis or lysed for RNA isolation for RT-qPCR analysis. With PMA and Doxorubicin treatments, cells were incubated with the indicated drug for 24 hours and analyzed using the cell viability assay described below.

2.3.5 Subcellular Fractionation

Benzonase (10U/mL) was used in all subcellular fractionation experiments to prevent post-lysis cGAS:DNA interactions unless otherwise stated. To separate membranes from the soluble cellular components, cells were washed once in hypotonic buffer (10mM Tris-HCl pH 7.4; 10mM KCl; 1.5mM $MgCl_2$) supplemented with a protease inhibitor cocktail (Roche), incubated on ice in hypotonic buffer, and lysed by Dounce homogenization. Lysates were centrifuged at 4°C for 5 minutes at 2,500xg to remove nuclei and cellular debris. The nuclear pellets were then washed 3

times in hypotonic buffer supplemented with 0.3% IGEPAL CA-630 to remove contaminating organelles and fully isolate nuclei, resulting in the nuclear fraction (P25). The supernatants from the 2,500xg spin (post-nuclear supernatants) were centrifuged further at 100,000xg for 1 hour at 4°C. The resultant pellets (P100) were resuspended in lysis buffer volumes equal to those of the supernatants (S100), stored with the addition of 6x Laemmli Buffer, and analyzed by western blot.

For membrane floatation assays, post-nuclear supernatants were collected and described above, mixed with Optiprep™-supplemented hypotonic buffer to yield a final concentration of 45% Optiprep™, laid at the bottom of an Optiprep™ step gradient ranging from 10% (top) to 45% (bottom), and spun at 52,000xg for 90 minutes. The gradient was then fractionated into 24 0.5mL fractions and analyzed by western blot. For gradients run in the presence of Triton-X100, post-nuclear supernatants were mixed with a 10% Triton-X100 solution to achieve a final concentration of 1%.

2.3.6 Confocal Microscopy

Cells were plated onto glass coverslips, treated as described, and fixed for 1.5 hours in a periodate-lysine-paraformaldehyde fixation buffer (20mM MES; 70mM NaCl; 5mM KCl; 70mM Lysine-HCl; 5mM $MgCl_2$; 2mM EGTA; 10mM $NaIO_4$; 2% Paraformaldehyde; 4.5% sucrose). Following fixation, cells were blocked and permeabilized in blocking buffer (0.1% saponin; 25mM Tris-HCl pH 7.5; 150mM NaCl; 4.5% sucrose; 2% goat serum; 50mM NH_4Cl), incubated overnight at 4°C with the indicated primary antibody at 1:100 dilution in blocking buffer, and incubated for 1 hour at RT with secondary antibodies and stains at a 1:400 dilution in blocking buffer. Cells were mounted onto glass slides with Prolong Gold Antifade (Thermo) and imaged using a 63x oil immersion objective on the LSM 880 with Airyscan (Zeiss). Images were processed using ZEN software (Zeiss) and ImageJ (NIH).

For imaging THP-1 cells, cells were attached to coverslips coated with Alcian Blue by incubation in serum free media for 20 minutes at 37°C in 5% CO_2. For imaging of zymosan

phagocytosis, cells were incubated for 10 minutes at 37°C in 5% CO_2 in media containing zymosan at a ratio of 5 particles per cell. For quantification of cGAS localization, at least 200 cells per replicate were counted of three replicates in total. Plasma membrane localization was characterized as co-localization with Phalloidin, while nuclear localization was characterized as co-localization with DAPI.

2.3.7 Real-Time Quantitative PCR

RNA was isolated from cells using Qiashredder (Qiagen) homogenizers and the PureLink Mini RNA Kit (Life Technologies). The resultant RNA was treated subsequently DNAse I (Thermo) to remove genomic DNA. Relative mRNA expression was analyzed using the TaqMan RNA-to-Ct 1-Step Kit (Applied Biosystems) with indicated probes on a CFX384 Real-Time Cycler (BioRad).

2.3.8 Cell Viability Assay

Cell viability was measured using the CellTiter-Glo kit (Promega), a luminescent assay for ATP in living cells. Assays were performed as described by the manufacturer with untreated cells used as a positive control for cell viability. These cells were considered as the 100% viable benchmark compared to treated cells. Luminescent outputs were read on a Tecan plate reader.

2.3.9 Phylogenetic Analysis

Ten vertebrate animals' cGAS sequences were analyzed by Clustal ω software (https://www.ebi.ac.uk/Tools/msa/clustalo/). The N- and C-termini were defined according to their alignments with human cGAS, and the isoelectric point (pI) of each domain was calculated using the ExPASy Compute pI/molecular weight tool (https://web.expasy.org/compute_pi/). Percent identity was calculated as the ratio of conserved residues to the total number of residues in the protein, using human cGAS as the reference.

2.3.10 Recombinant Protein Purification

Recombinant cGAS protein and corresponding variants were purified as previous described[138]3. Briefly, human cGAS and cGAS R71/75E variants were cloned into a custom pET

vector for expression as an N-terminal 6xHis-SUMO2-fusion protein using PCR amplification and standard cloning techniques. The pET-cGAS plasmids were transformed into *E. coli* BL21 DE3 (Aglient) bacteria harboring a pRARE2 tRNA plasmid. *E. coli* were grown in M9ZB media at 37 °C and protein expression was induced by IPTG for 16 h at 16°C. Bacterial pellets expressing cGAS were resuspended in lysis buffer and then lysed by sonication. After centrifugation, the supernatants were collected, and recombinant protein was isolated using Ni-NTA (QIAGEN) chromatography. The His-SUMO2 tag was then removed by digestion with human SENP2 protease except when used as His-tagged proteins for the PI-binding pulldown assay, in which case the tag was not cleaved. Recombinant cGAS proteins were further purified by Heparin HP ion-exchange (GE Healthcare) and 16/600 S75 size-exclusion chromatography (GE Healthcare). Final cGAS proteins were concentrated in storage buffer (20 mM HEPES-KOH pH 7.5, 250 mM KCl, 1 mM TCEP), flash-frozen in liquid nitrogen, and stored at –80 °C.

Recombinant human cGAS∆N and cGAS N were expressed using the pET50b vector containing an N-terminal 6xHis-NusA tag (gift from Dr. Sun Hur) in BL21 (DE3) *E. coli* at 16°C for 20 hours after induction with 5mM IPTG. Cells were lysed using an Emulsiflex-C5 (Avestin), and protein was batch purified using Ni-NTA affinity chromatography. Proteins were dialyzed overnight into a storage buffer (20mM HEPES pH 7.5; 150mM KCl; 10% Glycerol; 1mM TCEP) [30] and flash frozen in liquid nitrogen for use in biochemical assays. Preparation efficacy and purity was assessed by SDS-PAGE and SimplyBlue SafeStain (Thermo).

2.3.11 PIP Strip Lipid Binding Assay

Lipid binding assays were performed as described[69]. Briefly, PIP strips (Echelon) were blocked in blocking buffer(10mM Tris pH 8; 150mM NaCl; 0.1% Tween-20; 0.1% ovalbumin) for 1 hour, then incubated for 2 hours with purified hcGAS (500ng/mL) in the presence of an anti-hcGAS antibody (Sigma) in blocking buffer, washed 3 times with blocking buffer, and then probed

with an HRP-conjugated secondary antibody in blocking buffer for 30 minutes. Lipid bound protein was detected using enhanced chemiluminescence.

2.3.12 Liposome Preparation and Assays

Liposome preparation and subsequent binding assays were performed described[69]. In brief, phosphatidylcholine (PC) and phosphatidylethanolamine (PE) (Avanti) were mixed at a 3:1 ratio in a solution of 2:1 chloroform:methanol in borosilicate glass tubes and gently dried into a lipid film using inert nitrogen gas. For liposomes containing PIPs, the 3:1 PC:PE ratio was maintained with the addition of the specified percentage of PIP (Echelon). Dried lipids were resuspended in 300mM sucrose and vortexed aggressively to yield liposomes at a final concentration of 1μg/μL.

For sedimentation assays, 20μg of liposomes were incubated with 5μg of recombinant cGAS in a cytosol buffer (25mM HEPES pH 7.2; 25mM KCl; 2.5mM Magnesium Acetate; 150mM Potassium Glutamate) for 15 minutes at RT. Following incubation, samples were centrifuged at 100,000xg, and the pellets were analyzed by western blot for cGAS binding.

For fluorescent liposome pulldown assays, liposomes were prepared as described above, except fluorescently tagged PC (NBD-PC) was used in place of PC. 25μg of liposomes were mixed with 25μg of recombinant protein in cytosol buffer in the presence of Ni-NTA resin and incubated with gentle mixing for 30 minutes at RT. Ni-NTA resin was pelleted and washed two times before elution of liposomes with 10% SDS. Resultant fluorescence recovered was quantified by spectrofluorimetry using a Tecan plate reader. Interactions between the beads and liposomes alone were subtracted from all samples to account for nonspecific binding.

2.3.13 Luciferase Reporter Assays

293T cells were transiently transfected with the indicated plasmids using PEI at a 3:1 PEI:DNA ratio. After 24h, cells were lysed and incubated with Bright-Glo reagent (Promega) according to manufacturer's instructions, and luminescence was read on a Tecan plate reader.

2.3.14 Statistical Analysis

All statistical analysis was performed using Graphpad Prism7 software. All experiments were performed in triplicate as three independent biological replicates. For comparison in which multiple variables were at multiple timepoints, two-way ANOVA analysis was performed. For comparison of two data points, the student's two-tailed t test was used. Asterisk coding is as follows: * p<= 0.05; ** p<=0.01; *** p<=0.001; **** p<=0.0001. Data with error bars depict the average with the standard error of the mean (SEM).

2.4 Results

2.4.1 cGAS is located at the plasma membrane of human and mouse macrophages.

We sought to identify the site of cGAS residence in unstimulated macrophages, a cell type critical for immune responses to infection and tissue injury. We examined the distribution of cGAS in human THP1 monocytes through subcellular fractionation by differential ultracentrifugation. Fractionation fidelity was verified by detection of the cytosolic protein caspase-3 in the soluble fraction (S100), the ER-localized transmembrane protein calnexin in the insoluble, membrane fraction (P100), and Lamins A and C in the nuclear fraction (P25). We utilized a cGAS antibody, validated on cGAS knockout (KO) cells, to ensure accuracy (Figure S1A and S1B). The nuclease benzonase was included in all buffers to minimize post-lysis DNA binding by cGAS. This possibility was important to consider, as cGAS forms liquid droplets upon DNA binding that co-sediment with nuclei[129]. The bulk of endogenous cGAS was detected the membranous P100 fraction along with a small amount present in the nuclear P25 fraction (Figure 2.1A). No cGAS was detected in the S100 cytosolic fractions (Figure 2.1A). These data suggest that cGAS is not a cytosolic protein, but rather associates with membranes and nuclei.

Whereas the presence of cGAS in the nucleus is consistent with established literature[29,48], its predominant distribution in the membrane fraction warranted further investigation. Membrane-bound organelles should not only sediment after ultracentrifugation, but also migrate from dense to light fractions of a bottom-loaded density gradient, known as a membrane flotation assay. We therefore performed membrane flotation assays on Optiprep™ gradients bottom-loaded with post-nuclear supernatants of THP1 cells. As expected, the membrane protein calnexin floated from the site of gradient loading (fractions 21-24) into several contiguous fractions throughout the gradient (Figure 2.1B). Similar observations were made with cGAS, with nearly the entire population of this protein migrating into lighter membrane fractions (Figure 2.1B). These complementary procedures indicate that cGAS is present on a membrane-bound organelle.

If we eliminated benzonase from our buffers, cGAS fractionation patterns were distinct from those described above. In sedimentation assays, the absence of benzonase resulted in a greater amount of cGAS fractionating with nuclei (Figure 2.1A). Based on the knowledge that cGAS forms liquid droplets that approach the size of nuclei upon DNA binding, it is reasonable to suggest that post-lysis DNA binding causes cGAS to appear as a predominantly nuclear protein in biochemical assays. Consistent with this idea, elimination of benzonase from our flotation-based assays resulted in almost all cGAS remaining in the heaviest fractions 21-24, where the gradient was loaded (Figure 2.1B). These findings support the conclusion that in the absence of DNA exposure, cGAS is predominantly a membrane protein and highlight the importance of considering post-lysis DNA binding in any assay for cGAS function.

To complete our biochemical analysis, we determined if the flotation of cGAS into light membrane fractions was sensitive to the detergent Triton X-100. Whereas treatment of cell lysates with Triton X-100 prevented calnexin flotation, cGAS retained the ability to float into lower density fractions (Figure 2.1C). cGAS is therefore present on a membrane insensitive to solvation by Triton X-100. Triton X-100 resistant membranes include lipid rafts, which are subdomains of the plasma membrane[139,140]. These subdomains are rich in several lipids, including the $PI(4,5)P_2$, which will be discussed later.

Confocal microscopy was used to complement these analyses and identify the precise subcellular residency of cGAS. Staining of wild type (WT) or cGAS knockout (KO) THP1 monocytes was performed to identify conditions suitable for endogenous protein detection, using two different cGAS antibodies. Neither antibody generated a staining pattern that present in resting WT cells but absent in KO cells (Figure S1C and S1D). However, a short treatment (4 hours) of cells with 1000U/mL IFNβ increased the abundance of cGAS and permitted detection of the endogenous protein. The staining observed was concentrated at the plasma membrane (Figure 2.1D). Cross section confocal slices revealed a circumferential staining pattern that coincided with filamentous actin (F-actin), whereas confocal slices of the ventral side of the cell

(the site of attachment to the coverslip) revealed cGAS concentration in multiple foci scattered throughout the plasma membrane (Figure 2.1D). Quantification revealed that over 90% of cells displayed cGAS staining at the site of coverslip contact (Figure S1E). cGAS KO cells completely lacked staining with this antibody. We reasoned that if the cGAS antibody used (from Cell Signaling Technology (CST)) truly detected cGAS at the plasma membrane, then cells expressing a C-terminally HA-tagged cGAS (cGAS-HA) allele should display extensive colocalization when stained with antibodies specific for cGAS and HA. This possibility was tested by generating THP1 monocytes that stably express cGAS-HA (Figure S1F and S1G). Consistent with our studies of endogenous cGAS, cGAS-HA fractionated primarily with membranes in the presence of benzonase and localized to the plasma membrane (Figure 2.1E and 2.1F).

Also consistent with our microscopic studies of endogenous cGAS, the CST and HA antibodies displayed extensive plasma membrane co-distribution (Figure S1G). In contrast, the cGAS antibody from Sigma was unable to detect endogenous cGAS or cGAS-HA (Figure S1G). The abundance of cGAS-HA in our stable lines was modestly greater than the endogenous protein (Figure S1F), but these cells exhibited no evidence of cGAS activation, as basal IFNβ expression was comparable to what was observed in WT THP1 cells, as discussed below. These data, combined with our biochemical analysis, support the conclusion that in its inactive state, cGAS is a membrane protein that resides primarily at the surface of THP1 cells.

To determine if our findings extended to other cell populations, we examined the staining of cGAS-HA in primary murine bone marrow derived macrophages (BMDMs), where the transgene was expressed at levels that similar to the endogenous protein (Figure S1F). Staining for HA in these cells revealed a clear localization of cGAS to the plasma membrane, with a concentration in actin-rich membrane ruffles (Figure 2.1F). Additionally, immortalized BMDMs (iBMDMs) stably expressing cGAS-HA displayed similar staining patterns, with prominent cGAS staining detected at the cell surface in actin-rich ruffles (Figure 2.1F).

2.1A

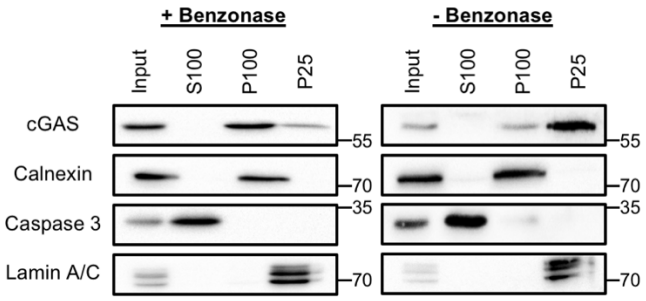

2.1B

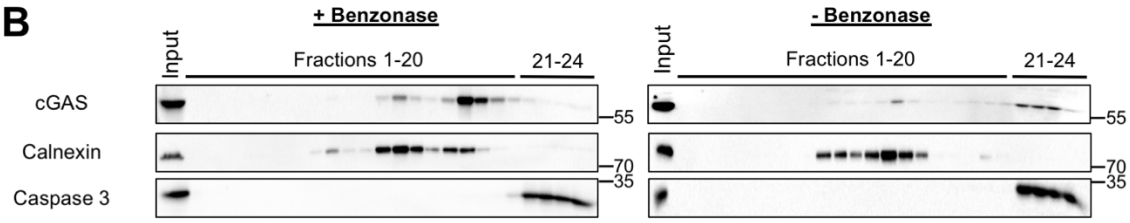

2.1C

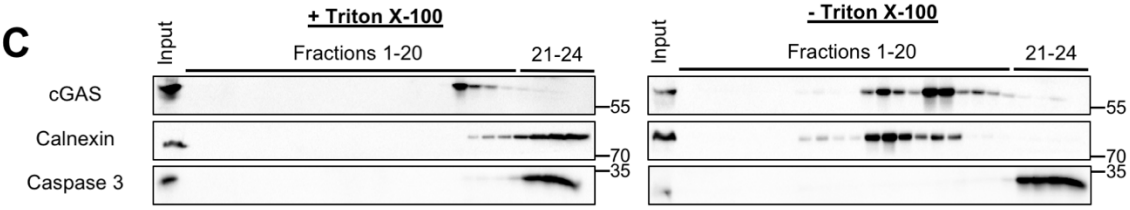

2.1D

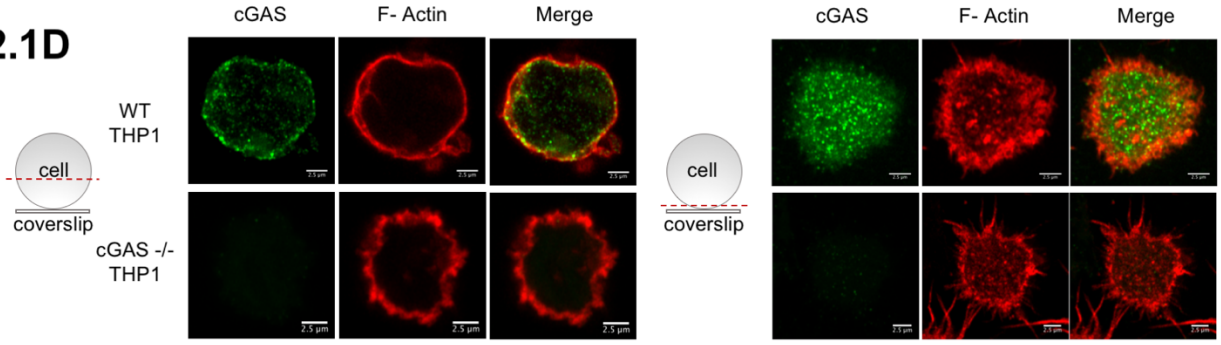

2.1E

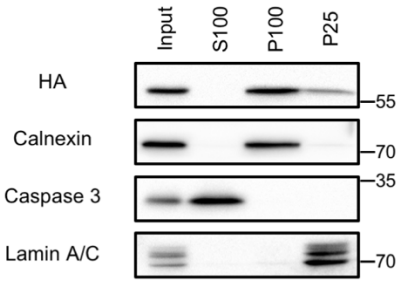

2.1F

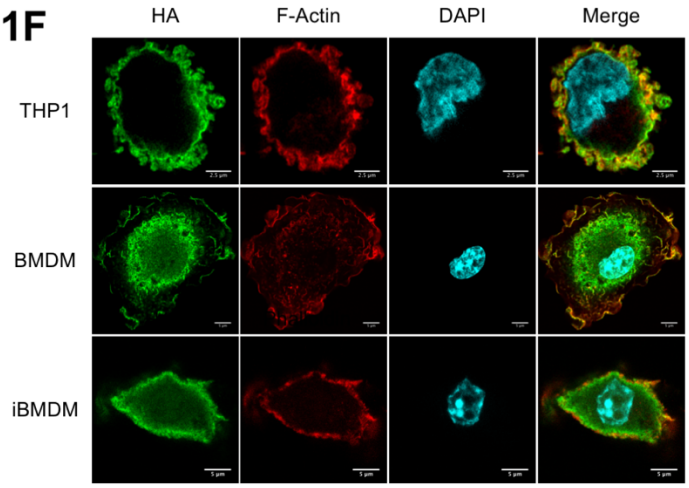

Figure 2.1: cGAS associates with the plasma membrane.

2.1A) Subcellular fractionation of WT THP1 cells in the presence or absence of benzonase. Western blot analysis was used to probe the cytosolic fraction (S100), membrane fraction (P100), and nuclear (P25) fractions for the indicated proteins. **2.1B)** Membrane floatation assays of THP1 post-nuclear lysates on a 10-45% Optiprep™ gradient in the presence or absence of benzonase. Fractions 1-24 were taken from the top to the bottom of the gradient, and western blot analysis was used to probe these fractions for the indicated proteins. **2.1C)** Membrane floatation assays of THP1 post-nuclear lysates on a 10-40% Optiprep™ gradient in the presence of benzonase in the presence or absence of 1% Triton-X 100. **2.1D)** Confocal micrographs cGAS in WT and cGAS-/- THP1 cells treated with 1000U/mL recombinant IFNβ1 for 4 hours. Diagrams to the left of micrographs, where the red dashed lines indicate the plane in view (not to scale). **2.1F)** Subcellular fractionation of WT THP1 expressing cGAS-HA cells in the presence of benzonase. **2.1G)** Confocal micrographs of various cell lines expressing cGAS-HA. Experiments shown are representative of n=3 biological replicates.

See also Figure S1.

Several studies have examined the localization of cGAS in non-phagocytes and have not observed plasma membrane localization[8,29,42,141]. To standardize our studies with those of others, we introduced the same cGAS-HA cDNA into THP1 monocytes, iBMDMs, Hela cells and L929 cells, the latter two of which were examined previously[8,42,141]. Whereas cGAS was almost singularly located at the plasma membrane of THP1 cells and iBMDMs, a heterogenous distribution of cGAS was observed in Hela and L929 cells (Figure S1H and S1I). While cGAS localization was predominantly nuclear in L929 cells and highly varied in Hela cells, all cell types displayed some proportion of plasma membrane localized cGAS (Figure S1H and S1I). Therefore, cell type specific factors influence cGAS localization.

Others have observed cGAS to be concentrated in cytosolic spots following DNA transfection[8,54,142]. Similarly, we found that within 30 minutes of DNA transfection, cGAS was no longer concentrated at the cell surface, but was rather detected in various cytoplasmic puncta (Figure S1J). These puncta are thought to be sites of cGAS-DNA interaction, in which cGAS oligomerizes, forms liquid droplets, and synthesizes cGAMP[54,129,142,143]. Collectively, these findings indicate that within resting phagocytic cells, cGAS primarily resides on the plasma membrane.

2.4.2 The N-Terminal domain of cGAS is necessary and sufficient for cGAS localization to the plasma membrane.

Human cGAS is a 522 amino acid protein with an unstructured N-terminus of 159 amino acids[30]. The structurally defined C-terminus (residues 160-522) is sufficient to recognize DNA, produce cGAMP *in vitro*[30,33], and produce IFNβ upon overexpression within cells[8]. The N-terminus of cGAS is poorly characterized, but contributes to DNA binding and to efficient DNA-induced assembly of lipid droplets[8,30,33,129]. To identify regions of cGAS that mediate plasma membrane localization, deletion analysis was performed. We separated cGAS into its N-terminal domain (residues 1-159 human; residues 1-147 murine) and its C-terminal domain (residues 160-522 human; residues 148-507 murine) (Figure 2.2A). The human alleles were stably expressed as C-

terminally HA-tagged proteins in THP1 monocytes. Western analysis verified production of each cGAS protein (Figure 2.2B). The allele lacking its N-terminus (cGASΔN) was expressed at lower levels than the WT protein or N-terminus alone (cGAS N) (Figure 2.2B).

cGAS N phenocopied the localization of the WT protein, localizing to the cell surface (Figure 2.2C). In contrast, cGASΔN was not located at the plasma membrane but was rather found throughout the cytoplasm and nucleus (Figure 2.2C). Similar to human cGAS, murine cGASΔN was expressed at lower levels than WT cGAS and cGAS N (Figure 2.2D). Furthermore, murine cGAS N localized to the plasma membrane, while cGASΔN did not associate with the plasma membrane (Figure 2.2E). Quantification revealed that all cells expressing the cGAS N-terminus displayed plasma membrane localization, while none of the cells expressing cGASΔN showed such localization (Figure S2A). Pseudo-3D renderings of WT cGAS and these mutants further illustrated the conclusions obtained from confocal slices, as WT and cGAS N proteins were concentrated at the plasma membrane and absent from the interior of the cell (Figure S2B). In contrast, cGASΔN was concentrated in the cytosol and nucleus (Figure S2B). As described above, cGAS localization varies by cell type. However, this heterogeneity of cGAS localization was not observed when we examined the distribution of the N-terminal domain alone. This domain was uniformly localized at the plasma membrane of all cell types examined (Figure 2.2F). These findings indicate the N-terminus of cGAS is necessary and sufficient for positioning at the cell surface, acting as a *bona fide* localization domain.

Alignment of the domains within cGAS from ten vertebrate animals revealed strong conservation of the catalytic domain, and while all species examined contained an N-terminal domain, this region of the protein was less conserved. Despite this weak degree of conservation, the N-termini of all species examined were highly charged, as compared to the catalytic domain, with an isoelectric point (pI) that was at least 2 pH units higher than the catalytic domain (Figure 2.2G). Thus, while the specific amino acids that comprise the cGAS N-terminus are not well conserved, the pI of this localization domain is conserved.

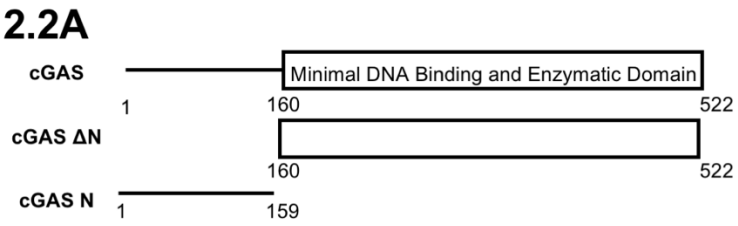
2.2A
cGAS
Minimal DNA Binding and Enzymatic Domain
1
160
522
cGAS ΔN
160
522
cGAS N
1
159

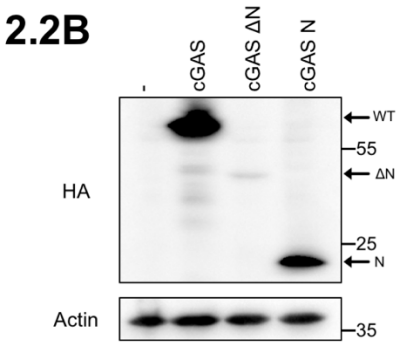
2.2B
-
cGAS
cGAS ΔN
cGAS N
HA
WT
55
ΔN
25
N
Actin
35

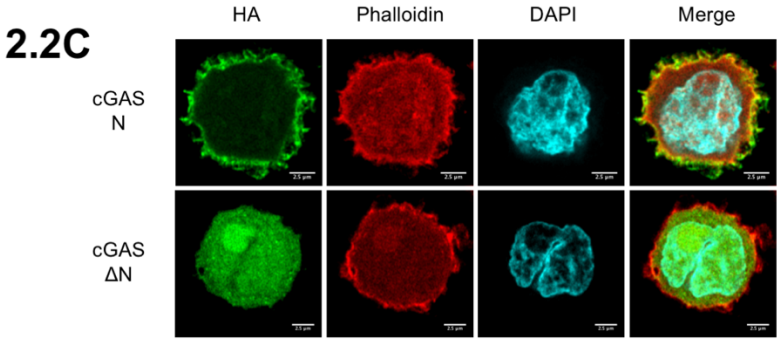
2.2C
HA
Phalloidin
DAPI
Merge
cGAS N
cGAS ΔN

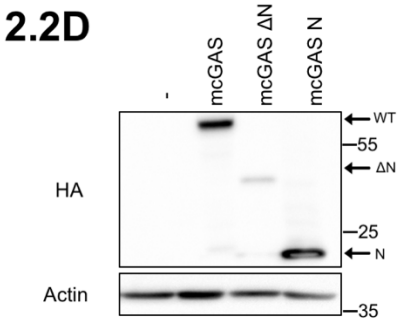
2.2D
-
mcGAS
mcGAS ΔN
mcGAS N
HA
WT
55
ΔN
25
N
Actin
35

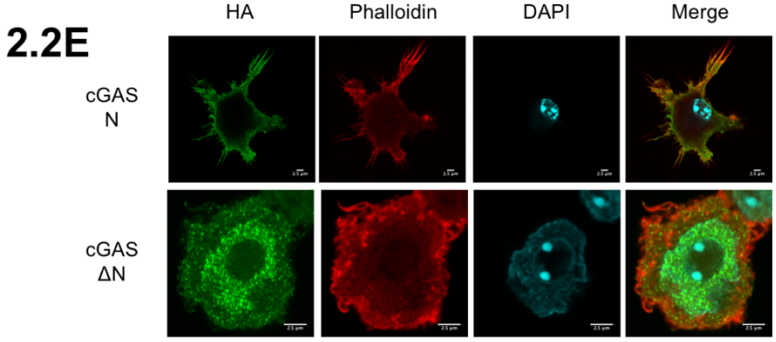
2.2E
HA
Phalloidin
DAPI
Merge
cGAS N
cGAS ΔN

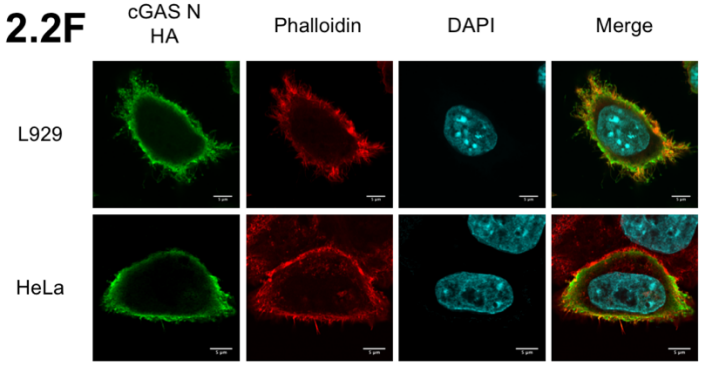
2.2F
cGAS N
HA
Phalloidin
DAPI
Merge
L929
HeLa

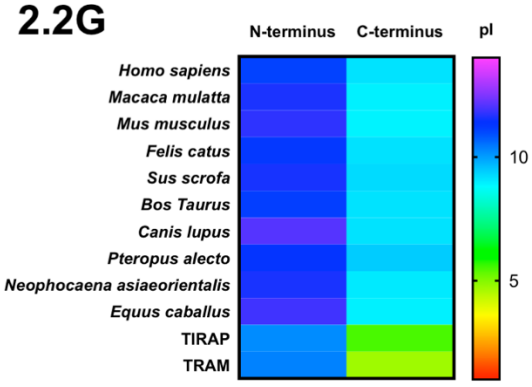
2.2G
N-terminus
C-terminus
pI
Homo sapiens
Macaca mulatta
Mus musculus
Felis catus
Sus scrofa
Bos Taurus
Canis lupus
Pteropus alecto
Neophocaena asiaeorientalis
Equus caballus
TIRAP
TRAM
10
5

Figure 2.2: The N-Terminus of cGAS is necessary and sufficient for plasma membrane association.

2.2A) Schematic of human cGAS domain architecture and truncation mutants. **2.2B)** Western blot analysis of mutant cGAS expression in THP1 cells. **2.2C)** Confocal micrograph of THP1 cells expressing human cGAS N or cGASΔN. **2.2D)** Western blot analysis of murine mutant cGAS expression in iBMDMs. **2.2E)** Confocal micrographs of iBMDMs expressing murine cGAS N or cGASΔN. **2.2F)** Confocal micrographs of L929 and Hela cells expressing cGAS N. **2.2G)** Heat map showing the relative pI of the N- and C- terminal domains of cGAS from various species (n=10) alongside innate immune adaptors TRIF and TRAM with N-terminal PIP-binding domains. Experiments shown are representative of n=3 biological replicates.

See also Figure S2.

2.4.3 The cGAS N-terminus binds PI(4,5)P_2 to mediate plasma membrane localization.

The pI of the cGAS N-terminus was comparable to that of the localization domains from TIRAP and TRAM, with a pI of 11.07 in the human cGAS N-terminus (Figure 2.2G). The high net positive charge of these domains mediates subcellular positioning through electrostatic interactions with negatively-charged PIPs and is a common feature of PIP-binding localization domains[72]. Considering the features of the cGAS N-terminus, we hypothesized that cGAS localizes to the plasma membrane through interactions with a PIP.

We examined the ability of recombinant cGAS to bind a panel of lipids immobilized on hydrophobic membranes (PIP Strips). Far western analysis revealed interactions between cGAS and several PIPs, but not the unphosphorylated lipid PI (Figure 2.3A). Additionally, no interactions were observed between cGAS and other membrane lipids (Figure 2.3A). To corroborate these findings, we examined the ability of recombinant cGAS to bind PIPs within lipid bilayers, the physiological context for protein-PIP interactions. We constructed liposomes consisting of PC and PE, abundant lipids present naturally in the plasma membrane, and select PIPs. Recombinant cGAS interacted with liposomes containing 18% of various PIPs, but not with liposomes lacking PIPs (Figure 2.3B). These collective experiments indicate that cGAS promiscuously interacts PIPs but does not associate with any other membrane lipids.

Quantitative analysis was performed using fluorescently labeled liposomes to determine if cGAS displays preference for individual PIPs. For these studies, we reduced the concentration of PIPs present in each liposome to 2%. Given the localization of cGAS, we focused on PIPs found at the plasma membrane at steady state: PI(4)P and PI(4,5)P_2[72], and another di-phosphorylated PIP found on the plasma membrane in an inducible manner: PI(3,4)P_2[144]. This quantitative analysis demonstrated that cGAS preferentially binds PI(4,5)P_2 (Figure 2.3C) and supports a model in which PI(4,5)P_2 directs cGAS association with the plasma membrane.

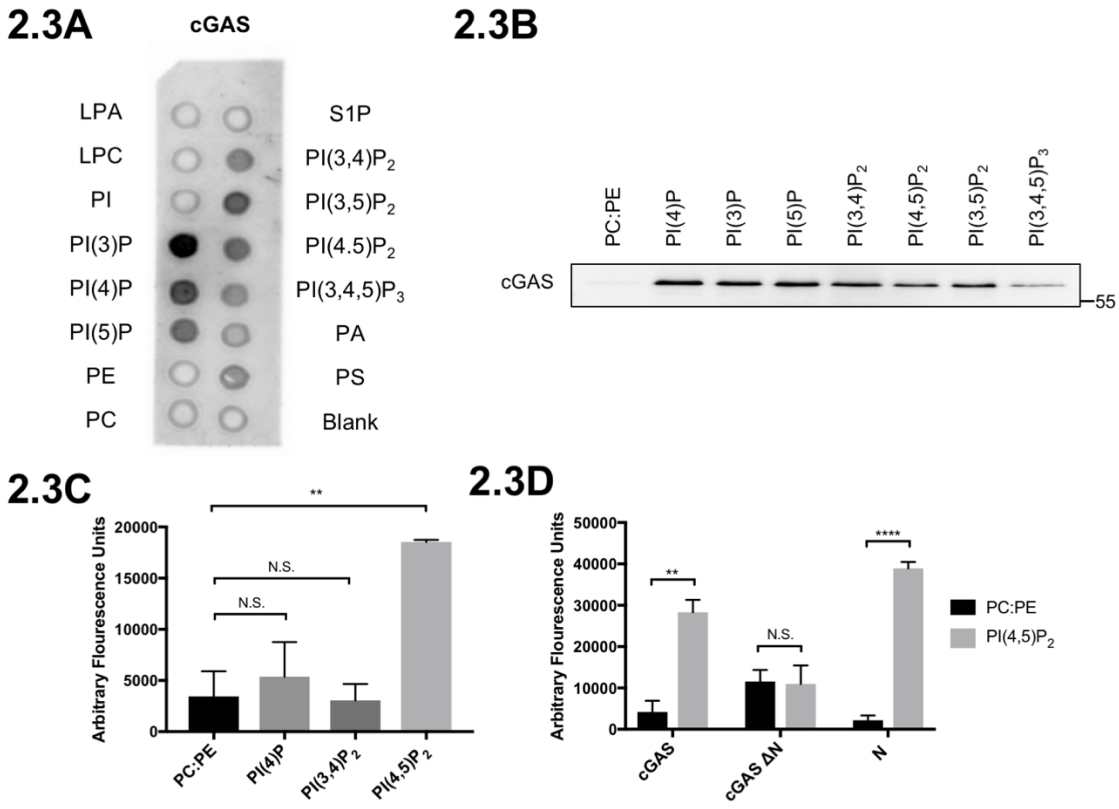
2.3A
cGAS
LPA
LPC
PI
PI(3)P
PI(4)P
PI(5)P
PE
PC
S1P
PI(3,4)P2
PI(3,5)P2
PI(4.5)P2
PI(3,4,5)P3
PA
PS
Blank
2.3B
PC:PE
PI(4)P
PI(3)P
PI(5)P
PI(3,4)P2
PI(4,5)P2
PI(3,5)P2
PI(3,4,5)P3
cGAS
55
2.3C
Arbitrary Flourescence Units
20000
15000
10000
5000
0
**
N.S.
N.S.
PC:PE
PI(4)P
PI(3,4)P2
PI(4,5)P2
2.3D
Arbitrary Flourescence Units
50000
40000
30000
20000
10000
0
**
N.S.
****
cGAS
cGAS ΔN
N
PC:PE
PI(4,5)P2
2.3E
PLCδ1
cGAS N
DAPI
Merge
2.3F
gp91phox
cGAS N
DAPI
Merge
2.3G
cGAS N
Zymosan
DAPI
Merge

Figure 2.3: cGAS binds PI(4,5)P_2 via its N-terminus.

2.3A) PIP strip analysis of recombinant cGAS. Recombinant cGAS was incubated with a membrane spotted with the indicated lipids and analyzed by far western. **2.3B)** Cosedimentation assay for cGAS interactions with liposomes containing 18% of the specified PIPs on a 3:1 PC:PE backbone. Recombinant cGAS was incubated with liposomes, after which the liposomes were isolated by ultracentrifugation and probed by western blot for cGAS association. **2.3C)** Fluorescent liposome pulldown assay. 6xHis-tagged cGAS was incubated with fluorescent liposomes containing the specified PIPs. cGAS was isolated by nickel affinity resin and cGAS-lipid interaction was measured by the amount of fluorescence pulled down with the resin. **2.3D)** Same as 3C, but 6x-His-tagged cGAS, cGASΔN, and cGAS N were probed for binding to PI(4,5)P_2. **2.3E)** Confocal micrographs of electroporated primary BMDMs expressing cGAS N-HA with PLCδ1-PH-YFP. **2.3F)** Confocal micrographs of electroporated primary BMDMs expressing $gp91^{phox}$-PX-YFP. **2.3G)** Confocal micrograph of an iBMDM expressing cGAS N phagocytosing a fluorescent zymosan particle. Experiments shown are representative of or averages of n=3 biological replicates. Data is represented as a mean ± standard error of the mean (SEM), and statistical analysis was preformed using a student's T test with asterisk coding as follows: * p<= 0.05; ** p<=0.01; *** p<=0.001; **** p<=0.0001.

Using the deletion mutants described above, we determined which domain within cGAS interacts with PI(4,5)P_2. We found that the N-terminal localization domain phenocopied WT cGAS, as both proteins interacted with liposomes containing PI(4,5)P_2, but not with liposomes containing only PC:PE (Figure 2.3D). In contrast, cGASΔN interacted weakly with PC:PE liposomes and displayed no preference for PI(4,5)P_2 (Figure 2.3D). The cGAS N-terminus also displayed preferential co-localization with PI(4,5)P_2 within cells. We observed extensive colocalization in primary BMDMs expressing the cGAS N-terminus and the PI(4,5)P_2-specific PH domain of PLCδ1 (Figure 2.3E)[91]. These experimental conditions resulted in partial mislocalization of both binding proteins as a result of competition for PI(4,5)P_2, which is observed when two PI(4,5)P2 binding proteins are co-expressed[74]. In contrast, cGAS did not colocalize with the PI(3)P-binding PX domain from gp91^{phox91} (Figure 2.3F). Furthermore, the cGAS N-terminus displays a canonical behavior of PI(4,5)P_2 distribution on forming phagosomes[75]. cGAS was detected on phagocytic protrusions but was absent from the base of the phagocytic cup (Figure 2.3G). These independent assays demonstrate that interactions with PI(4,5)P_2 direct cGAS to the plasma membrane.

2.4.4 Plasma membrane localization of cGAS is important to prevent recognition of self-DNA.

cGAS has dual functions in innate immunity; it must minimize detection of self-DNA while simultaneously being capable of pathogenic DNA detection. To determine if either of these tasks are influenced cGAS membrane localization, functional analysis was performed. For these studies, we aimed to utilize a cellular system that closely matched physiological contexts. Tonic signaling via the cGAS pathway sets the expression level of numerous IFNs and ISGs, and cGAS-deficient cells express low levels of these genes[3]. Expression of WT cGAS in THP1 cells did not influence basal IFN and ISG levels (Figure 2.4A and 2.4B), allowing us to perform functional studies in this genetic background. In addition to WT cGAS, we engineered THP1 cell lines stably expressing the N-terminal localization domain (cGAS N) or the mislocalized cGASΔN. Additional THP1 lines were generated that expressed GFP, a mutant cGAS allele defective for DNA-binding

(C396/397A)[33] or a cGASΔN allele defective for DNA binding (C396/397A). Western analysis verified the presence of each protein, with cGASΔN produced at lower levels than other proteins (Figure S3A).

Although the cGASΔN allele was expressed at lower levels than its WT counterpart (Figure S3A), cells producing this protein displayed high expression of *IFNβ1* and *RSAD2* (Figure 2.4A and 2.4B). Cells producing the DNA-binding deficient cGASΔN (C396/397A) allele did not display a similar phenotype (Figure 2.4A and 2.4B), indicating that high basal IFN expression was due to detection of endogenous DNA. These data suggest that localization of cGAS is important to avoid detection of self-DNA.

If this prediction was correct, then cells expressing cGASΔN should be more sensitive to genotoxic stress. Indeed, the cGAS pathway is activated in several experimental settings of DNA damage[44-51]. This idea was tested by treating cells with the DNA damaging agent hydrogen peroxide (H_2O_2). Treatment with H_2O_2 for six hours induced minimal *IFNβ1* expression in most of the transgenic THP1 lines examined (Figure 2.4C). In contrast, cells expressing mislocalized cGASΔN induced substantial increases in *IFNβ1* expression in response to H_2O_2 (Figure 2.4C). This H_2O_2-induced IFN response was not observed in cells expressing the DNA-binding deficient cGASΔN C396/397A (Figure 2.4C). Western analysis demonstrated that cells expressing cGASΔN responded to H_2O_2 by inducing the phosphorylation of STAT1 (Figure 2.4D), a hallmark of an IFN response. No other transgene induced potent STAT1 phosphorylation in response to H_2O_2, suggesting that loss of localization leads to heightened sensitivity to genotoxic stress.

We performed similar analyses with two additional DNA-damage inducing agents: doxorubicin and phorbol myristate acetate (PMA)[145,146]. Treatment with doxorubicin induced *IFNβ1* expression in THP1 cells expressing cGASΔN but not cGASΔN C396/7A or WT cGAS (Figure 2.4E). Notably, this upregulation was accompanied by the death of cGASΔN expressing cells. At 14 hours post treatment with doxorubicin, only 22.2% of cGASΔN expressing cells remained viable compared to untreated controls as measured by cellular ATP content (Figure

2.4F). This phenotype was not observed in cells expressing WT cGAS or cGASΔN C396/7A (Figure 2.4F).

Treatments with PMA also demonstrated a stark contrast between cells expressing WT cGAS and mislocalized cGASΔN. PMA stimulations for as little as three hours induced a 2-3 log increase in *IFNβ1* expression in cells expressing cGASΔN (Figure 2.4G). Expression of the ISG *RSAD2* correlated with IFNβ expression, although with delayed kinetics (Figure 2.4G). This increase in IFN and ISG expression was not observed in cells expressing cGASΔN C396/397A (Figure 2.4G), an observation that further implicates endogenous DNA detection as the cause of this response. Cells expressing WT cGAS also induced an IFN and ISG response to PMA treatment (Figure 2.4G), but this response was not evident for several hours and the extent of IFN and ISG induction was lower than observed in cells expressing cGASΔN.

As observed with doxorubicin treatment, overnight stimulation demonstrated specific toxicity of PMA in cells expressing cGASΔN (Figure 2.4H and S3B). Whereas all other transgenic cell populations attached to the tissue culture plate upon PMA treatment, cells expressing cGASΔN remained unattached and only 10.82% of cells remained viable (Figure 2.4H and S3B). Cells expressing WT cGAS or cGASΔN C396/397A did not display these phenotypes (Figure 2.4H and S3B). These data support the idea that mislocalized cGAS cannot avoid detection of self-DNA and triggers unusually high IFN responses that correlate with loss of viability upon genotoxic stress.

The above findings suggest that cGAS localization to the plasma membrane is necessary to prevent self-DNA detection. However, these findings could also be explained if the N-terminal domain of cGAS operated as an intrinsic inhibitor of catalytic activity. If this alternative explanation were correct, then any DNA stimulus should induce a more robust response from cells expressing cGASΔN than those expressing WT cGAS. This possibility was examined by infecting cells with Modified Vaccinia Ankara (MVA), an attenuated DNA virus that stimulates cGAS-dependent IFN responses[147].

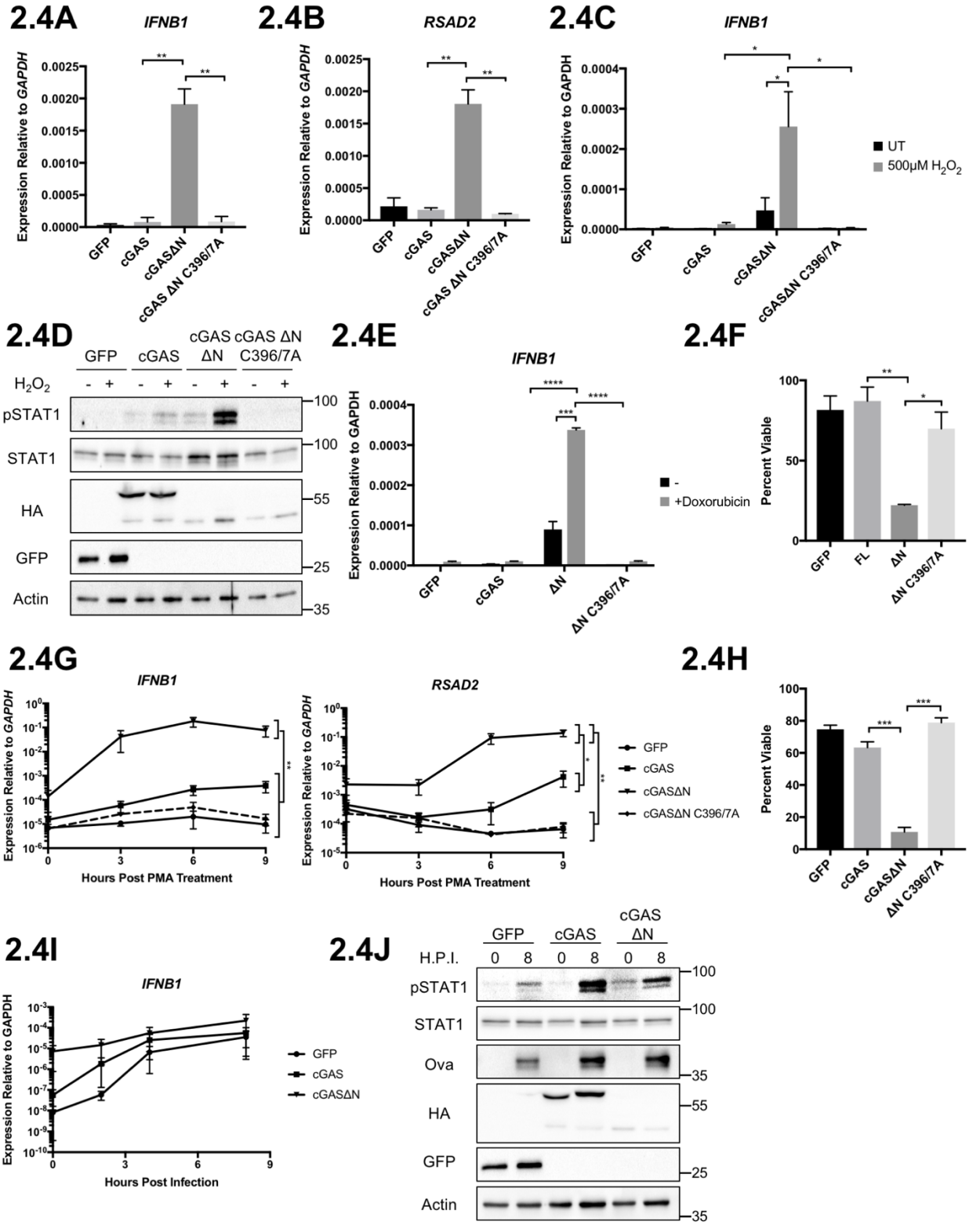
2.4A
IFNB1
Expression Relative to GAPDH
GFP
cGAS
cGASΔN
cGAS ΔN C396/7A
2.4B
RSAD2
2.4C
IFNB1
UT
500μM H2O2
2.4D
GFP
cGAS
cGAS ΔN
cGAS ΔN C396/7A
H2O2
pSTAT1
STAT1
HA
GFP
Actin
2.4E
IFNB1
-
+Doxorubicin
ΔN
ΔN C396/7A
2.4F
Percent Viable
FL
2.4G
IFNB1
RSAD2
Hours Post PMA Treatment
2.4H
2.4I
Hours Post Infection
2.4J
H.P.I.
Ova

Figure 2.4: Loss of the cGAS N-Terminus leads to heightened basal IFN signaling and increased responses to genotoxic stress.

2.4A) qRT-qPCR analysis of *IFNβ1* expression in THP1 cell lines at steady-state. **2.4B)** qRT-qPCR analysis of *RSAD2* expression in THP1 cell lines at steady-state. **2.4C)** qRT-qPCR analysis of *IFNβ1* expression following a 6-hour treatment with 500μM H_2O_2 in the indicated THP1 cell lines. **2.4D)** Western blot analysis for the indicated proteins before and after 6-hour treatment with 500μM H_2O_2. **2.4E)** qRT-qPCR analysis of *IFNβ1* expression following a 14-hour treatment with 500nM Doxorubicin in the indicated THP1 cell lines. **2.4F)** Viability of THP1 cell lines following a 14-hour treatment with 500nM Doxorubicin, shown as a percentage of untreated controls, as measured by intracellular ATP content. **2.4G)** qRT-qPCR analysis of *IFNβ1* and *RSAD2* expression at the indicated time points following treatment with 50ng/mL PMA in the indicated THP1 cell lines. **2.4H)** Viability of THP1 cell lines following overnight treatment with 50ng/mL PMA, as described in 4F. **2.4I)** qRT-qPCR analysis of *IFNβ1* expression at the indicated time points following infection with MVA-Ova (MOI 3) in the indicated THP1 cell lines. **2.4J)** Western blot analysis of the indicated proteins before and after infection with MVA-Ova (MOI 3) in the indicated cell lines. H.P.I. (Hours Post Infection). Experiments shown are representative of or averages of n=3 biological replicates. Data is shown as a mean ± SEM. Statistical analysis comparing two data points was preformed using a student's T test and statistical analysis of time course experiment trends (4H and 4J) were preformed using Two-Way ANOVA with asterisk coding as follows: * p<= 0.05; ** p<=0.01; *** p<=0.001; **** p<=0.0001.

We infected THP1 cells with an MVA strain expressing an Ovalbumin (Ova) transgene, which we utilized as a reporter for the establishment of infection[148]. Upon MVA infection, cells expressing GFP or WT cGAS upregulated *IFNβ1* expression (Figure 2.4I). This increase in *IFNβ1* expression correlated with increases in the intracellular abundance of phospho-STAT1 (Figure 2.4J). However, cGASΔN-expressing cells were less responsive to MVA infection. Whereas MVA induced a multi-log increase in *IFNβ1* transcripts in cells expressing GFP or WT cGAS, only a log fold-change was observed in cells expressing cGASΔN over 8 hours (Figure 2.4I). Additionally, STAT1 phosphorylation was less robust in cGASΔN expressing cells, as compared to cells expressing WT cGAS (Figure 2.4J). Expression of the virus-encoded Ova transgene was observed across all cells examined (Figure 2.4J).

The mislocalized cGASΔN allele is therefore potently responsive to cell intrinsic DNA ligands, as compared to the WT allele, yet a similar hyper-responsiveness is not observed with stimulation by foreign DNA through MVA infection. The differential sensitivity of mislocalized cGASΔN to genotoxic stresses and viral infections rules out the possibility that the N-terminus serves as an intrinsic catalytic inhibitor. Rather, these findings demonstrate the importance of plasma membrane localization via $PI(4,5)P_2$ for cGAS activities.

2.4.5 Molecular basis for cGAS interactions with $PI(4,5)P_2$.

As $PI(4,5)P_2$ is the first lipid identified to interact with cGAS, additional mechanistic insight into this interaction was of interest. As $PI(4,5)P_2$ binding correlates with membrane localization, deletion analysis was performed within the cGAS N-terminus to identify a minimal region necessary for plasma membrane association (Figure 2.5A). This analysis identified amino acids 64 to 75 as necessary for plasma membrane localization (Figure 2.5A). Within this region are two arginine residues that are conserved or charge-conserved between humans, mice and several other mammalian species (Figure 2.5A). As phosphoinositide interactions are often electrostatic, these residues were of interest. We mutated both arginine residues to glutamic acid in the context

of the full length human cGAS protein (cGAS R71/75E) and examined its ability to localize in cells, induce IFN responses, and bind $PI(4,5)P_2$.

We found that the recombinant cGAS R71/75E protein was completely defective for $PI(4,5)P_2$ interactions *in vitro*, thus indicating an essential role of the mutated amino acids in protein-lipid interactions (Figure 2.5B). Notably, this protein was difficult to produce in 293T cells, as compared to its WT counterpart (Figure 2.5C). Despite the low abundance of cGAS R71/75E, expression of this gene drove IFN stimulatory response element (ISRE) reporter activation to levels comparable to WT cGAS (Figure 2.5D). The high signaling activity of low amounts of cGAS R71/75E is consistent with the idea that $PI(4,5)P_2$ interactions prevent access of cGAS to cytosolic DNA. Direct evidence in support of this model was provided when we generated a point mutant deficient for plasma membrane association and DNA binding (cGAS R71/75E C396/7A). This mutant was unable to induce ISRE responses upon expression in 293T cells and was produced at high abundance (Figure 2.5C and 2.5D). Similar protein stability trends were observed in primary cells, as transduction of murine marrow with cGAS R71/75E did not yield any detectable protein after a week of macrophage differentiation, but parallel transductions demonstrated the robust expression of the DNA binding deficient cGAS R71/75E C396/7A allele (Figure 2.5C). This mutant did not associate with the plasma membrane upon stable expression in primary BMDMs, THP1 cells, and L929 cells and upon transient transfection of Hela cells (Figure 2.5E). Thus, amino acids 71 and 75 are critical for cGAS interactions with $PI(4,5)P_2$ and are consequently critical for plasma membrane localization within cells. Interfering with these interactions, either by deletion or amino acid substitution, renders cGAS responsive to cytosolic DNA, even when produced at very low levels.

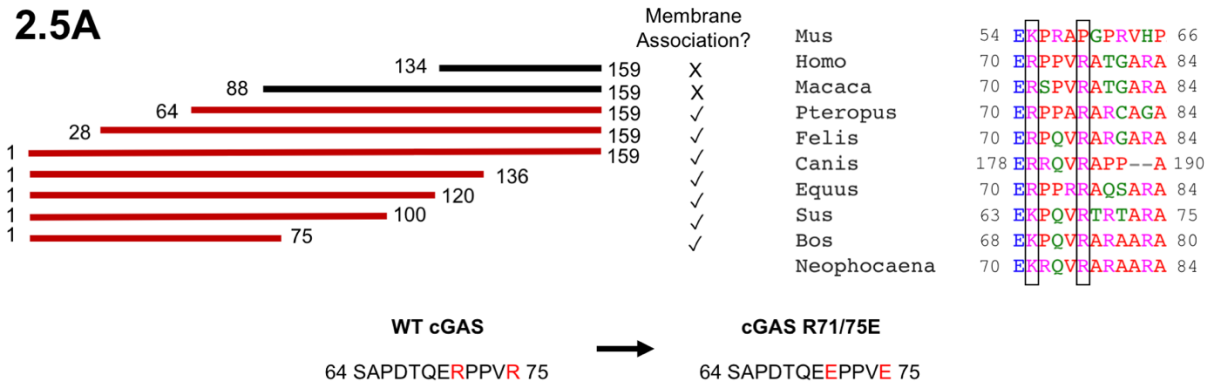

WT cGAS

64 SAPDTQERPPVR 75

cGAS R71/75E

64 SAPDTQEEPPVE 75

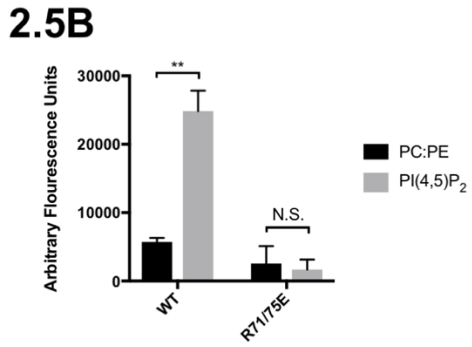

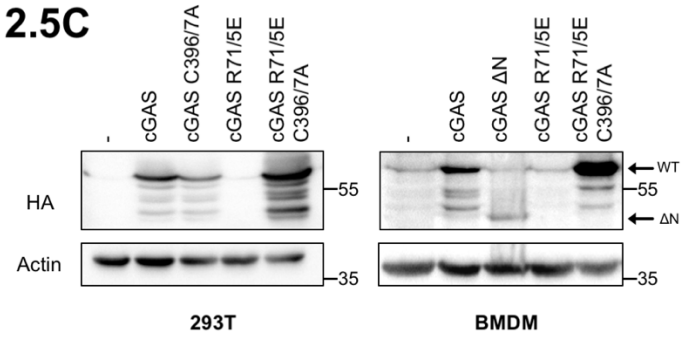

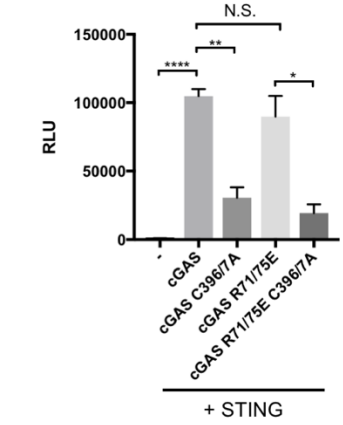

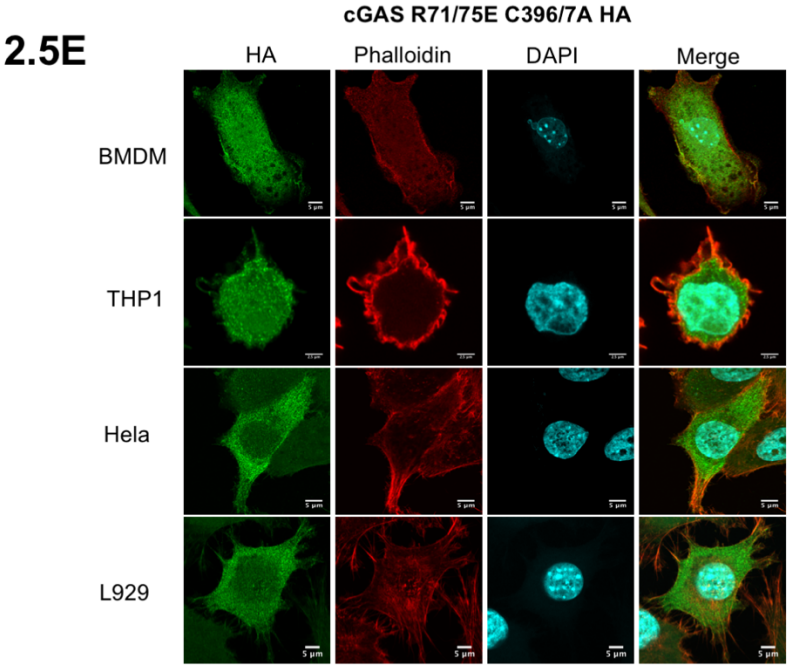

Figure 2.5: The cGAS R71/75E mutant does not bind PI(4,5)P_2 and does not associate with the plasma membrane.

2.5A) *Left*: Schematic of truncation mutants screened in the cGAS N-terminus in Hela cells and their ability to associate with the plasma membrane. *Bottom center:* Residues identified as essential for cGAS membrane association with mutated residues indicated in red and the indicated point mutations. *Right:* Alignment of mutated residues in several species (same as 2H) with R71 and R75 boxed. **2.5B)** Fluorescent liposome pulldown assay with the indicated mutants, as described in 3C. **2.5C)** Western blot analysis of expression of indicated cGAS mutants in transiently transfected 293T cells and BMDMs stably expressing mutants via lentiviral transduction. **2.5D)** ISRE luciferase assay of 293Ts expressing the indicated constructs 24 hours post transfection. – indicates cells transfected with the ISRE reporter construct alone. All cGAS constructs were co-transfected with STING to enable pathway signaling. **2.5E)** Confocal micrographs of indicated cell lines expressing cGAS R71/75E C396/7A. Experiments shown are representative of or averages of n=3 biological replicates. Data is shown as a mean ± SEM, and statistical analysis was preformed using a student's T test with asterisk coding as follows: * p<= 0.05; ** p<=0.01; *** p<=0.001; **** p<=0.0001.

Thus far, all experiments indicate that cGAS interactions with $PI(4,5)P_2$ are necessary for localization and function. To determine if these interactions are sufficient for plasma membrane localization and prevention of self-DNA recognition, we replaced the N-terminus of cGAS with a heterologous PIP binding domain from the TLR adaptor TIRAP (TIRAP-ΔN; Figure 2.6A). Like the cGAS N-terminus, this domain directs TIRAP to the plasma membrane via interactions with $PI(4,5)P_2$. We generated stable THP1 lines expressing this cDNA as well as WT cGAS, cGASΔN or cGASΔN C396/7A (Figure 2.6B). The TIRAP localization domain was sufficient to direct cGASΔN to the plasma membrane (Figure 2.6C). Functionally, the TIRAP localization domain reversed the basal IFN expression and the lethal PMA-induced IFN responses associated with cGASΔN in THP1 cells (Figure 2.6D and 2.6E). Resting cells expressing cGASΔN displayed high basal IFNβ and ISG expression, as compared to cells expressing TIRAP-ΔN or WT cGAS (Figure 2.6D). Moreover, whereas cGASΔN responded to PMA by producing copious amounts of IFNβ transcripts and subsequently dying, cells expressing TIRAP-ΔN or WT cGAS did not induce such responses (Figure 2.6D and 2.6E).

While these experiments demonstrate that $PI(4,5)P_2$ binding is sufficient to prevent aberrant cGASΔN activation, they do not determine if this interaction allows for cGASΔN activation in contexts that activate WT cGAS. To test if $PI(4,5)P_2$ binding is both necessary and sufficient for cGAS activation, we generated a second cGASΔN fusion protein, Fyn-ΔN, which contains the N-terminal dual acylation sequence of the kinase Fyn (Figure 2.6F). This lipidation motif anchors cGAS in the plasma membrane and prevents cGAS movement from this membrane (Figure 2.6F). Like TIRAP-ΔN, this protein localized to the plasma membrane of THP1 cells (Figure 2.6G). Once this activity was confirmed, we transfected both of these mutants into 293T cells along with plasmids encoding STING and the ISRE reporter (Figure 2.6H and 2.6I). While TIRAP-ΔN stimulated ISRE reporter activity to similar levels as WT cGAS, reporter activity in cells expressing Fyn-ΔN was significantly dampened (Figure 2.6H). Despite these differences in activation, these constructs were expressed at comparable levels (Figure 2.6I).

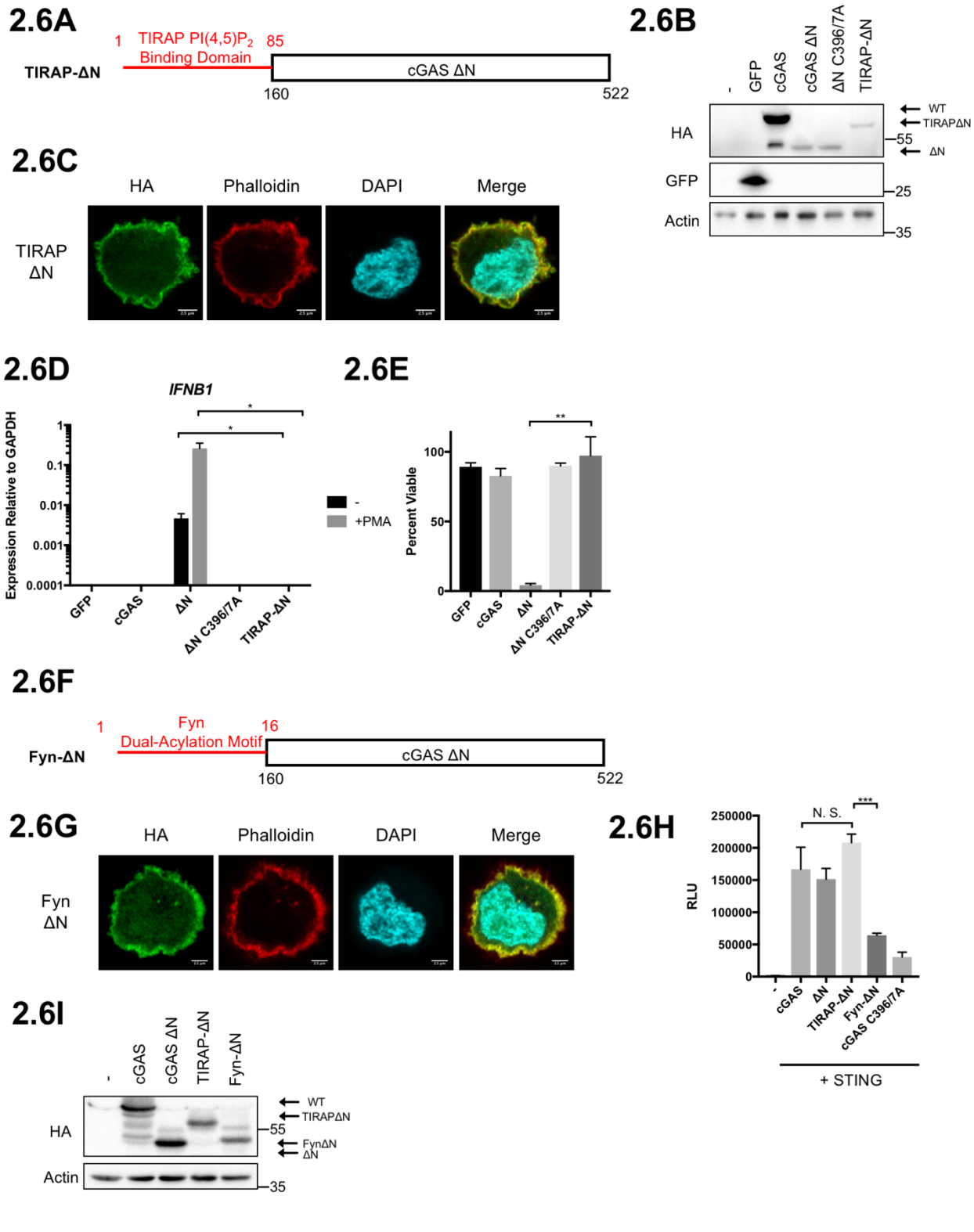
2.6A
TIRAP-ΔN
1
TIRAP PI(4,5)P2
Binding Domain
85
cGAS ΔN
160
522
2.6B
-
GFP
cGAS
cGAS ΔN
ΔN C396/7A
TIRAP-ΔN
HA
GFP
Actin
WT
TIRAPΔN
ΔN
55
25
35
2.6C
HA
Phalloidin
DAPI
Merge
TIRAP ΔN
2.6D
IFNB1
Expression Relative to GAPDH
1
0.1
0.01
0.001
0.0001
*
*
GFP
cGAS
ΔN
ΔN C396/7A
TIRAP-ΔN
-
+PMA
2.6E
Percent Viable
100
50
0
**
GFP
cGAS
ΔN
ΔN C396/7A
TIRAP-ΔN
2.6F
Fyn-ΔN
1
Fyn
Dual-Acylation Motif
16
cGAS ΔN
160
522
2.6G
HA
Phalloidin
DAPI
Merge
Fyn ΔN
2.6H
RLU
250000
200000
150000
100000
50000
0
N. S.
***
-
cGAS
ΔN
TIRAP-ΔN
Fyn-ΔN
cGAS C396/7A
+ STING
2.6I
-
cGAS
cGAS ΔN
TIRAP-ΔN
Fyn-ΔN
HA
Actin
WT
TIRAPΔN
FynΔN
ΔN
55
35

Figure 2.6: Artificial localization of cGASΔN to the plasma membrane through the TIRAP PI(4,5)P_2 binding domain rescues localization and prevents hyper responsiveness to genotoxic stress.

2.6A) Schematic of the synthetic TIRAP PI(4,5)P_2 binding domain fused to cGASΔN. **2.6B)** Western blot analysis of THP1 cells stably expressing the indicated mutants. **2.6C)** Confocal micrograph of THP1 cells stably expressing TIRAP-ΔN-HA. **2.6D)** qRT-qPCR analysis of *IFNβ1* expression 3 hours post treatment with 50ng/mL PMA in the indicated THP1 cell lines. **2.6E)** Viability of THP1 cell lines following overnight treatment with 50ng/mL PMA, shown as a percentage of untreated controls, as measured by intracellular ATP content. **2.6F)** Schematic of the synthetic Fyn myristoylation motif fused to cGASΔN. **2.6G)** Confocal micrograph of THP1 cells stably expressing Fyn-ΔN-HA. **2.6H)** ISRE luciferase assay of 293Ts expressing the indicated constructs 24 hours post transfection, as described in 5D. **2.6 I)** Western blot analysis of 293T cells expressing indicated constructs. Experiments shown are representative of or averages of n=3 biological replicates. Data is shown as a mean ± SEM, and statistical analysis was preformed using a student's T test with asterisk coding as follows: * p<= 0.05; ** p<=0.01; *** p<=0.001; **** p<=0.0001.

2.5 Discussion

The importance of localization for proteins lacking transmembrane domains is often overlooked, and it is generally assumed that innate immune regulators lacking such domains must operate as cytosolic proteins. In this study, we tested the predictions of this model through a detailed analysis of the subcellular positioning and functions of cGAS. Several lines of evidence support the conclusion that cGAS is not a cytosolic protein but is rather a plasma membrane protein whose localization is mediated by $PI(4,5)P_2$. First, subcellular fractionation of endogenous cGAS reveals that a majority of cGAS cofractionates with membranes through both sedimentation and floatation, while being present at low levels in the nucleus and absent from the cytosol. Second, confocal microscopy of endogenous and tagged cGAS show that it is concentrated at the plasma membrane of human and murine monocytes and macrophages. Third, using multiple independent assays for protein-lipid interactions, cGAS interacts with acidic PIPs and selectively binds $PI(4,5)P_2$. Finally, subcellular localization and the $PI(4,5)P_2$ binding activity of cGAS map to the same amino acids in the N-terminus of this protein, providing a mechanism to explain how cGAS can be positioned at the plasma membrane of resting cells. cGAS must therefore be considered a plasma membrane protein, whose localization is dictated by protein-lipid interactions.

Although we found cGAS located primarily at the plasma membrane, we also observed a pool of nuclear cGAS biochemically and microscopically. While the mechanisms of nuclear localization are unclear, some technical considerations must be made. First, our use of benzonase in fractionations was critical to prevent post-lysis DNA binding, which could drive cGAS oligomerization into nucleus-sized aggregates[129]. Second, microscopic detection of lipid-binding proteins is sensitive to methods of cell fixation. For example, paraformaldehydes immobilize lipid-binding proteins within cells, whereas methanol fixatives extract lipids and their associated proteins. These latter conditions may exaggerate the appearance of selective pools of intracellular cGAS. With these statements made, we do not consider cGAS to be absent from

the nucleus, but rather consider the plasma membrane to be the most common site of its residence in phagocytes. While we found that the frequency of nuclear- or plasma membrane-localized cGAS varied among cell types, the cGAS N terminus localizes to the plasma membrane regardless of cell type. These findings suggest this association is a fundamental feature of the N terminus that is actively modulated by cells and is dependent on cGAS activity. We suggest that cGAS localization may emerge as a mechanism of regulation that varies in a context-dependent manner.

While our analysis identified the N-terminus of cGAS as the domain responsible for lipid binding and localization, this domain also facilitates DNA binding and assembly of cGAS into liquid droplets[129]. DNA binding and liquid droplet formation are cornerstone features of active cGAS, whereas $PI(4,5)P_2$ binding and plasma membrane localization are activities consistent with inactive cGAS. Based on this collection of data, we propose a unifying model whereby the cGAS N-terminus serves distinct functions in its resting and active states. In resting cells, the N-terminus positions cGAS at the cell surface, where it is least likely to detect self-DNA and prevent aberrant activation. Upon DNA detection, the N-terminus may release from $PI(4,5)P_2$ and facilitate liquid droplet formation and signaling. Consistent with this idea is our finding that DNA transfection results in the movement of cGAS from the cell surface to cytosolic foci, and that restricting cGAS release from the plasma membrane prevents signal transduction.

Our phylogenetic analysis revealed that the high pI of the cGAS N terminus relative to its C terminus is conserved across several species. These features indicate that the strong positive charge of the N-terminus is conserved across species and that its electrostatic interactions with PIPs may be conserved as well. In further support of this concept, we determined that the two residues essential for cGAS interaction with $PI(4,5)P_2$ and membrane localization (R71/R75) were conserved or charge-conserved across these species. We therefore suggest plasma membrane localization of cGAS is a fundamental and evolutionarily conserved feature of this PRR.

To date, access to DNA ligands has been the focal point of discussions surrounding the ability of cGAS to maintain the balance of self-nonself discrimination[137,149,150]. The cytosol of mammalian cells should be DNA-free, with genomic DNA and mitochondria DNA confined to distinct subcellular sites. Any DNA released into the cytosol is hydrolyzed by well-defined nucleases, and genetic defects in these nucleases lead to cGAS-dependent pathologies[151]. Thus, current models predict that the sole mechanism of preventing inappropriate cGAS activation is by restricting access of DNA to the cytosol. It is with this model in mind that our findings may be most notable, as we can now propose that DNA is not only hidden from cGAS, but cGAS via membrane localization is also hidden from mislocalized DNA that escapes nuclease-mediated hydrolysis.

By positioning cGAS at the cell periphery, the most distal site from the nucleus in the cell, this PRR may be localized to a site that is free of DNA entirely. Under such a model, we speculate that mislocalized cGAS is no longer geographically restricted from DNA that leaks from the nucleus. Thus, mislocalized cGAS is prone to induce IFN responses in the absence of infection or major genomic damage. Why mislocalized cGAS did not induce similarly potent IFN responses to viral DNA is also worth considering. Positioning at the plasma membrane places cGAS at and near portals of pathogen entry, which may enable it to sense foreign DNA as it enters the cell. Alternatively, the defect in virus detection by cGASΔN may not be linked directly with its inability to localize properly, but instead may be related to its inefficient ability to assemble into liquid droplets upon DNA binding[129]. While future work is necessary to dissect the relative activities present in the cGAS N-terminus, our functional studies with TIRAP-ΔN and Fyn-ΔN suggest that $PI(4,5)P_2$ binding is an activity necessary for cGAS function.

Finally, the similarities in subcellular positioning of TLR adaptors and cGAS suggest an evolutionary theme may have been uncovered by our study. The use of PIP binding domains to position a sensor of viral infection (cGAS) and sensors of activated TLRs (TIRAP, TRAM and dMyD88) raises the possibility that other innate immune pathways may use similar strategies to ensure signaling fidelity. This study provides a mandate to explore this possibility, as well as the

localization of other seemingly cytosolic PRRs that may operate by principles similar to those described for cGAS.

Chapter 3: RIG-I

Characterization of RIG-I Interactions

with Phosphatidylinositol-3,5-Bisphosphate

3.1 Abstract

RIG-I is a germline-encoded helicase that serves as a major sensor of viral RNA (vRNA) in the host cell cytosol, activating proinflammatory cytokine and IFN production in the presence of its ligands. Little is known about specific positioning of RIG-I within the intracellular space, though specific positioning of this receptor could maximize its ability to sense vRNA as it enters the cell. Here, we observe RIG-I in the membrane fraction of several cell lines and present evidence that RIG-I specifically interacts with the membrane lipid $PI(3,5)P_2$ *in vitro*. Further investigation of this interaction demonstrated that $PI(3,5)P_2$ inhibits RIG-I interactions with RNA ligands in a competitive manner and that $PI(3,5)P_2$ selectively inhibits ATP hydrolysis by RIG-I in a ligand-dependent manner. These data suggest that $PI(3,5)P_2$ may not only play a role in positioning RIG-I within the cells but also influence which ligands RIG-I interacts with in a productive manner, providing a directive to research these interactions further *in vitro* and *in vivo*.

3.2 Introduction

RNA viruses are the causative agents of many significant public health threats, including Influenza A Virus, Dengue Virus, and Respiratory Syncytial Virus[152]. While pathological effects of these viruses vary greatly, their genomes are based in RNA and replicate through dsRNA intermediates[152]. dsRNA molecules produced by these infections are detected by the protein RIG-I to induce an inflammatory response[9,13]. This innate immune sensor induces an antiviral defense program and initiates inflammation upon binding vRNA, which is essential for the activation of the adaptive immune system and often host survival.

RIG-I is a PRR that recognizes vRNA to activate an immune response through an interaction with the transmembrane protein MAVS[6]. As vRNA is similar to host RNA, RIG-I specifically recognizes a 5' di- or tri-phosphate (5'PPP; 5'PP) motif through its C-Terminal Domain (CTD)[14,127,153]. Furthermore, the helicase domain of RIG-I specifically recognizes RNA ligands with some amount of double stranded character[6,153,154], a motif not commonly present in the mammalian cell. Specificity for these motifs allows for efficient self-nonself discrimination, despite sensing a nucleic acid commonly found in the host cell. Upon ligand recognition, RIG-I releases from an auto-inhibitory conformation, oligomerizes, and acquires K63-linked ubiquitin chains through the activity of the E3 ubiquitin ligase Riplet[16-19]. These activities allow the CARD domains of RIG-I to interact with the CARD domain of MAVS, a resident protein of the mitochondria, peroxisomes, and MAM of the ER[20-25]. This CARD-CARD interaction aggregates MAVS within its resident membrane[26]. This prion-like aggregate serves as SMOC to activate IRF3, NF-κB, and AP-1 and promote production of antiviral interferons and proinflammatory cytokines[13]. The activities of these molecules allow for the recruitment of immune cells to the site of infection and the upregulation of ISGs, which have specific activities for fighting viral infection within the infected cell and its neighbors[155].

Effective blockade of viral infection relies upon rapid recognition of the infection, as recognition triggers the immune response. Therefore, a lack of or delay in recognition provides

the virus with a clear replicative advantage, as the virus is free to generate progeny and spread without restriction by the host cell. RIG-I serves as the key sensor for several viral infections, yet its expression prior to activation is low, once estimated at 15 molecules per cell[126]. Despite this, RIG-I remains an effective PRR for vRNA and efficiently recognizes its ligand with as low as an estimated 20 molecules of 5'PPP RNA present in the cell[126]. This efficacy of detection is unexpected, given the nanomolar affinity of RIG-I for its 5'PPP RNA[156], and suggests that diffusion alone does not account for the mechanism of RIG-I interactions with vRNA.

Therefore, we propose that RIG-I does not rely only on diffusion for interacting with viral RNA and is instead poised through positioning on a cellular membrane to interact with vRNA. A potential site of RIG-I localization must be common to all viral life cycles to be efficacious. As all viruses must breach a host cell membrane to expose its genome to the cytoplasm and begin replication, an ideal site of RIG-I localization may be at these portals of entry, such as the acidified endosome[152]. Furthermore, positioning at the site of viral entry would allow RIG-I to sense viral infection at its absolute earliest step of replication, entry, and provide the host cell with an advantage to suppress the infection in its most nascent stage.

In the experiments detailed below, we demonstrate that RIG-I is capable of interacting with membrane component lipids *in vitro* and fractionates with cellular membranes in several cell types. *In vitro*, RIG-I selectively interacts with $PI(3,5)P_2$, a PIP found on the membranes of late endosomes, in a manner that is competitive with 5'PPP RNA and inhibits the ATPase activity of RIG-I. Together, these data suggest that RIG-I is specifically positioned at sites of viral entry and warrant further investigation into the localization of this critical PRR.

3.3 Materials and Methods

3.3.1 Cell Lines

All cell lines were maintained at 37°C in 5% CO_2 in DMEM supplemented with 10% FBS, Penicillin/Streptomycin (Pen+Strep), L-glutamine, and sodium pyruvate, referred to as complete DMEM. For passage, immortalized mouse embryonic fibroblasts (MEFs) and the human hepatocellular carcinoma cell line Huh7 were lifted using 0.25% Trypsin and split 1:10 every 2-3 days, while immortalized bone marrow derived macrophages (iBMDMs) were lifted with 2.5mM EDTA in PBS and split 1:10 every 2-3 days.

To generate lentiviral particles for the stable expression of transgenes, HEK293T cells were transfected with the packaging plasmids psPAX2 and pCMV-VSV-G along with the transgene in pRRL-PGK-GFP-WPRE. All truncation mutant genes of interest were subcloned into the GFP site. Plasmids were transfected into 10cm^2 dishes of HEK293Ts at 50%-80% confluency using polyethyleneimine (PEI) at a ratio of 3:1 PEI:DNA. 16 hours after transfection the media was changed, and virus-containing supernatants were harvested 24 hours following the media change. Viral supernatants were passed through a 0.45μm filter to remove cellular debris. Filtered viral supernatants were placed onto target cells for 24 hours and then replaced with the appropriate complete media. Transgene expression was assessed by western analysis.

3.3.2 Subcellular Fractionation

For subcellular fractionation through sedimentation, 2x10^7 cells were isolated through trypsinization and then washed with PBS. Cells were washed once with and then incubated in hypotonic buffer (10mM Tris pH 7.4, 10mM KCl, 1.5mM $MgCl_2$) with protease inhibitors (Roche) and Dounce homogenized. Following homogenization, nuclei were pelleted through centrifugation for 5 minutes at 2,500xg, and the resultant supernatant was subjected to further centrifugation at 100,000xg for 1 hour. The resulting supernatant (S100; cytosolic fraction) and pellet (P100; membranous fraction) were probed by western blot.

3.3.3 Recombinant Protein Expression and Purification

Recombinant RIG-I was produced as described previously[17]. Briefly, following induction with 0.5mM IPTG, NusA-6x-His tagged RIG-I was expressed in *E. coli* at 20°C overnight. Following expression, the cells were lysed, and recombinant RIG-I was purified from the resultant lysates through a combination of nickel affinity chromatography, heparin affinity chromatography, and size exclusion chromatography. In some instances, the NusA-6xHis tag was cleaved using the Human Rhinovirus C3 protease (Thermo) following nickel affinity purification, and in others, the tag was left on the protein for use in *in vitro* assays that are described below.

3.3.4 PIP Strip Lipid Binding Assay

Lipid binding assays were performed as described[69]. Briefly, PIP strips (Echelon) were blocked in (10mM Tris pH 8; 150mM NaCl; 0.1% Tween-20; 0.1% ovalbumin) for 1 hour, then incubated for 2 hours with purified RIG-I (500ng/mL) in the presence of an anti-RIG-I antibody (Cell Signaling) in blocking buffer, washed 3 times with blocking buffer, and then probed with an HRP-conjugated secondary antibody in blocking buffer for 30 minutes. Lipid bound protein was detected using enhanced chemiluminescence.

3.3.5 Liposome Preparation and Assays

Liposome preparation and subsequent binding assays were performed as previously described[69]. In brief, PC:PE (Avanti) were mixed at a 3:1 ratio in a solution of 2:1 chloroform:methanol in borosilicate glass tubes and gently dried into a lipid film using inert nitrogen gas. For liposomes containing PIPs, the 3:1 PC:PE ratio was maintained with the addition of the specified percentage of PIP (Echelon). Dried lipids were resuspended in 300mM sucrose and vortexed aggressively to yield liposomes at a final concentration of 1µg/µL.

For sedimentation assays, 20µg of liposomes were incubated with 5µg of recombinant RIG-I in a cytosol buffer (25mM HEPES pH 7.2; 25mM KCl; 2.5mM Magnesium Acetate; 150mM Potassium Glutamate) for 15 minutes at 37°C. Following incubation, samples were centrifuged at 100,000xg, and the pellets were analyzed by western blot for RIG-I binding.

3.3.6 RNA Synthesis and RNA Binding Assays

5'PPP RNA was synthesized using the MEGAshortscript™ T7 transcription kit (Invitrogen) from a 114bp template. To generate fluorescent RNA ligands to measure RIG-I: RNA interactions, Flourescein-12-UTP (Sigma) was included in the reaction. In addition to the 114bp construct, a 19bp dsRNA was purchased from Invivogen for use in ATPase assays.

To measure RIG-I interactions with RNA ligands, 6xHis-RIG-I (100nM) was incubated with a fluorescent RNA ligand (250nM) with or without liposomes (25µg, ~100µM) in cytosol buffer and incubated at 37°C for 30 minutes. Following this incubation, RIG-I and any bound RNA was pulled down using Nickel Agarose resin (Qiagen), eluted using 3M Imidazole, and the resultant RNA fluorescence intensity was measured by plate reader.

3.3.7 ATPase Assay

To measure the ATPase activity of RIG-I under various conditions *in vitro*, inorganic phosphate (P_i) production, as a result of ATP cleavage, was measured using the PiColorLock™ Gold Colorimetric Assay Kit (Novus Biologicals). In brief, recombinant 10nM RIG-I was incubated with 250nM RNA (or indicated concentration), 10µg liposomes containing 2% of the specified PIP, and 10mM ATP for 5 minutes at 37ºC. The reaction was quenched with 50mM EDTA, and PiColorLock™ reagent mix was added at a ratio of 1:4 (detection mix: reaction mix) and incubated for 30 minutes at RT to develop the colorimetric readout. Following this incubation, absorbance at 635nm was read on a Tecan plate reader. To ensure fidelity of the reactions, single component mixtures (i.e. RIG-I alone, RNA alone, etc.) and non-reactive mixtures (i.e. RIG-I+ATP without RNA or RIG-I+RNA without ATP) were used as negative controls and run alongside a phosphate standard curve.

3.4 Results

3.4.1 RIG-I Fractionates with Cell Membranes

To pinpoint the site of RIG-I residence in the absence of stimuli, we first isolated total membranes from the soluble, cytosolic portion of cells through subcellular fractionation. In brief, we subjected Dounce homogenized cells to low speed centrifugation to pellet nuclei, and then further subjected the resultant supernatant to centrifugation at 100,000xg. The resultant supernatant is considered the soluble, cytosolic fraction (S100), and the resultant pellet contains all cellular membranes (P100). These fractions were assessed for the presence of RIG-I through western blot. The quality of these fractionations was monitored through the use of Caspase-3 as a marker for the S100 fraction and Calnexin as a marker for the P100 fraction.

Upon performing these fractionations in immortalized mouse embryonic fibroblasts (iMEFs), we observed two pools of RIG-I, as it was present in both the soluble S100 fraction and the membranous P100 fraction (Figure 3.1A). This distribution was not limited to fibroblasts, as we observed a similar distribution of RIG-I residence in murine immortalized bone marrow derived macrophages (iBMDMs) (Figure 3.1A). Furthermore, a population of RIG-I sediments with cellular membranes in the human hepatocellular cell line, Huh7 (Figure 3.1A). As all of these experiments were performed in the absence of stimuli, we hypothesized that inactive RIG-I was capable of interacting with cellular membranes at steady state.

However, RIG-I is known to interact with one transmembrane protein, MAVS[20-23], though this interaction is thought to only occur when RIG-I is active and bound to RNA. To determine if RIG-I had a basal interaction with MAVS, we performed subcellular fractionation in MAVS$^{-/-}$ iBMDMs and probed for RIG-I in the S100 and P100 fractions. Even in the absence of MAVS, RIG-I was still found in the membrane fraction (Figure 3.1B). This demonstrates RIG-I sediments with cell membranes in both the presence and absence of its only known membrane-bound interacting protein. Together, these data suggest that RIG-I may associate with cell membranes through a unique interaction in the absence of activation.

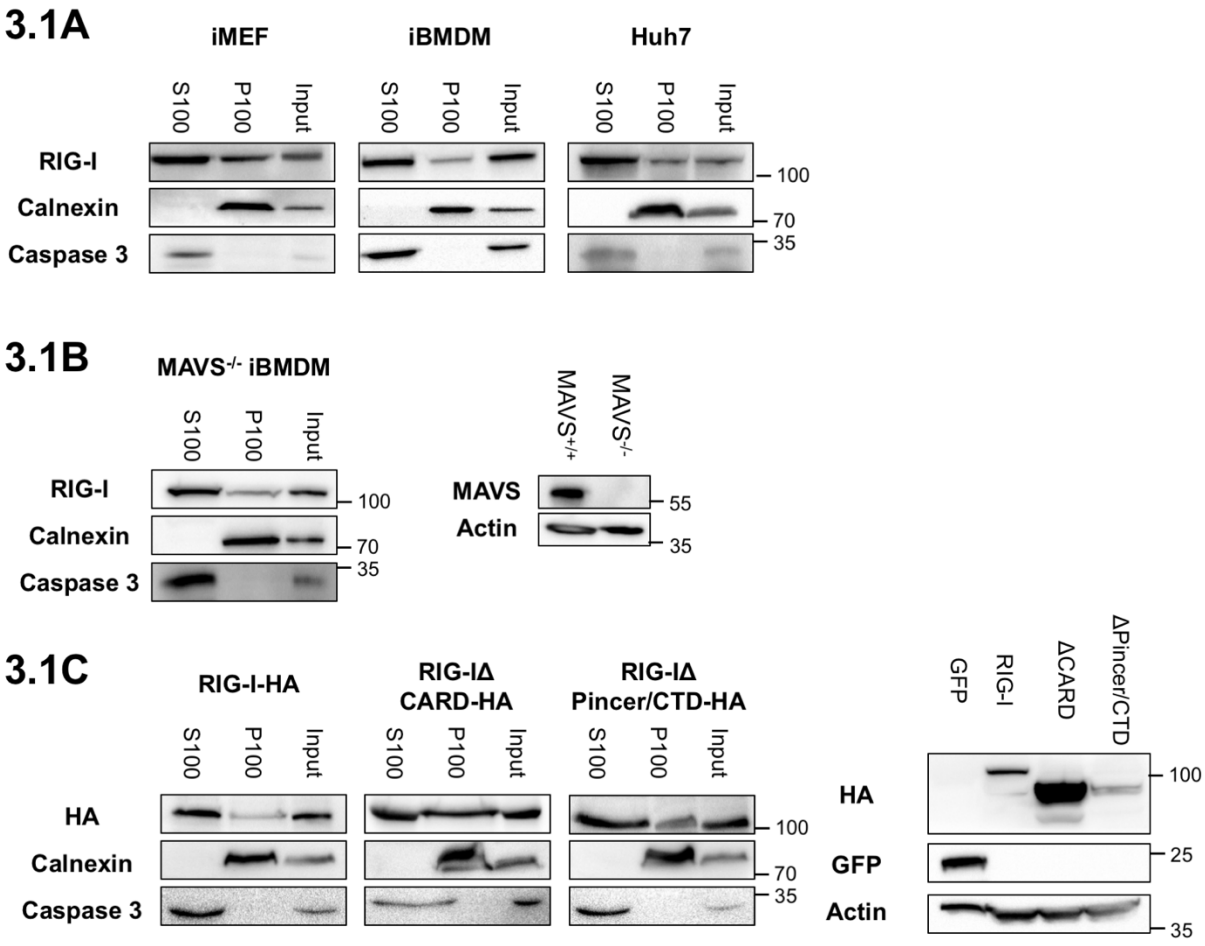

Figure 3.1: RIG-I associates with membranes in human and murine cells independently of MAVS.

3.1A) Subcellular fractionation through membrane pelleting of WT iMEFs, iBMDMs, and Huh7 cell lines. The soluble, cytosolic fraction (S100), pelleted membrane fraction (P100), and whole cell lysates (Input) were probed for the indicated proteins by western blot. **3.1B)** Subcellular fractionation of (left) and validation of (right) MAVS$^{-/-}$ iBMDMs, where the indicated fractions were probed for the indicated proteins by western blot. **3.1C)** iBMDM cell lines expressing various RIG-I truncation mutants with an HA tag were generated alongside a GFP control line (right). The cell lines expressing RIG-I truncation mutants were fractionated through membrane pelleting and probed for the indicated proteins by western blot (left). Experiments shown are representative of or averages of n=3 biological replicates.

To determine the domain(s) necessary for RIG-I sedimentation with membranes, we generated stable iBMDM cell lines expressing various RIG-I truncation mutants alongside WT RIG-I and a GFP control (Figure 3.1C). First, we generated a mutant of RIG-I lacking both of its N-terminal CARDs (RIG-IΔCARD), which are required for RIG-I signaling and activation of MAVS[13,26]. Next, we generated a second truncation mutant of RIG-I that lacked its Pincer domain and C-terminal domains (RIG-IΔPincer/CTD), which are important to stabilize the ATPase activity of its helicase domains and confer specificity 5'PPP or 5'PP RNA, respectively[157-159]. Upon subcellular fractionation of cells expressing these constructs, HA-tagged RIG-I, RIG-IΔCARD, and RIG-IΔPincer/CTD were all found in the both the P100 and S100 fractions (Figure 3.1C). This suggests that the CARDs, the Pincer domain, and the CTD are all unnecessary for the membrane association of RIG-I. Rather, these suggest that the helicase domains of RIG-I, which were present in each of these constructs, confers the membrane association activity of RIG-I.

3.4.2 RIG-I Interacts with PI(3,5)P_2 *in vitro*

RIG-I lacks transmembrane domains, which led us to consider that RIG-I may interact with cell membranes through an electrostatic interaction. Because of this hypothesis, we opted to test RIG-I interactions with PIPs, as they frequently mediate electrostatic interactions between proteins that lack transmembrane domains and specific membranes[72]. To screen for interactions between RIG-I and membrane lipids, we performed PIP strip analysis (Figure 3.2A). Through this analysis, we observed that recombinant human RIG-I interacted with several PIP species containing a phosphorylation on the 3' carbon of the PIP inositol ring, including PI(3)P, PI(3,5)P_2, and PIP_3 (Figure 3.2A). Notably, no interactions between RIG-I and other membrane component lipids, such PC or PE, were detected (Figure 3.2A). When using recombinant RIG-IΔCARD, we observed a similar pattern of PIP interactions (Figure 3.2A). Given these data, we surmised that RIG-I is capable of interacting with PIPs *in vitro* and that this interaction is not dependent on its CARDs.

3.2A

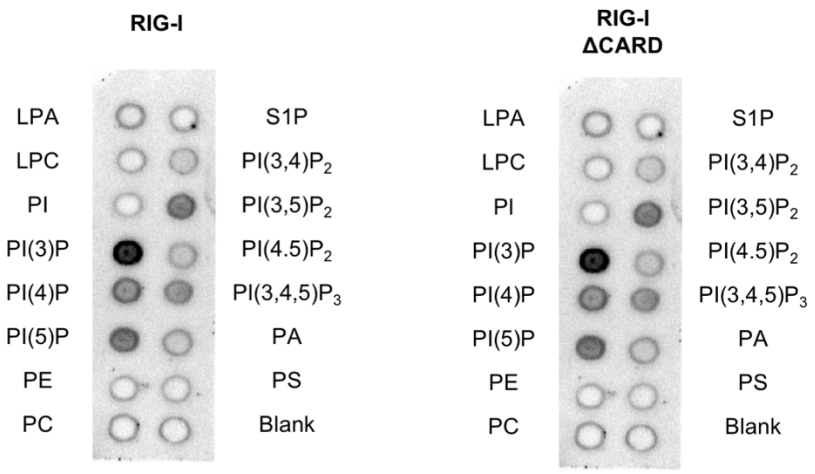

3.2B

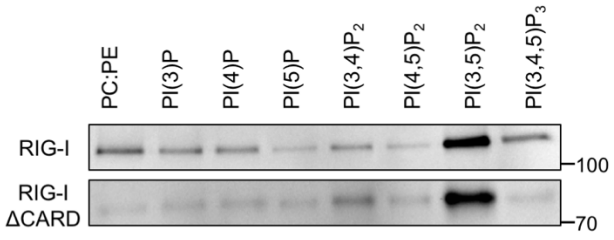

3.2C

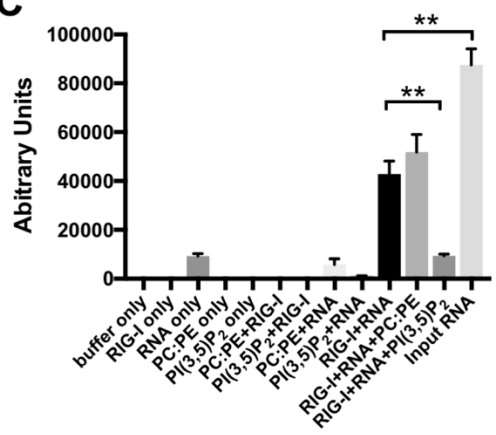

3.2D

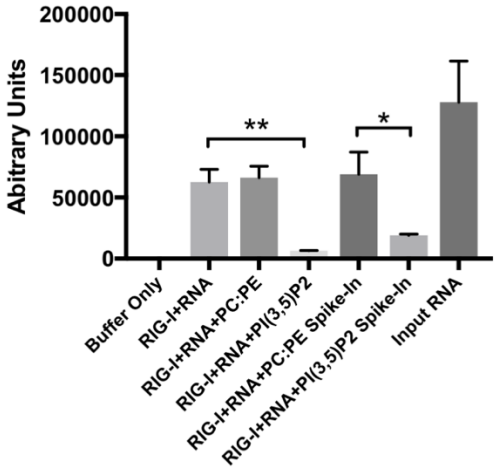

3.2E

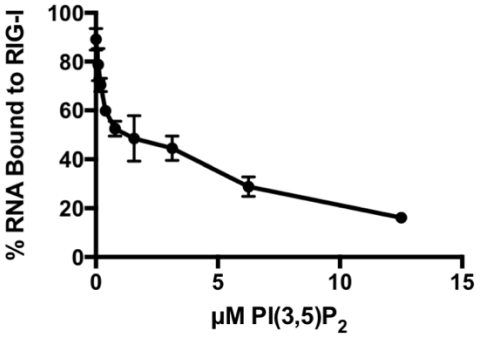

Figure 3.2: RIG-I interacts with PI(3,5)P_2, and PI(3,5)P_2 competes with 5'PPP RNA for RIG-I binding.

3.2A) PIP strip analysis of recombinant RIG-I and recombinant RIG-IΔCARD. Recombinant protein was incubated with membranes spotted with the indicated lipid species. RIG-I lipid interactions were detected with primary and secondary antibodies through enhanced chemiluminescence. **3.2B)** Cosedimentation assay for RIG-I or RIG-IΔCARD interactions with liposomes containing 18% of the specified PIPs on a 3:1 PC:PE backbone. Recombinant RIG-I or RIG-IΔCARD was incubated with liposomes, after which the liposomes were isolated by ultracentrifugation and probed by western blot for RIG-I or RIG-IΔCARD association. **3.2C)** Fluorescence assay for RNA bound by 6xHis-tagged recombinant RIG-I. Fluorescent RNA and RIG-I were incubated with or without liposomes containing PI(3,5)P_2 under the specified conditions. Following incubation, RIG-I and any bound RNA was recovered through isolation by nickel affinity resin, and bound RNA was measured by fluorescence recovered on a Tecan plate reader. **3.2D)** Same as in C, but in some conditions PI(3,5)P_2 liposomes were added after RIG-I incubated with RNA ("Spike-In" condition). **3.2E)** Fluorescent RNA pulled down by RIG-I in the presence of liposomes containing varying concentrations of PI(3,5)P_2 as compared to RNA pulled down in the presence of liposomes containing only PC:PE. Experiments shown are representative of or averages of n=3 biological replicates. Data is shown as a mean ± SEM, and statistical analysis was preformed using a student's T test with asterisk coding as follows: * p<= 0.05; ** p<=0.01; *** p<=0.001; **** p<=0.0001.

If RIG-I is tethered to an organelle through an interaction with PIP, this interaction does not occur between a single lipid in solution and RIG-I. Rather it must occur within the context of a membrane, in which RIG-I interacts specifically with the headgroup of a target PIP surrounded by the headgroups of other membrane component lipids. Because of this, PIP strips serve best as a screen for PIP interactions. However, liposomes containing the PIP species of interest and other lipids commonly found in cell membranes allow for these interactions to be assessed in a more physiological setting that mimics the three-dimensional requirements of the membrane and its interacting partners.

Given this, we next generated liposomes with a PC:PE backbone supplemented with individual PIPs to pinpoint the specific PIP that interacts with RIG-I. To determine if RIG-I interacts with a specific PIP species, recombinant RIG-I or RIG-IΔCARD was incubated with liposomes at 37°C to allow for binding. Following this incubation, the liposomes were pelleted at 100,000xg and probed for the presence of RIG-I in these pellets through western blot (Figure 3.2B). Through this experiment, we observed a strong and specific interaction between RIG-I and only liposomes containing PI(3,5)P_2 (Figure 3.2B), a species of PIP enriched on the membranes of acidified endosomes[72,160]. As observed in the previous experiment, RIG-IΔCARD phenocopied the WT protein and only interacted with PI(3,5)P_2-containing liposomes (Figure 2B). Together, these experiments demonstrate that RIG-I interacts with PI(3,5)P_2 *in vitro* in a CARD-independent manner.

3.4.3 PI(3,5)P_2 competes with 5'PPP RNA for RIG-I binding

Our data suggest that RIG-I has a previously unknown interacting ligand, PI(3,5)P_2 in addition to its known ligands of 5'PPP RNA and ATP. Our truncation mutant analysis suggests that the helicase domains of RIG-I may mediate its membrane association (Figure 3.1C) and presumably its PI(3,5)P_2 binding activity. Given the known RNA-binding activity of these domains, we were curious to understand how the presence of PI(3,5)P_2 influenced interactions between RIG-I and its other ligands, particularly 5'PPP RNA.

To test this, we performed competition assays between RIG-I, RNA, and liposomes containing PI(3,5)P_2. To quantitatively assess RIG-I RNA interactions, we utilized T7 *in vitro* transcribed (IVT) RNA labeled with Fluorescein-12-UTP, allowing for the amount of RNA bound by RIG-I to be measured by spectrofluorimetry. The template for these RNAs is predicted to generate a ssRNA of 114bp. However, given the nature of T7 transcription, this 114mer likely contains hairpin regions of dsRNA, making it a potent RIG-I ligand[153]. In addition, liposomes were generated as described, and recombinant 6xHis-NusA-RIG-I was utilized. For these assays, we incubated recombinant NusA-6xHis-RIG-I with the specified ligands at 37°C for 30 minutes, pulled down on tagged RIG-I, and measured the amount of RNA bound.

Through these experiments, we observed that the presence of PI(3,5)P_2-containing liposomes, but not PC:PE control liposomes, prevented RIG-I from interacting with the fluorescently labeled IVT-generated 114mer (Figure 3.2C). However, in the absence of liposomes, RIG-I readily pulled down this ligand, as measured by spectrofluorimetry (Figure 3.2C). Furthermore, the addition of PI(3,5)P_2-containing liposomes, but not the control PC:PE liposomes, following RIG-I pre-incubation with labeled 5'PPP RNA led to a loss of fluorescent signal (Figure 3.2D). This suggests that the addition of PI(3,5)P_2 liposomes was sufficient to cause RIG-I to release bound 5'PPP RNA. Finally, incubating RIG-I with excess 5'PPP RNA and various concentrations of PI(3,5)P_2 shows that PI(3,5)P_2 inhibits RIG-I:RNA interactions in a dose-dependent manner (Figure 3.2E). Together, these data suggest that PI(3,5)P_2 directly competes with RNA for access to RIG-I.

3.4.4 PI(3,5)P_2 influences RIG-I ATPase Activity in a Ligand-Dependent Manner

In addition to its RNA binding activity, the helicase domains of RIG-I possess ATPase activity, which is activated upon RNA binding[161,162]. Current models of this activity implicate ATP hydrolysis following RNA binding as a mechanism of self-nonself discrimination beyond the 5'PPP recognition by the RIG-I CTD, allowing for selective engagement of dsRNA[154,163,164]. Furthermore, this activity powers the oligomerization of RIG-I through its translocation along the bound RNA[165].

Because of this, the ATPase activity of RIG-I also serves to displace viral RNA binding proteins and suppress viral replication. As $PI(3,5)P_2$ competes with RNA for binding to RIG-I, we were curious to understand how $PI(3,5)P_2$ influences this essential enzymatic function of RIG-I.

Inorganic phosphate production was quantified over time to measure the rate of RIG-I mediated ATP hydrolysis in the presence of various ligands. RIG-I only hydrolyses ATP when bound to an RNA ligand[161,162], and the rate of hydrolysis is heavily dependent the nature of the RNA ligand[157,161]. Because of this phenomenon, we chose to examine the effect of $PI(3,5)P_2$-containing membranes on RIG-I ATPase activity in the context of two different RNA ligands: an IVT-generated 5'PPP 114mer and 5'PPP dsRNA 19mer. Both of these ligands activate RIG-I ATPase activity, though the rate of activation varied slightly (Figure 3.3A).

With the addition of liposomes containing 2% $PI(3,5)P_2$, we observed differential effects on the ATPase activity of RIG-I with each ligand (Figure 3.3A). In the presence of 250nM dsRNA 19mer, RIG-I hydrolyzed ATP at an average rate of 1.73μM/min of PO_4^- release (Figure 3.3A), and this rate was dampened to 0.98μM/min of PO_4^- release in the presence of $PI(3,5)P_2$ liposomes but not the control PC:PE liposomes (Figure 3.3A). This inhibitory effect $PI(3,5)P_2$ but not PC:PE alone was observed at a wide range of concentrations of 19mer RNA (Figure 3.3B). However, this effect was not nearly as pronounced when RIG-I hydrolyzed ATP in the presence of the 114mer (Figure 3.3A and 3.3B). At a maximal concentration of 250nM 114mer, RIG-I hydrolyzed ATP at an average rate of 1.11μM/min of PO_4^- release, which was unchanged in the presence of PC:PE liposomes as well as $PI(3,5)P_2$ liposomes (Figure 3.3A). While over a range of lower concentrations, a modest inhibitory effect of the presence of $PI(3,5)P_2$ liposomes in the reaction was observed.

3.3A

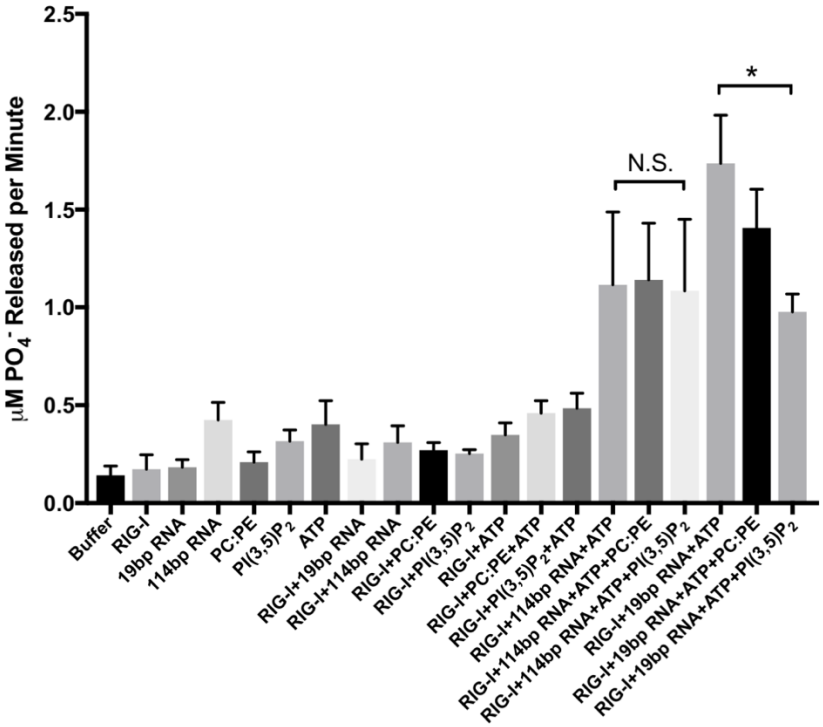
μM PO4- Released per Minute
2.5
2.0
1.5
1.0
0.5
0.0
N.S.
*
Buffer
RIG-I
19bp RNA
114bp RNA
PC:PE
PI(3,5)P2
ATP
RIG-I+19bp RNA
RIG-I+114bp RNA
RIG-I+PC:PE
RIG-I+PI(3,5)P2
RIG-I+ATP
RIG-I+PC:PE+ATP
RIG-I+PI(3,5)P2+ATP
RIG-I+114bp RNA+ATP
RIG-I+114bp RNA+ATP+PC:PE
RIG-I+114bp RNA+ATP+PI(3,5)P2
RIG-I+19bp RNA+ATP
RIG-I+19bp RNA+ATP+PC:PE
RIG-I+19bp RNA+ATP+PI(3,5)P2

3.3B

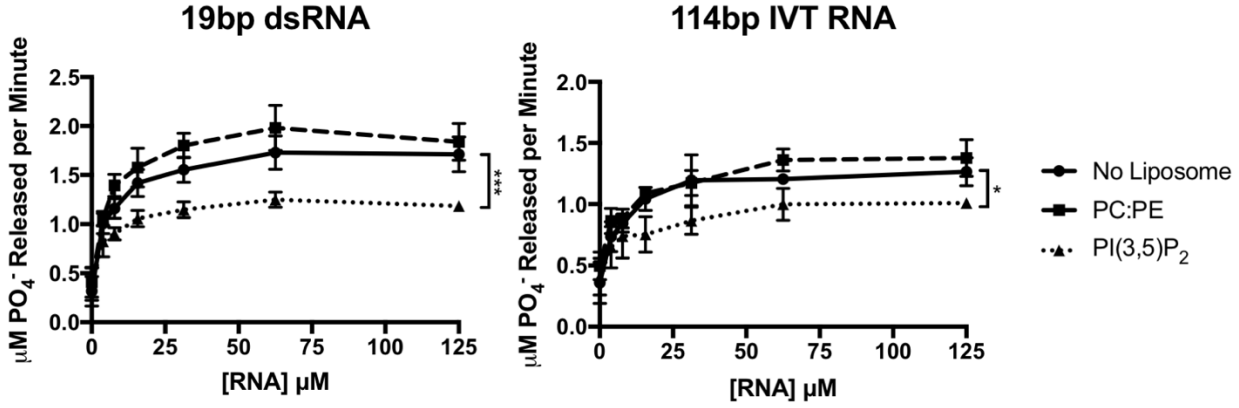
19bp dsRNA
114bp IVT RNA
μM PO4- Released per Minute
[RNA] μM
***
*
No Liposome
PC:PE
PI(3,5)P2

Figure 3.3: PI(3,5)P_2 alters the rate of ATP hydrolysis in a ligand-dependent manner

3.3A) The rate of inorganic phosphate release was measured to monitor RIG-I ATP hydrolysis. Minimal inorganic phosphate release was measured in conditions lacking the productive combination of RIG-I, RNA, and ATP. Rates of hydrolysis in the presence of a dsRNA 19mer or a 5'PPP IVT RNA by RIG-I were measured in the presence and absence of PI(3,5)P_2 liposomes. **3.3B)** Same as in A, but inorganic phosphate production through RIG-I ATP hydrolysis was measured in the presence of varying concentrations of a dsRNA 19mer or a 5'PPP IVT RNA with PI(3,5)P_2 liposomes, PC:PE liposomes, or no liposomes. Experiments shown are representative of or averages of n=3 biological replicates. Data is shown as a mean ± SEM, and statistical analysis was preformed using a student's T test with asterisk coding as follows: * p<= 0.05; ** p<=0.01; *** p<=0.001; **** p<=0.0001.

Through these experiments, we found that $PI(3,5)P_2$-containing membranes inhibited ATPase activity in a ligand-dependent manner. Given that $PI(3,5)P_2$ inhibited the interaction with the IVT-generated 114mer RNA, we were surprised to observe that this did not lead to a similar decrease in ATPase activity, which is typically stimulated through RNA binding[17,161,162]. Notably, the presence of $PI(3,5)P_2$ liposomes alone did not stimulate the ATPase activity of RIG-I (Figure 3.3A), ruling out the possibility that $PI(3,5)P_2$ binding could lead to ATPase activation. However, the clear inhibition of ATPase activity observed in the presence of dsRNA 19mer suggests that $PI(3,5)P_2$ binding leads to different rates ATP hydrolysis in a ligand-dependent manner. As ATP hydrolysis plays a critical role in self-nonself discrimination by RIG-I, $PI(3,5)P_2$ may be another regulator of this activity, but further investigation is required.

3.5 Discussion

The RIG-I signaling pathway is essential for the control of many RNA virus infections[9,10], while mutations in this gene are implicated in autoinflammatory disease[11,12]. Through our study of RIG-I, we determined that protein is capable of associating with membranes through an interaction with PI(3,5)P_2 *in vitro* and present evidence suggestive of a pool of membrane-bound RIG-I in multiple cell lines. Further analysis of the interaction between PI(3,5)P_2 and RIG-I *in vitro* revealed that PI(3,5)P_2 competes with T7 IVT RNA for RIG-I binding and displaces RNA already bound to RIG-I. Measurement of RIG-I's ATPase activity stimulated by binding this 114bp ligand showed no change in the rate of ATP hydrolysis in the presence or absence PI(3,5)P_2, while a significant suppression of the rate of ATP hydrolysis was observed in the presence of PI(3,5)P_2 with a dsRNA 5'PPP 19mer. Together, these data suggest that PI(3,5)P_2 may play a role in regulating the interactions between RIG-I and potential RNA ligands.

Lacking specific transmembrane domains, RIG-I is presumed to be a resident of the cytosol. However, many proteins without distinct transmembrane domains are capable of interacting with cell membranes through electrostatic interactions with lipid head groups, such as those of PIPs[72]. Our data suggest that RIG-I may behave as a peripheral membrane protein, as it both sediments with cellular membranes separated from the soluble cytosol and interacts specifically with PI(3,5)P_2-containing liposomes *in vitro*. In particular, the specificity for PI(3,5)P_2 over other PIPs is quite striking, as many PIP-binding are promiscuous and able to interact with many PIP species *in vitro*[166]. As PI(3,5)P_2 is one of the least abundant species of PIP in the cell[160], such specificity may be necessary to prevent off-target interactions. PI(3,5)P_2 is enriched on the surface of late endosomes, where it is generated from PI(3)P on early endosomes through the activity of the kinase PIKfyve[160]. PI(3,5)P_2 has also been found albeit in lower abundance on other organelles, such as the late autophagosome and the lysosome[160,167].

Because PI(3,5)P_2 is enriched on the acidified endosome, it is tempting to speculate that RIG-I may associate with this compartment through binding PI(3,5)P_2. Such positioning would be

optimal for this viral sensor, as many viruses enter the host cell cytoplasm through breach of the late endosomal membrane[152]. To determine if $PI(3,5)P_2$ could mediate subcellular positioning of RIG-I on late endosomes, immunocytochemistry or other microscopic analysis of RIG-I positioning within the cell is required. Ultimately, understanding how the ability of RIG-I to bind $PI(3,5)P_2$ alters its subcellular positioning mandates further experimental analysis.

Our investigation of RIG-I interactions with $PI(3,5)P_2$ revealed that $PI(3,5)P_2$ differentially regulated interactions between RIG-I, ATP, and potential RNA ligands. Given both its effect on RIG-I ATPase activity and RNA binding, $PI(3,5)P_2$ may potentially play a role in self/nonself discrimination by RIG-I. In addition to its effector functions in viral infection[165], the ATPase activity of RIG-I is thought to play an essential role in stabilizing or disengaging the protein on target RNAs[154,161,164]. Although 5' di- or triphosphate motifs are crucial for RIG-I recognition of an RNA ligand through its CTD[14,127,153], RIG-I binding to the RNA backbone through its helicase domains is modulated by ATP hydrolysis. When the helicase domains bind the RNA backbone, ATP is hydrolyzed, which promotes the release of the RNA when interacting with non-ideal ligands or the translocation of RIG-I along the target RNA to form filaments and activate MAVS[154]. Analysis of mutants reveals that both hyperactive and hypoactive ATPase activity leads to deleterious effects on RIG-I signaling[164]. As mutants of RIG-I that lack ATPase activity cannot induce an IFN response through MAVS, while mutants with hyperactive ATPase activity promotes an autoinflammatory phenotype[164].

By differentially altering ATP hydrolysis rates and RNA binding in the presence of various ligands, $PI(3,5)P_2$-containing membranes may add another layer to the regulation of self/nonself interactions by RIG-I. However, much more investigation is necessary to understand this potential phenomenon. Extensive analysis of RIG-I interaction with a wide array of different ligands is must be performed to understand how $PI(3,5)P_2$ alters RIG-I-RNA interactions and ATP hydrolysis. Furthermore, analysis of mutants of RIG-I that cannot bind $PI(3,5)P_2$ are necessary to understand the functional effects of this interaction *in vivo*.

Taken together, our data demonstrate that RIG-I is capable of interacting with lipid bilayers through an interaction with $PI(3,5)P_2$ and suggest a potential role for this interaction in ligand recognition and licensing of RIG-I filament formation through ATP hydrolysis. Furthermore, this work serves as a directive to understand if this interaction occurs *in vivo* and how this interaction alters RIG-I activity and positioning within the cell. If $PI(3,5)P_2$ does position RIG-I at sites of viral entry and preferentially allows for interaction between RIG-I and ideal RNA ligands, this interaction could be a potential target for therapeutics looking to stimulate or dampen RIG-I activity. Further study will better elucidate this mechanism as well as any potential for druggable targets for therapeutic intervention.

Chapter 4: Discussion

Membrane Lipids as Regulators of Intracellular Innate Immune Sensing

4.1 Overview

The aim of this work was to investigate the subcellular localization of the intracellular nucleic acid sensors cGAS and RIG-I. Localization orchestrates innate immunity, controlling PRR activation and downstream signal transduction. This phenomenon is well appreciated in regard to transmembrane proteins of the innate immune system and their accessory proteins. However, cGAS and RIG-I lack transmembrane domains and have no apparent requirement for specific localization within the cell. As such, many assume these proteins are soluble residents of the cell cytosol, encountering ligands through diffusion. However, this model does not account for several aspects of cGAS and RIG-I signaling. For instance, dsDNA, the ligand detected by cGAS, is present within the cell at steady state in both the mitochondria and the nucleus. Therefore, a mechanism to avoid inappropriate sensing self-DNA is vital to prevent autoimmunity. Additionally, the low abundance of these proteins in unstimulated cells refutes a model of ligand encounter based solely on diffusion, as this necessitates significant viral replication in order for sensing to occur. Therefore, we hypothesized that these sensors were positioned within the host cell in such a way to avoid detection of self-ligands and to promote the detection of nonself-ligands.

Through our study of these sensors, we found that the intracellular DNA sensor cGAS localizes to the plasma membrane through an interaction with the lipid $PI(4,5)P_2$. The N terminus of cGAS mediates the interaction with $PI(4,5)P_2$ *in vitro* and localization to the plasma membrane in cells. Loss of the N terminus, and therefore cGAS localization, heightened basal IFN signatures, triggered hyperresponsiveness to genotoxic stress but not viral infection, and instigated cell death in some instances. This phenotype was rescued with a mutant allele of cGAS in which the N terminus was replaced with a heterologous $PI(4,5)P_2$-binding domain, demonstrating that these phenotypes were due to mislocalization of the protein rather than other unknown activities of the N terminus. Our research supports a model in which the interaction between the cGAS N terminus and the plasma membrane prevents aberrant sensing of self-DNA and subsequent autoimmunity.

While our study of RIG-I warrants a more thorough investigation, the data generated suggested that PIP-mediated localization may be a common mechanism intracellular nucleic acid sensor regulation. Our *in vitro* studies RIG-I revealed an interaction with $PI(3,5)P_2$, a lipid enriched on late endosomes. In addition, we observed that $PI(3,5)P_2$ competes with RNA ligands for RIG-I binding and modulates RIG-I ATPase activity. Together, these studies highlight the importance of electrostatic membrane association in innate immune sensing and challenge the notion that sensors lacking transmembrane domains must also lack any specific subcellular positioning.

As our work on RIG-I is incomplete, much of this discussion will focus on our study of cGAS as well as shared aspects between the sensors. Through studying cGAS, we uncovered a mechanism of self/nonself discrimination through subcellular localization that is mediated by a its N terminus. However, there are many aspects of this model and our work that warrant further investigation and suggest new avenues for research. cGAS activity is implicated in a wide range of cellular activities and pathologies, including cell cycle progression[48-50], viral infection[3,29,130], cell death[168-173], and cancer[46,48]. Understanding the regulatory landscape of this sensor will inform the development of new therapeutics for a range of diseases and enhance our knowledge of innate immunity and cell biology.

4.2 cGAS

4.2.1 The cGAS N-Terminus

Our study of cGAS localization focused on its intrinsically disordered N-terminal domain. A small domain with poor primary sequence conservation, the N terminus of cGAS was initially considered dispensable. While the N terminus tightly bound DNA *in vitro*, it was not necessary or sufficient for DNA binding or cGAMP synthesis and was considered an accessory DNA-binding domain[8]. However, further study elucidated that this domain is required for biomolecular condensation of cGAS and DNA into liquid droplets[129], and our work revealed the essential role of the N terminus in localization through its interaction with $PI(4,5)P_2$. With these discoveries, the N terminus is emerging as a regulatory domain of cGAS, its localization, and its ability to sense dsDNA.

These roles of the N terminus are diametric, acting as a positive regulator of signaling through facilitation of liquid droplet formation[129] and as a negative regulator of signaling through sequestration of cGAS at the plasma membrane. Such opposing functions may be a consequence of the nature of the N terminus. Intrinsically disordered proteins are able to take on multiple conformations, and presumably multiple functions, dependent on their molecular context and available binding partners[174]. Therefore, its ability to bind both $PI(4,5)P_2$ and DNA in liquid droplets may be derived from its inherent ability to adopt different conformations, changing its 3D structure when the local concentration of dsDNA reaches a certain threshold and promoting cGAMP production. In this way, the N terminus may act as a molecular switch, permitting cGAS to be “off” or “on” as consequence of its surroundings.

In addition to its DNA-bound liquid droplet and plasma membrane associated states, cGAS also localizes to the nucleus, as observed in this study and many others[29,48,175]. While this is considered dependent on the cell cycle[48], the molecular cues that dictate cGAS localization to the nucleus during cell division or otherwise remain unexplored, though the N terminus is implicated in this event as well[175]. Given that the interaction between the N terminus and $PI(4,5)P_2$

is electrostatic, one possibility for dissociating these components and re-localizing cGAS to the nucleus could be a post-translational modification of the N terminus that switches or neutralizes its strong positive charge. One such modification is phosphorylation, which could be mediated by one of the many cyclin dependent kinases (CDKs) that regulate the cell cycle[176]. Though this theory is speculative, it highlights how the N terminus of cGAS could regulate the multiple states of activity and localization. Therefore, identifying modifications of the cGAS N terminus and additional interacting molecules is an area that warrants in-depth investigation. To date, the only published modification of the cGAS N terminus is its cleavage by caspase 1 during inflammasome activation, which upregulates IFN production in the context of pyroptosis[177]. With more work needed, it is clear that better understanding the activities and modifications of this domain will shape our understanding of cGAS itself.

4.2.2 Thermodynamics of cGAS Activation

Our model dictates that cGAS must release from $PI(4,5)P_2$ on the plasma membrane to bind DNA and produce cGAMP to activate STING and upregulate the production of IFN. Recently, DNA-bound cGAS was described as forming biomolecular condensates within the cell with liquid-like properties[129]. Liquid-like properties of several membraneless compartments of the cell have been described, including protein and RNA rich compartments like P granules of *C. elegans*[178], the nucleolus[179], and other RNA-protein complexes[180,181]. These biomolecular condensates are phase-separated from the surrounding cellular compartment and concentrate proteins with other biomolecules, allowing for rapid and specific interactions to occur[182,183]. In the context of cGAS activation, liquid droplet formation is thought to be necessary for maximal cGAMP production and requires the N terminus for formation[129]. Such a requirement could be expected, as intrinsically disordered domains frequently are found in biomolecular condensates[181-183].

How these droplets are nucleated from membrane-bound cGAS and cytosolic DNA is unclear. However, a simple thermodynamic hypothesis emerges, as cGAS-DNA phase separation is dependent on the concentration of its components *in vitro*[129]. At steady state, the

cGAS N terminus may remain bound to $PI(4,5)P_2$ at the plasma membrane to prevent accidental nucleation of cGAS liquid droplets on any cytosolic DNAs. However, if the cellular concentration of DNA significantly increases due to viral infection or genotoxic stress, for instance, cGAS may release from the plasma membrane to preferentially bind DNA. As this occurs, other molecules of cGAS or cGAS:DNA complexes may interact, as it has been proposed that the N terminus may crosslink cGAS:DNA complexes and increase the valency of this interaction, ultimately leading to the formation of a biomolecular condensate[129]. The presence of $PI(4,5)P_2$ may increase the necessary concentration of DNA needed to nucleate this event or perhaps alter requirements for DNA length. Longer DNA ligands promote more efficient phase separation, which is presumably due to increased available cGAS binding sites[129]. Additionally, other biomolecules may facilitate nucleation of cGAS liquid droplets. Recently, the stress granule-associated protein G3BP1 was proposed to facilitate cGAS:DNA interactions *in* vitro and in cells[184]. Given that stress granules are another form of biomolecular condensate with liquid-like properties[182,183], this protein could serve as a common nucleating mechanism for different liquid droplets, but such a model requires additional experimental evidence. Investigating how phase separation is nucleated and regulated in the context of membrane-bound cGAS is necessary to understand the activation of this critical innate immune sensor.

4.2.3 cGAS Localization States

Our study focused on cGAS localization at the plasma membrane, its interaction with $PI(4,5)P_2$, and the consequences of this localization in monocytes and macrophages. However, this is not the only state of cGAS localization. While we found cGAS predominantly at the plasma membrane in human and murine monocytes, we did observe cGAS concentrated in the nucleus, which others have noted[29,48,175]. Furthermore, when cGAS was discovered, it was considered a resident of the cytosol[8]. Our experiments comparing cGAS localization in multiple cell lines revealed that the distribution of cGAS varied between cell types. This variation in localization

suggests that cGAS may not reside at one specific site within any given cell and that cGAS localization is likely dynamic and actively regulated.

Outside of our work on the plasma membrane, the best characterized states of cGAS localization are its localization to liquid droplets, as described above, and its localization to the nucleus. Some aspects of its nuclear localization are inflammatory. This is evident in its antiviral functions, as cGAS is found in the nucleus during HSV1 infection through an association with IFI16[29] and HIV infection through association with the protein NONO[185]. However, some population associates with the nucleus at steady state in a way that appears not be inherently inflammatory, as many have noted that cGAS in nucleus at steady state in various cell lines[29,175]. Additionally, cGAS associates with chromatin during mitosis and is more likely to localize to the nucleus in rapidly dividing cells[48]. Together, these observations suggest that cGAS has both inflammatory and more fundamental roles in the nucleus.

We observed significant differences in cGAS localization states between cell lines. However, when we expressed the N terminus alone in any given cell type, this construct localized exclusively to the plasma membrane. In addition to demonstrating that the N terminus is a *bona fide* localization domain, these data suggest that differences in localization observed with WT cGAS are tied to its enzymatic domain and imply that cGAS localization is actively regulated. Understanding how the localization states of cGAS are regulated and why these states vary with cell type is an intriguing avenue of research.

A potential reason for the differences of cGAS localization observed by us and others in different cell lines may have to do with their immortalized state. The most variability in cGAS localization we observed was in HeLa cells, which is one of the earliest immortalized cell lines known for its genetic instability and phenotypic variation[186,187]. Furthermore, many immortalized cell lines lack cGAS expression entirely[8,188,189], and cGAS and STING are frequently lost or mutated in tumors[188-190]. Given it associates with the nucleus during cell division and is activated during both senescence[48-50] and DNA damage[44,45,47,51], it is likely cGAS activity is fundamental to

cellular transformation, which relies upon genomic instability, bypassing senescence, and generates DNA damage[191]. Because of this, studying cGAS localization in immortalized cells may not properly inform on its regulation in a non-transformed cell. For these reasons, we chose to confirm our localization observations in primary murine macrophages. However, understanding how cGAS is misregulated as cells immortalize may provide insight into the inflammatory responses to immortalization and to the transformed state of genetic plasticity. Given these possibilities, we must strive to understand cGAS and its localization in both health and disease, through the study of primary cells, cells undergoing immortalization, and cells of established tumors.

4.2.4 cGAS, PI(4,5)P_2, and the Plasma Membrane

The plasma membrane defines the cell periphery, interfaces with other cells, and coordinates interactions with the extracellular space and the molecules that occupy it. Many different events arise at the plasma membrane, including endocytic uptake, cell movement, and cell surface receptor activation. PI(4,5)P_2 is a resident lipid of the intracellular face of the plasma membrane, which is involved in many of these events. PI(4,5)P_2 plays a role in multiple forms of endocytosis and actin-based activities by recruiting proteins involved in these activities to the plasma membrane[192]. For instance, PI(4,5)P_2 interacts with AP-2[74], a protein essential for clathrin-mediated endocytosis. Additionally, PI(4,5)P_2 directs the actin cytoskeleton during phagocytosis[75], facilitating the formation of phagocytotic protrusions and the engulfment of the target particle. In addition to endocytic uptake, PI(4,5)P_2 coordinates a number of events at the plasma membrane through the activity peripheral membrane proteins and through its conversion to other forms of PIPs as events such as endocytosis and movement occur[82,193].

Our data demonstrates that cGAS interacts PI(4,5)P_2 as its mechanism of recruitment to the plasma membrane. *In vitro*, both recombinant cGAS and its N-terminal localization domain interacted strongly and specifically with liposomes containing PI(4,5)P_2. In cells, we observed that both cGAS and the cGAS N terminus localized to the plasma membrane, a subcellular site

enriched in $PI(4,5)P_2$. During phagocytosis of zymosan particles, the N terminus localized to phagocytic protrusions but not the base of the phagocytic cup, a localization pattern specific to $PI(4,5)P_2$ in this process[76]. The interaction between the cGAS N terminus and $PI(4,5)P_2$ is essential for cGAS function, as loss of the N-terminal $PI(4,5)P_2$ binding domain was coupled with heightened basal IFN signaling and increased sensitivity to endogenous DNA ligands produced during genotoxic stress. These observations led us to conclude that the interaction between cGAS and $PI(4,5)P_2$ creates a threshold for the recognition of endogenous ligands and prevents autoimmune responses.

However, outside of this thresholding effect, the purpose of cGAS recruitment to the plasma membrane over other organelles is unclear. A tempting hypothesis for this specific localization hinges on the subcellular distribution of self- and nonself-DNA. Our data with MVA-Ova infection demonstrated that mislocalized cGAS did not have heightened sensitivity to viral DNA, which is in stark contrast to the strong responses it generated to self-DNA. Therefore, plasma membrane localization may place cGAS at an advantage to specifically sense foreign DNA. The plasma membrane coordinates the uptake of foreign particles, and as $PI(4,5)P_2$ is converted to other PIPs during endocytosis[192], cGAS may specifically lose membrane association at sites of endocytic uptake. Such an event would prime cGAS to interact with DNA if this molecule is released from an endosome, an event that typically occurs during infection. In contrast, the nucleus is arguably the organelle furthest from the plasma membrane, as the plasma membrane defines the cell periphery. Small bursts of DNA generated from this area due to mild genotoxic stress may not significantly alter the local concentration of DNA near the plasma membrane, while severe genotoxic stress would increase the concentration of DNA throughout the cell. Similarly, DNA released from mitochondria is likely local to the organelle under mild stressors and abundant throughout the cell upon severe stress. In this manner, cGAS positioning at the plasma membrane could promote its sensitivity to nonself-DNA over self-DNA.

Understanding the relationship between cGAS, $PI(4,5)P_2$ and the plasma membrane requires further investigation. The plasma membrane fundamentally defines the cellular self and nonself, and this barrier influences cGAS-mediated immune responses to the self and nonself. $PI(4,5)P_2$ is involved in many events mediated by this organelle, identifying how and when $PI(4,5)P_2$ directs cGAS activity will provide significant insight into cGAS function.

4.2.5 cGAS Sensing of Nonself-DNA

Accumulation of cytosolic DNA frequently occurs in infection, and one of the best characterized functions of cGAS is its ability to sense infection. cGAS activates an IFN response to a wide range of pathogens, including viruses[3,29,130,131], bacteria[40,41,194], and parasites[43]. Frequently, these responses are required for control of infection[3,28] and are antagonized by many pathogens[52,195,196]. Clearly, control of pathogenic infection is a fundamental function of the cGAS-STING pathway and an active area of ongoing research.

While our work on cGAS localization focused on responses to endogenous ligands, we examined how loss of cGAS localization altered its responses to attenuated Vaccinia Virus infection. Using a strain of MVA with an Ova reporter gene, we found that mislocalized cGAS produced an IFN response at the same order of magnitude as cells overexpressing WT cGAS or GFP. These data stand in stark comparison to stimuli of genotoxic stress, in which mislocalized cGAS produces a much stronger IFN response than the WT protein. Despite increased basal IFN signaling in cells expressing mislocalized cGAS, MVA-Ova was able to replicate in these cells, as Ova transgene expression was observed, ruling out the possibility that the IFN response was dampened by lack of productive infection. Furthermore, because cells expressing mislocalized cGAS have higher basal IFN expression, their responsiveness to MVA-Ova infection appears slightly weaker than in cells expressing WT cGAS or GFP.

These data suggest that cGAS has differential responses to endogenous and exogenous DNA. Loss of cGAS plasma membrane association biases the protein toward sensing endogenous DNA and has no effect or perhaps dampens the sensing exogenous DNA. As

discussed earlier, this may be a consequence of cGAS plasma membrane association, enhancing its ability to detect DNA entering the cell. However, this effect may also be a consequence of loss of the N terminus outside of its function as a localization domain, as the N terminus also facilitates liquid droplet formation and cGAMP production[129]. Clearly, more research is required to understand the relationship between cGAS plasma membrane association and its sensing of foreign DNA.

4.2.6 cGAS Sensing of Self-DNA

Outside of its role in sensing foreign DNA, cGAS detects self-DNA to generate an IFN response in several different contexts. For instance, cGAS recognizes DNA derived from the nucleus, producing an immune response to chromatin fragments released from the nucleus as cells senesce[48-50] and to micronuclei generated from aberrant cell division[44,45]. Both high doses of several genotoxic agents[47,197,198] and loss of genes involved in DNA repair, including BRCA2[199], ATM[51], and PARP1[200], lead to cGAS-mediated IFN production. In addition to nuclear DNA, cGAS recognizes and responds to mitochondrial DNA, which is released from mitochondria under various forms of cellular stress such as oxidative stress or viral infection[52,53]. These activities of cGAS in sensing endogenous DNA are underscored by the importance of this pathway in cancer progression and its necessity for effective checkpoint blockade therapy[46]. The ability of cGAS to detect self-DNA in the event of significant DNA damage and genetic instability is an integral aspect of cGAS activity with clear clinical relevance.

However, our data demonstrates that cGAS localization to the plasma membrane inhibits detection of self-DNA. We observed that loss of cGAS interaction with the plasma membrane led to heighted IFN production at steady-state, significant increases in IFN production in response to genotoxic stressors, and in some instances, cell death. Such responses were not observed in cells expressing WT cGAS. These observations suggest that cGAS inherently tolerates low levels of cytosolic DNA, setting a threshold for the amount of endogenous DNA in the cytosol necessary to generate an IFN response.

Tolerance of low levels of cytosolic DNA is likely essential to prevent autoinflammatory responses to normal cellular processes. Cytosolic DNA can be generated through DNA damage or mitochondrial stress mediated by reactive oxygen species (ROS). Notably, ROS are produced by at low levels as a consequence of oxidative phosphorylation[201,202], an indispensable process of cellular life. Other cellular functions lead to ROS production as well, such as the activity of NADPH oxidases (NOX), which produce superoxide from oxygen to facilitate a number of cellular activities[203]. Because cGAS is not active in unstimulated cells, it is likely that the DNA generated by these normal cellular processes is too minimal to lead to its activation. Further evidence for the existence and tolerance of cytosolic DNA at steady state comes from the study of extra-nuclear nucleases, such as the exonuclease TREX1[149]. Such nucleases degrade cytosolic DNA or DNA:RNA hybrids[135], which are both cGAS ligands[8,136], and mutations in these genes are linked to autoimmune disease[135]. Indeed, loss of TREX1 or other such nucleases causes a cGAS-dependent IFN response in the absence of stimulation[132,134,137] and autoinflammatory disease[27,135]. Given these data, it becomes apparent that cytosolic DNA is produced by cells at equilibrium, but its concentration remains low through the activity of TREX1 and other extra-nuclear nucleases.

Therefore, in order for cGAS sensing to occur, DNA produced as a result of damage or viral infection must overwhelm these nucleases and reach a sufficient concentration for cGAS dissociation from the plasma membrane and the formation of liquid droplets. Because of these barriers to activation, cGAS likely senses drastic increases in cytosolic DNA concentration rather than subtle changes. Together, nuclease activity and cGAS plasma membrane association set a threshold for reasonable cytosolic DNA concentrations in the cell, only activating cGAS when significant changes occur. A thorough understanding of how this threshold is maintained and how it can be altered will be essential to understand cGAS activity in different contexts, such as viral infection, oxidative stress, and cancer.

4.2.7 cGAS-Mediated Cell Death

One of the most striking observations in our study was the ability of mislocalized cGAS to activate cell death in response to stimuli that did not cause cell death or significant IFN production in cells expressing WT cGAS. Such a stark difference in cell fate decisions suggests that cGAS may be directly involved in initiating cell death. Additionally, this phenotype was dependent on cGAS:DNA interaction, implicating its sensory capacity in its ability to initiate cell death. Outside of our work, many others observed cGAS-dependent cell death[168-173]. However, many aspects of cGAS-mediated cell death are unclear, including the type of death induced, the general requirements for cell death initiation, and the molecules involved.

Multiple mechanisms have been described for cGAS-mediated cell death, but none converge around a single model. Some studies suggest that cGAS is involved in pyroptotic cell death through activation of the inflammasome[168-171]. Of these, some argue that IFN production stimulated by cGAS recognition of DNA serves as the priming step for inflammasome activation, through IFN-mediated upregulation of inflammasome components and the pyroptotic cytokine IL-1β[170,171]. However, others propose more direct involvement of cGAS in initiating the NLRP3 inflammasome. One model suggests that cGAMP interacts directly with NLRP3 or AIM2 to form the inflammasome[168], while another supports a model by which cGAS-STING activation leads to leads to lysosomal rupture and K^+ efflux from the cell to activate NLRP3[169].

Outside of pyroptotic cell death, other mechanisms of cGAS-mediated cell death have been proposed. For instance, in the context of HSV-1 and HCMV infection, cGAS appears to play a pro-apoptotic role[173]. In addition, two recent reports describe cGAS-mediated cell death during mitotic delay[172,204]. One study investigated the role of cGAS in cells undergoing replicative crisis[172], a critical barrier to tumorigenesis driven by shortened telomeres leading to mitotic arrest and cell death[205,206]. In this report, cGAS mediates an autophagic cell death, dependent on several component of the autophagy pathway but independent of caspase-3 activation[172]. While another study observed that prolonged mitotic arrest driven by Taxol treatment led to the activation of apoptosis in a cGAS-dependent manner[204].

Given the diversity of these reports, a central cGAS-dependent cell death pathway is not apparent, though it is possible multiple mechanisms may exist. This is further clouded by the known DNA-mediated pyroptotic pathway in which the inflammasome is formed through the DNA binding protein AIM2[207]. Some investigations of cGAS-mediated cell death have shown independence from AIM2[169], which suggests multiple pathways for dsDNA-dependent cell death may exist. Gaining a better understanding of how cGAS-mediated cell death is initiated and executed will add to our understanding of this protein and its role in driving cell fate decisions.

4.3 Localization of Intracellular Nucleic Acid Sensors

Our initial hypothesis alleged that spatial regulation of innate immune sensing was not limited to transmembrane proteins. Our investigation of cGAS and RIG-I demonstrated that both of these soluble proteins interact with PIPs within membranes. Study of the interaction between cGAS and $PI(4,5)P_2$ revealed that plasma membrane localization of cGAS maintains basal IFN signaling and sets a threshold for sensing of self-DNA. With these data, we conclude that cGAS is subject to spatial regulation. While our experiments with RIG-I were mainly *in vitro* and require further investigation, we demonstrated that RIG-I association with the membrane lipid $PI(3,5)P_2$ altered its ability to associate with RNA and to hydrolyze ATP. Although further work is needed, this preliminary data suggests that membrane association by RIG-I, like cGAS, directly regulates its interactions with ligands. Through these observations, we can conclude that soluble, intracellular PRRs are governed by the same principles as their integral membrane counterparts in which localization governs access to proinflammatory ligands.

Regulating ligand access through subcellular localization may play an important role in self-nonself discrimination. Our work with cGAS demonstrates that plasma membrane localization of this protein prevents recognition of endogenous nucleic acids. Similarly, TLR9, a transmembrane PRR that detects dsDNA, resides in the acidified endosome, and mislocalization of this protein causes autoinflammation and death in a mouse model[58]. Additionally, our data on RIG-I suggests that its interaction with $PI(3,5)P_2$ alters its rate of ATP hydrolysis in the presence of certain ligands. Given ATPase activity plays an important role in self-nonself discrimination by RIG-I[154,163], $PI(3,5)P_2$ binding may further influence this discriminatory activity. Taken together, these data reveal a commonality between nucleic acid sensing PRRs, in which subcellular localization regulates ligand access and subsequently self-nonself discrimination.

However, the avoidance of self-ligands is only one aspect of the regulation of ligand access. Sensing of foreign PAMPs is the principal role of PRRs, and their subcellular localization cannot unnecessarily hinder this activity. Unlike stimulation of genotoxic stress, viral infection did

not induce a potent IFN response in cells expressing mislocalized cGAS. Although this phenotype needs further validation and study, it suggests that localization of cGAS to the plasma membrane does not indiscriminately prevent cGAS from accessing its ligand. Rather, $PI(4,5)P_2$-mediated plasma membrane association by cGAS appears to serve as both a mechanism to prevent sensing of self-ligands and promote sensing of nonself-ligands. Therefore, the subcellular localization of PRRs may not only prevent sensing of self-ligands but allows PRRs to strike an important balance by actively promoting sensing of nonself ligands over those of the self. This is likely not limited to cGAS, and subcellular localization may emerge as an essential regulator of many intracellular PRRs. Our data, together with the work done on transmembrane PRRs, add to the mandate to study PRR localization, enriching our understanding of innate immune sensing and opening up new avenues for its manipulation to treat disease.

Chapter 5: Conclusion

The cGAS-STING pathway is a central regulator of the immune response to dsDNA. As such, cGAS-STING signaling is critical for the control of a wide range of infectious diseases[3,29,52,130,131], autoimmune disease[27,132,150], and cancer[46,48]. At the apex of this pathway is the recognition of dsDNA by cGAS, which leads to the production of cGAMP and the activation of IFN production via STING. Understanding this critical interaction and how it is regulated is essential to understand when and how this pathway is activated. Because cGAS activity is implicated in a myriad of diseases, studying cGAS activity not only enriches our understanding of its biology, but also has practical implications for human health.

Our work on cGAS revealed its regulation through subcellular localization via its N-terminal domain. By localizing to the plasma membrane, cGAS avoids recognition of self-DNA, preventing autoimmune responses. The charged, intrinsically disordered N-terminus of cGAS serves as its localization domain and binds to the membrane lipid $PI(4,5)P_2$. Previously, this domain was implicated in facilitating cGAS:DNA interactions through the formation of biomolecular condensates, but our work demonstrates that this domain has a bipartite function in both suppression and activation of cGAS signaling. In addition, cells expressing mislocalized cGAS were also more likely to die in the event of genotoxic stress, suggesting that the N terminus of cGAS may also regulate cGAS-mediated cell fate decisions. This multifunctionality of this domain may be a consequence of its inherent disorder, allowing the domain to adopt different conformations in different molecular contexts. Although initially overlooked, the N terminus is emerging as a key regulator of cGAS activation and localization. Understanding the structural states of this domain, its potential binding partners, and its post-translational modifications will further reveal how this domain shapes cGAS activity.

We also further elucidated the role of cGAS in sensing endogenous DNA. Several studies have found that cGAS detects cytosolic dsDNA as a consequence of DNA damage[44,45,47,51,198], and its loss facilitates cancer progression[46,48]. These data demonstrate an essential role of cGAS in responding to DNA damage and promoting an immune response in cases of severe genotoxic

stress. However, our work demonstrates that not all DNA damage or the accumulation of cytosolic DNA steady state is sufficient to activate cGAS. Its sensitivity is controlled through its localization to the plasma membrane, setting a threshold for sensing of self-DNA. Identifying further regulatory mechanisms of this threshold will enhance our understanding of how the cell recognizes its own damage and how such a threshold could be altered in disease.

Through this work, we have defined a state of cGAS localization required to maintain cellular homeostasis and prevent autoimmunity. With its emerging role in tumorigenesis, understanding the states of cGAS activity and their regulation will shape our understanding of this protein in both health and disease. More broadly, our data highlight the importance of studying protein localization in innate immune sensors with poorly defined subcellular states and demonstrate how proteins lacking transmembrane domains interact with membranes in a functionally relevant manner. Further study of PRR localization and its functional consequences is indispensable to understand innate immunity, cell biology, and human disease.

Appendix 1: References

1. Takeuchi, O. & Akira, S. Pattern Recognition Receptors and Inflammation. *Cell* **140,** 805–820 (2010).

2. Kato, H. *et al.* Differential roles of MDA5 and RIG-I helicases in the recognition of RNA viruses. *Nature* **441,** 101–105 (2006).

3. Schoggins, J. W. *et al.* Pan-viral specificity of IFN-induced genes reveals new roles for cGAS in innate immunity. *Nature* **505,** 691–695 (2014).

4. Roers, A., Hiller, B. & Hornung, V. Recognition of Endogenous Nucleic Acids by the Innate Immune System. *Immunity* **44,** 739–754 (2016).

5. Chow, J., Franz, K. M. & Kagan, J. C. PRRs are watching you: Localization of innate sensing and signaling regulators. *Virology* **479-480,** 104–109 (2015).

6. Hur, S. Double-Stranded RNA Sensors and Modulators in Innate Immunity. *Annu. Rev. Immunol.* **37,** 349–375 (2019).

7. Bhat, N. & Fitzgerald, K. A. Recognition of cytosolic DNA by cGAS and other STING-dependent sensors. *Eur. J. Immunol.* **44,** 634–640 (2014).

8. Sun, L., Wu, J., Du, F., Chen, X. & Chen, Z. J. Cyclic GMP-AMP Synthase Is a Cytosolic DNA Sensor That Activates the Type I Interferon Pathway. *Science* **339,** 786–791 (2013).

9. Loo, Y. M. *et al.* Distinct RIG-I and MDA5 Signaling by RNA Viruses in Innate Immunity. *J. Virol.* **82,** 335–345 (2007).

10. Kell, A. M. & Gale, M., Jr. RIG-I in RNA virus recognition. *Virology* **479-480,** 110–121 (2015).

11. Jang, M.-A. *et al.* Mutations in DDX58, which Encodes RIG-I, Cause Atypical Singleton-Merten Syndrome. *The American Journal of Human Genetics* **96,** 266–274 (2015).

12. Crow, Y. J. & Manel, N. Aicardi-Goutières syndrome and the type I interferonopathies. *Nature Publishing Group* **15,** 429–440 (2015).

13. Yoneyama, M. *et al.* The RNA helicase RIG-I has an essential function in double-stranded RNA-induced innate antiviral responses. *Nat Immunol* **5,** 730–737 (2004).

14. Goubau, D. *et al.* Antiviral immunity via RIG-I-mediated recognition of RNA bearing 5′-diphosphates. *Nature* **514,** 372–375 (2014).

15. Lu, C. *et al.* The Structural Basis of 5' Triphosphate Double-Stranded RNA Recognition by RIG-I C-Terminal Domain. *Structure* **18,** 1032–1043 (2010).

16. Leung, D. W. & Amarasinghe, G. K. Structural insights into RNA recognition and activation of RIG-I-like receptors. *Current Opinion in Structural Biology* **22,** 297–303 (2012).

17. Peisley, A., Bin Wu, Yao, H., Walz, T. & Hur, S. RIG-I Forms Signaling-Competent Filaments in an ATP-Dependent, Ubiquitin-Independent Manner. *Molecular Cell* **51,** 573–583 (2013).

18. Oshiumi, H., Matsumoto, M., Hatakeyama, S. & Seya, T. Riplet/RNF135, a RING finger protein, ubiquitinates RIG-I to promote interferon-beta induction during the early phase of viral infection. *J. Biol. Chem.* **284,** 807–817 (2009).

19. Cadena, C. *et al.* Ubiquitin-Dependent and -Independent Roles of E3 Ligase RIPLET in Innate Immunity. *Cell* **177,** 1187–1200.e16 (2019).

20. Seth, R. B., Sun, L., Ea, C.-K. & Chen, Z. J. Identification and Characterization of MAVS, a Mitochondrial Antiviral Signaling Protein that Activates NF-κB and IRF3. *Cell* **122,** 669–682 (2005).

21. Kawai, T. *et al.* IPS-1, an adaptor triggering RIG-I- and Mda5-mediated type I interferon induction. *Nat Immunol* **6,** 981–988 (2005).

22. Meylan, E. *et al.* Cardif is an adaptor protein in the RIG-I antiviral pathway and is targeted by hepatitis C virus. *Nature* **437,** 1167–1172 (2005).

23. Xu, L.-G. *et al.* VISA Is an Adapter Protein Required for Virus-Triggered IFN-β Signaling. *Molecular Cell* **19,** 727–740 (2005).

24. Dixit, E. *et al.* Peroxisomes Are Signaling Platforms for Antiviral Innate Immunity. *Cell* **141,** 668–681 (2010).

25. Horner, S. M., Liu, H. M., Park, H. S., Briley, J. & Gale, M. Mitochondrial-associated endoplasmic reticulum membranes (MAM) form innate immune synapses and are targeted by hepatitis C virus. *Proc Natl Acad Sci USA* **108,** 14590–14595 (2011).

26. Hou, F. *et al.* MAVS Forms Functional Prion-like Aggregates to Activate and Propagate Antiviral Innate Immune Response. *Cell* **146,** 448–461 (2011).

27. Gao, D. *et al.* Activation of cyclic GMP-AMP synthase by self-DNA causes autoimmune diseases. *Proc Natl Acad Sci USA* **112,** E5699–E5705 (2015).

28. Li, X.-D. *et al.* Pivotal Roles of cGAS-cGAMP Signaling in Antiviral Defense and Immune Adjuvant Effects. *Science* **341,** 1387–1390 (2013).

29. Orzalli, M. H. *et al.* cGAS-mediated stabilization of IFI16 promotes innate signaling during herpes simplex virus infection. *Proc Natl Acad Sci USA* **112,** E1773–E1781 (2015).

30. Kranzusch, P. J., Lee, A. S.-Y., Berger, J. M. & Doudna, J. A. Structure of Human cGAS Reveals a Conserved Family of Second-Messenger Enzymes in Innate Immunity. *CellReports* **3,** 1362–1368 (2013).

31. Ablasser, A. *et al.* cGAS produces a 2′-5′-linked cyclic dinucleotide second messenger that activates STING. *Nature* **498,** 380–384 (2013).

32. Wu, J. *et al.* Cyclic GMP-AMP is an endogenous second messenger in innate immune signaling by cytosolic DNA. *Science* **339,** 826–830 (2013).

33. Civril, F. *et al.* Structural mechanism of cytosolic DNA sensing by cGAS. *Nature* **498,** 332–337 (2013).

34. Ishikawa, H., Ma, Z. & Barber, G. N. STING regulates intracellular DNA-mediated, type I interferon-dependent innate immunity. *Nature* **461,** 788–792 (2009).

35. Ishikawa, H. & Barber, G. N. STING is an endoplasmic reticulum adaptor that facilitates innate immune signalling. *Nature* **455,** 674–678 (2008).

36. Haag, S. M. *et al.* Targeting STING with covalent small-molecule inhibitors. *Nature* 1–22 (2018). doi:10.1038/s41586-018-0287-8

37. Ouyang, S. *et al.* Structural Analysis of the STING Adaptor Protein Reveals a Hydrophobic Dimer Interface and Mode of Cyclic di-GMP Binding. *Immunity* **36,** 1073–1086 (2012).

38. Mukai, K. *et al.* Activation of STING requires palmitoylation at the Golgi. *Nature Communications* **7,** 1–10 (2016).

39. Zhong, B. *et al.* The Adaptor Protein MITA Links Virus-Sensing Receptors to IRF3 Transcription Factor Activation. *Immunity* **29,** 538–550 (2008).

40. Storek, K. M., Gertsvolf, N. A., Ohlson, M. B. & Monack, D. M. cGAS and Ifi204 Cooperate To Produce Type I IFNs in Response to *Francisella* Infection. *J.I.* **194,** 3236–3245 (2015).

41. Hansen, K. *et al.* Listeria monocytogenes induces IFN expression through an IFI16-, cGAS- and STING-dependent pathway. *The EMBO Journal* **33,** 1654–1666 (2014).

42. Zhang, Y. *et al.* The DNA Sensor, Cyclic GMP–AMP Synthase, Is Essential for Induction of IFN-β during *Chlamydia trachomatis* Infection. *J.I.* **193,** 2394–2404 (2014).

43. Gallego-Marin, C. *et al.* Cyclic GMP-AMP Synthase Is the Cytosolic Sensor of Plasmodium falciparum Genomic DNA and Activates Type I IFN in Malaria. *J. Immunol.* **200,** 768–774 (2018).

44. Mackenzie, K. J. *et al.* cGAS surveillance of micronuclei links genome instability to innate immunity. *Nature* **548,** 461–465 (2017).

45. Harding, S. M. *et al.* Mitotic progression following DNA damage enables pattern recognition within micronuclei. *Nature* **548,** 466–470 (2017).

46. Wang, H. *et al.* cGAS is essential for the antitumor effect of immune checkpoint blockade. *Proc Natl Acad Sci USA* **114,** 1637–1642 (2017).

47. Pépin, G. *et al.* Activation of cGAS-dependent antiviral responses by DNA intercalating agents. *Nucleic Acids Res* **45,** 198–205 (2017).

48. Yang, H., Wang, H., Ren, J., Chen, Q. & Chen, Z. J. cGAS is essential for cellular senescence. *Proc Natl Acad Sci USA* **114,** E4612–E4620 (2017).

49. Dou, Z. *et al.* Cytoplasmic chromatin triggers inflammation in senescence and cancer. *Nature* 1–21 (2017). doi:10.1038/nature24050

50. Glück, S. *et al.* Innate immune sensing of cytosolic chromatin fragments through cGAS promotes senescence. *Nat Cell Biol* **19,** 1061–1070 (2017).

51. Härtlova, A. *et al.* DNA Damage Primes the Type I Interferon System via the Cytosolic DNA Sensor STING to Promote Antimicrobial Innate Immunity. 1–13 (2017). doi:10.1016/j.immuni.2015.01.012

52. Aguirre, S. *et al.* Dengue virus NS2B protein targets cGAS for degradation and prevents mitochondrial DNA sensing during infection. *Nature Microbiology* 1–11 (2017). doi:10.1038/nmicrobiol.2017.37

53. West, A. P. *et al.* Mitochondrial DNA stress primes the antiviral innate immune response. *Nature* **520,** 553–557 (2015).

54. Andreeva, L. *et al.* cGAS senses long and HMGB/TFAM-bound U-turn DNA by forming protein–DNA ladders. *Nature* **549,** 394–398 (2017).

55. Murphy, K. & Weaver, C. Janeway's Immunobiology. (2016).

56. Ewald, S. E. *et al.* The ectodomain of Toll-like receptor 9 is cleaved to generate a functional receptor. *Nature* **456,** 658–662 (2008).

57. Lee, B. L. *et al.* UNC93B1 mediates differential trafficking of endosomal TLRs. *eLife* **2,** 13145–22 (2013).

58. Mouchess, M. L. *et al.* Transmembrane Mutations in Toll-like Receptor 9 Bypass the Requirement for Ectodomain Proteolysis and Induce Fatal Inflammation. *Immunity* **35,** 721–732 (2011).

59. Pfeiffer, A. *et al.* Lipopolysaccharide and ceramide docking to CD14 provokes ligand-specific receptor clustering in rafts. *Eur. J. Immunol.* **31,** 3153–3164 (2001).

60. Triantafilou, M., Miyake, K., Golenbock, D. T. & Triantafilou, K. Mediators of innate immune recognition of bacteria concentrate in lipid rafts and facilitate lipopolysaccharide-induced cell activation. *Journal of Cell Science* **115,** 2603–2611 (2002).

61. Płóciennikowska, A., Hromada-Judycka, A., Borzęcka, K. & Kwiatkowska, K. Co-operation of TLR4 and raft proteins in LPS-induced pro-inflammatory signaling. *Cell. Mol. Life Sci.* **72,** 557–581 (2014).

62. Kagan, J. C. *et al.* TRAM couples endocytosis of Toll-like receptor 4 to the induction of interferon-β. *Nat Immunol* **9,** 361–368 (2008).

63. Brandt, K. J., Fickentscher, C., Kruithof, E. K. O. & de Moerloose, P. TLR2 Ligands Induce NF-κB Activation from Endosomal Compartments of Human Monocytes. *PLoS ONE* **8,** e80743–11 (2013).

64. Sasai, M., Linehan, M. M. & Iwasaki, A. Bifurcation of Toll-like receptor 9 signaling by adaptor protein 3. *Science* **329,** 1530–1534 (2010).

65. Honda, K. *et al.* Spatiotemporal regulation of MyD88-IRF-7 signalling for robust type-I interferon induction. *Nature* **434,** 1035–1040 (2005).

66. Saitoh, T. *et al.* Atg9a controls dsDNA-driven dynamic translocation of STING and the innate immune response. *Proc. Natl. Acad. Sci. U.S.A.* **106,** 20842–20846 (2009).

67. Kagan, J. C. Defining the subcellular sites of innate immune signal transduction. *Trends in Immunology* **33,** 442–448 (2012).

68. Kagan, J. C., Magupalli, V. G. & Wu, H. SMOCs: supramolecular organizing centres that control innate immunity. *Nature Reviews Immunology* **14,** 821–826 (2014).

69. Kagan, J. C. & Medzhitov, R. Phosphoinositide-Mediated Adaptor Recruitment Controls Toll-like Receptor Signaling. *Cell* **125,** 943–955 (2006).

70. Bonham, K. S. *et al.* A Promiscuous Lipid-Binding Protein Diversifies the Subcellular Sites of Toll-like Receptor Signal Transduction. *Cell* **156,** 705–716 (2014).

71. Franchi, L. *et al.* Cytosolic Double-Stranded RNA Activates the NLRP3 Inflammasome via MAVS-Induced Membrane Permeabilization and K +Efflux. *J.I.* **193,** 4214–4222 (2014).

72. Balla, T. Phosphoinositides: Tiny Lipids With Giant Impact on Cell Regulation. *Physiological Reviews* **93,** 1019–1137 (2013).

73. Garcia, P. *et al.* The pleckstrin homology domain of phospholipase Cδ1 binds with high affinity to phosphatidylinositol 4,5-bisphosphate in bilayer membranes. *Biochemistry* **34,** 16228–16234 (1995).

74. Jost, M., Simpson, F., Kavran, J. M., Lemmon, M. A. & Schmid, S. L. Phosphatidylinositol-4,5-bisphosphate is required for endocytic coated vesicle formation. *Curr. Biol.* **8,** 1399–1402 (1998).

75. Scott, C. C. *et al.* Phosphatidylinositol-4,5- bisphosphate hydrolysis directs actin remodeling during phagocytosis. *J Cell Biol* **169,** 139–149 (2005).

76. Botelho, R. J. *et al.* Localized Biphasic Changes in Phosphatidylinositol-4,5-Bisphosphate at Sites of Phagocytosis. *J Cell Biol* **151,** 1353–1368 (2000).

77. He, K. *et al.* Dynamics of phosphoinositide conversion in clathrin-mediated endocytic traffic. *Nature* 1–31 (2017). doi:10.1038/nature25146

78. Kanai, F. *et al.* The PX domains of p47phox and p40phox bind to lipid products of PI(3)K. *Nat Cell Biol* **3,** 675–678 (2001).

79. Gillooly, D. J. *et al.* Localization of phosphatidylinositol 3-phosphate in yeast and mammalian cells. *The EMBO Journal* **19,** 4577–4588 (2000).

80. Dove, S. K., Dong, K., Kobayashi, T., Williams, F. K. & Michell, R. H. Phosphatidylinositol 3,5-bisphosphate and Fab1p/PIKfyve underPPIn endo-lysosome function. *Biochem. J.* **419,** 1–13 (2009).

81. Idevall-Hagren, O. & Pietro De Camilli. Detection and manipulation of phosphoinositides. *BBA - Molecular and Cell Biology of Lipids* **1851,** 736–745 (2015).

82. Schink, K. O., Tan, K.-W. & Stenmark, H. Phosphoinositides in Control of Membrane Dynamics. *Annu. Rev. Cell Dev. Biol.* **32,** 143–171 (2016).

83. Dickson, E. J. & Hille, B. Understanding phosphoinositides: rare, dynamic, and essential membrane phospholipids. *Biochem. J.* **476,** 1–23 (2019).

84. Nagata, S., Suzuki, J., Segawa, K. & Fujii, T. Exposure of phosphatidylserine on the cell surface. **23,** 952–961 (2016).

85. Resh, M. D. Covalent lipid modifications of proteins. *Current Biology* **23,** R431–R435 (2013).

86. Patra, M. C. & Choi, S. Insight into Phosphatidylinositol-Dependent Membrane Localization of the Innate Immune Adaptor Protein Toll/Interleukin 1 Receptor Domain-Containing Adaptor Protein. *Front. Immunol.* **9,** 291–16 (2018).

87. Fitzgerald, K. A. *et al.* LPS-TLR4 Signaling to IRF-3/7 and NF-κB Involves the Toll Adapters TRAM and TRIF. *J. Exp. Med.* **198,** 1043–1055 (2003).

88. Rowe, D. C. *et al.* The myristoylation of TRIF-related adaptor molecule is essential for Toll-like receptor 4 signal transduction. *Proc Natl Acad Sci USA* **103,** 6299–6304 (2006).

89. Valanne, S., Wang, J. H. & Ramet, M. The Drosophila Toll Signaling Pathway. *J.I.* **186,** 649–656 (2011).

90. Horng, T. & Medzhitov, R. Drosophila MyD88 is an adapter in the Toll signaling pathway. *Proc Natl Acad Sci USA* **98,** 12654–12658 (2001).

91. Marek, L. R. & Kagan, J. C. Phosphoinositide Binding by the Toll Adaptor dMyD88 Controls Antibacterial Responses in Drosophila. *Immunity* **36,** 612–622 (2012).

92. Liu, X. & Lieberman, J. A Mechanistic Understanding of Pyroptosis: The Fiery Death Triggered by Invasive Infection. *Adv. Immunol.* **135,** 81–117 (2017).

93. Weinlich, R., Oberst, A., Beere, H. M. & Green, D. R. Necroptosis in development, inflammation and disease. *Nat Rev Mol Cell Biol* **18,** 127–136 (2016).

94. Kayagaki, N. *et al.* Caspase-11 cleaves gasdermin D for non-canonical inflammasome signalling. *Nature* **526,** 666–671 (2015).

95. Shi, J. *et al.* Cleavage of GSDMD by inflammatory caspases determines pyroptotic cell death. *Nature* **526,** 660–665 (2015).

96. Liu, X. *et al.* Inflammasome-activated gasdermin D causes pyroptosis by forming membrane pores. *Nature* **535,** 153–158 (2016).

97. Aglietti, R. A. *et al.* GsdmD p30 elicited by caspase-11 during pyroptosis forms pores in membranes. *Proc Natl Acad Sci USA* **113,** 7858–7863 (2016).

98. Sborgi, L. *et al.* GSDMD membrane pore formation constitutes the mechanism of pyroptotic cell death. *The EMBO Journal* **35,** 1766–1778 (2016).

99. Evavold, C. L. *et al.* The Pore-Forming Protein Gasdermin D Regulates Interleukin-1 Secretion from Living Macrophages. *Immunity* **48,** 35–44.e6 (2018).

100. Ding, J. *et al.* Pore-forming activity and structural autoinhibition of the gasdermin family. *Nature* **535,** 111–116 (2016).

101. Dudek, J. Role of Cardiolipin in Mitochondrial Signaling Pathways. *Front. Cell Dev. Biol.* **5,** 8383–17 (2017).

102. Wood, J. M. Perspective: challenges and opportunities for the study of cardiolipin, a key player in bacterial cell structure and function. *Current Genetics* **64,** 795–798 (2018).

103. Feng, S., Fox, D. & Man, S. M. Mechanisms of Gasdermin Family Members in Inflammasome Signaling and Cell Death. *Journal of Molecular Biology* **430,** 3068–3080 (2018).

104. Chao, K. L., Kulakova, L. & Herzberg, O. Gene polymorphism linked to increased asthma and IBD risk alters gasdermin-B structure, a sulfatide and phosphoinositide binding protein. *Proc Natl Acad Sci USA* **114,** E1128–E1137 (2017).

105. Sun, L. *et al.* Mixed Lineage Kinase Domain-like Protein Mediates Necrosis Signaling Downstream of RIP3 Kinase. *Cell* **148,** 213–227 (2012).

106. Xia, B. *et al.* MLKL forms cation channels. *Cell Research* **26,** 517–528 (2016).

107. Wang, H. *et al.* Mixed Lineage Kinase Domain-like Protein MLKL Causes Necrotic Membrane Disruption upon Phosphorylation by RIP3. *Molecular Cell* **54,** 133–146 (2014).

108. Dondelinger, Y. *et al.* MLKL Compromises Plasma Membrane Integrity by Binding to Phosphatidylinositol Phosphates. *CellReports* **7,** 971–981 (2014).

109. Quarato, G. *et al.* Sequential Engagement of Distinct MLKL Phosphatidylinositol-Binding Sites Executes Necroptosis. *Molecular Cell* **61,** 589–601 (2016).

110. Voskoboinik, I., Whisstock, J. C. & Trapani, J. A. Perforin and granzymes: function, dysfunction and human pathology. *Nature Reviews Immunology* **15,** 388–400 (2015).

111. Bubeck, D. The Making of a Macromolecular Machine: Assembly of the Membrane Attack Complex. *Biochemistry* **53,** 1908–1915 (2014).

112. Monteleone, M. *et al.* Interleukin-1β Maturation Triggers Its Relocation to the Plasma Membrane for Gasdermin-D-Dependent and -Independent Secretion. *CellReports* **24,** 1425–1433 (2018).

113. Chang, M.-K. *et al.* Apoptotic Cells with Oxidation-specific Epitopes Are Immunogenic and Proinflammatory. *J. Exp. Med.* **200,** 1359–1370 (2004).

114. Imai, Y. *et al.* Identification of Oxidative Stress and Toll-like Receptor 4 Signaling as a Key Pathway of Acute Lung Injury. *Cell* **133,** 235–249 (2008).

115. Leitinger, N. Oxidized phospholipids as modulators of inflammation in atherosclerosis. *Curr. Opin. Lipidol.* **14,** 421–430 (2003).

116. Berliner, J. A. & Watson, A. D. A role for oxidized phospholipids in atherosclerosis. *N. Engl. J. Med.* **353,** 9–11 (2005).

117. Zanoni, I. *et al.* An endogenous caspase-11 ligand elicits interleukin-1 release from living dendritic cells. *Science* **352,** 1232–1236 (2016).

118. Zanoni, I., Tan, Y., Di Gioia, M., Springstead, J. R. & Kagan, J. C. By Capturing Inflammatory Lipids Released from Dying Cells, the Receptor CD14 Induces Inflammasome-Dependent Phagocyte Hyperactivation. *Immunity* **47,** 697–709.e3 (2017).

119. Stemmer, U. *et al.* Toxicity of oxidized phospholipids in cultured macrophages. *Lipids Health Dis* **11,** 110 (2012).

120. Erridge, C., Kennedy, S., Spickett, C. M. & Webb, D. J. Oxidized phospholipid inhibition of toll-like receptor (TLR) signaling is restricted to TLR2 and TLR4: roles for CD14, LPS-binding protein, and MD2 as targets for specificity of inhibition. *J. Biol. Chem.* **283,** 24748–24759 (2008).

121. Yeon, S. H., Yang, G., Lee, H. E. & Lee, J. Y. Oxidized phosphatidylcholine induces the activation of NLRP3 inflammasome in macrophages. *J Leukoc Biol* **101,** 205–215 (2017).

122. Bochkov, V. N. *et al.* Protective role of phospholipid oxidation products in endotoxin-induced tissue damage. *Nature* **419,** 77–81 (2002).

123. Chen, J. & Chen, Z. J. PtdIns4P on dispersed trans-Golgi network mediates NLRP3 inflammasome activation. *Nature* 1–26 (2018). doi:10.1038/s41586-018-0761-3

124. Iyer, S. S. *et al.* Mitochondrial cardiolipin is required for Nlrp3 inflammasome activation. *Immunity* **39,** 311–323 (2013).

125. Elliott, E. I. *et al.* Cutting Edge: Mitochondrial Assembly of the NLRP3 Inflammasome Complex Is Initiated at Priming. *J. Immunol.* **200,** 3047–3052 (2018).

126. Zeng, W. *et al.* Reconstitution of the RIG-I Pathway Reveals a Signaling Role of Unanchored Polyubiquitin Chains in Innate Immunity. *Cell* **141,** 315–330 (2010).

127. Hornung, V. *et al.* 5'-Triphosphate RNA Is the Ligand for RIG-I. *Science* **314,** 994–997 (2006).

128. Zhang, X. *et al.* Cyclic GMP-AMP Containing Mixed Phosphodiester Linkages Is An Endogenous High-Affinity Ligand for STING. *Molecular Cell* **51,** 226–235 (2013).

129. Du, M. & Chen, Z. J. DNA-induced liquid phase condensation of cGAS activates innate immune signaling. *Science* **361,** 704–709 (2018).

130. Gao, D. *et al.* Cyclic GMP-AMP Synthase Is an Innate Immune Sensor of HIV and Other Retroviruses. *Science* **341,** 903–906 (2013).

131. Paijo, J. *et al.* cGAS Senses Human Cytomegalovirus and Induces Type I Interferon Responses in Human Monocyte-Derived Cells. *PLoS Pathog* **12,** e1005546–24 (2016).

132. Gray, E. E., Treuting, P. M., Woodward, J. J. & Stetson, D. B. Cutting Edge: cGAS Is Required for Lethal Autoimmune Disease in the Trex1-Deficient Mouse Model of Aicardi–Goutières Syndrome. *J.I.* **195,** 1939–1943 (2015).

133. Vincent, J. *et al.* Small molecule inhibition of cGAS reduces interferon expression in primary macrophages from autoimmune mice. *Nature Communications* 1–12 (2017). doi:10.1038/s41467-017-00833-9

134. Bartsch, K. *et al.* Absence of RNase H2 triggers generation of immunogenic micronuclei removed by autophagy. *Human Molecular Genetics* **26,** 3960–3972 (2017).

135. Crow, Y. J. *et al.* Characterization of human disease phenotypes associated with mutations in TREX1, RNASEH2A, RNASEH2B, RNASEH2C, SAMHD1, ADAR, and IFIH1. *Am. J. Med. Genet. A* **167A,** 296–312 (2015).

136. Mankan, A. K. *et al.* Cytosolic RNA:DNA hybrids activate the cGAS–STING axis. *The EMBO Journal* **33,** 2937–2946 (2014).

137. Ablasser, A. *et al.* TREX1 Deficiency Triggers Cell-Autonomous Immunity in a cGAS-Dependent Manner. *J.I.* **192,** 5993–5997 (2014).

138. Zhou, W. *et al.* Structure of the Human cGAS-DNA Complex Reveals Enhanced Control of Immune Surveillance. *Cell* **174,** 300–311.e11 (2018).

139. Brown, D. A. & Rose, J. K. Sorting of GPI-anchored proteins to glycolipid-enriched membrane subdomains during transport to the apical cell surface. *Cell* **68,** 533–544 (1992).

140. Lingwood, D. & Simons, K. Lipid rafts as a membrane-organizing principle. *Science* **327,** 46–50 (2010).

141. Liang, Q. *et al.* Crosstalk between the cGAS DNA Sensor and Beclin-1 Autophagy Protein Shapes Innate Antimicrobial Immune Responses. *Cell Host and Microbe* **15,** 228–238 (2014).

142. Li, X. *et al.* Cyclic GMP-AMP Synthase Is Activated by Double-Stranded DNA-Induced Oligomerization. *Immunity* **39,** 1019–1031 (2013).

143. Zhang, X. *et al.* The Cytosolic DNA Sensor cGAS Forms an Oligomeric Complex with DNA and Undergoes Switch-like Conformational Changes in the Activation Loop. *Cell Reports* **6,** 421–430 (2014).

144. Hawkins, P. T. & Stephens, L. R. Emerging evidence of signalling roles for PI(3,4)P2 in Class I and II PI3K-regulated pathways. *Biochemical Society Transactions* **44,** 307–314 (2016).

145. Emerit, I. & Cerutti, P. A. Tumour promoter phorbol-12-myristate-13-acetate induces chromosomal damage via indirect action. *Nature* **293,** 144–146 (1981).

146. Tewey, K. M., Rowe, T. C., Yang, L., Halligan, B. D. & Liu, L. F. Adriamycin-induced DNA damage mediated by mammalian DNA topoisomerase II. *Science* **226,** 466–468 (1984).

147. Dai, P. *et al.* Modified Vaccinia Virus Ankara Triggers Type I IFN Production in Murine Conventional Dendritic Cells via a cGAS/STING-Mediated Cytosolic DNA-Sensing Pathway. *PLoS Pathog* **10,** e1003989–13 (2014).

148. Albrecht, M. *et al.* Vaccination with a Modified Vaccinia Virus Ankara-based vaccine protects mice from allergic sensitization. *J. Gene Med.* **10,** 1324–1333 (2008).

149. Stetson, D. B., Ko, J. S., Heidmann, T. & Medzhitov, R. Trex1 Prevents Cell-Intrinsic Initiation of Autoimmunity. *Cell* **134,** 587–598 (2008).

150. Gentili, M. & Manel, N. cGAS-STING do it again: pivotal role in RNase H2 genetic disease. *The EMBO Journal* **35,** 796–797 (2016).

151. Chen, Q., Sun, L. & Chen, Z. J. Regulation and function of the cGAS–STING pathway of cytosolic DNA sensing. *Nat Immunol* **17,** 1142–1149 (2016).

152. Knipe, D. M. & Howley, P. *Fields Virology.* (Wolters Kluwer, 2015).

153. Schmidt, A. *et al.* 5'-triphosphate RNA requires base-paired structures to activate antiviral signaling via RIG-I. *Proc. Natl. Acad. Sci. U.S.A.* **106,** 12067–12072 (2009).

154. Devarkar, S. C., Schweibenz, B., Wang, C., Marcotrigiano, J. & Patel, S. S. RIG-I Uses an ATPase-Powered Translocation-Throttling Mechanism for Kinetic Proofreading of RNAs and Oligomerization. *Molecular Cell* **72,** 355–368.e4 (2018).

155. Schneider, W. M., Chevillotte, M. D. & Rice, C. M. Interferon-Stimulated Genes: A Complex Web of Host Defenses. *Annu. Rev. Immunol.* **32,** 513–545 (2014).

156. Vela, A., Fedorova, O., Ding, S. C. & Pyle, A. M. The Thermodynamic Basis for Viral RNA Detection by the RIG-I Innate Immune Sensor. *J. Biol. Chem.* **287,** 42564–42573 (2012).

157. Rawling, D. C., Kohlway, A. S., Luo, D., Ding, S. C. & Pyle, A. M. The RIG-I ATPase core has evolved a functional requirement for allosteric stabilization by the Pincer domain. *Nucleic Acids Res* **42,** 11601–11611 (2014).

158. Luo, D. *et al.* Structural Insights into RNA Recognition by RIG-I. *Cell* **147,** 409–422 (2011).

159. Lu, C., Ranjith-Kumar, C. T., Hao, L., Kao, C. C. & Li, P. Crystal structure of RIG-I C-terminal domain bound to blunt-ended double-strand RNA without 5′ triphosphate. *Nucleic Acids Res* **39,** 1565–1575 (2010).

160. McCartney, A. J., Zhang, Y. & Weisman, L. S. Phosphatidylinositol 3,5-bisphosphate: Low abundance, high significance. *BioEssays* **36,** 52–64 (2013).

161. Rawling, D. C., Fitzgerald, M. E. & Pyle, A. Establishing the role of ATP for the function of the RIG-I innate immune sensor. *eLife* doi:10.7554/eLife.09391.001

162. Civril, F. *et al.* The RIG-I ATPase domain structure reveals insights into ATP-dependent antiviral signalling. *EMBO Reports* **12,** 1128–1135 (2011).

163. Lässig, C. *et al.* ATP hydrolysis by the viral RNA sensor RIG-I prevents unintentional recognition of self-RNA. *eLife* 1–20 (2015). doi:10.7554/eLife.10859.001

164. Fitzgerald, M. E. *et al.* Selective RNA targeting and regulated signaling by RIG-I is controlled by coordination of RNA and ATP binding. *Nucleic Acids Res* **45,** 1442–1454 (2017).

165. Yao, H. *et al.* ATP-Dependent Effector-like Functions of RIG-I-like Receptors. *Molecular Cell* **58,** 541–548 (2015).

166. Kavran, J. M. *et al.* Specificity and Promiscuity in Phosphoinositide Binding by Pleckstrin Homology Domains. *J. Biol. Chem.* **273,** 30497–30508 (1998).

167. Dall'Armi, C., Devereaux, K. A. & Di Paolo, G. The Role of Lipids in the Control of Autophagy. *Current Biology* **23,** R33–R45 (2013).

168. Swanson, K. V. *et al.* A noncanonical function of cGAMP in inflammasome priming and activation. *J. Exp. Med.* **214,** 3611–3626 (2017).

169. Gaidt, M. M. *et al.* The DNA Inflammasome in Human Myeloid Cells Is Initiated by a STING-Cell Death Program Upstream of NLRP3. *Cell* 1–34 (2017). doi:10.1016/j.cell.2017.09.039

170. Man, S. M. *et al.* The transcription factor IRF1 and guanylate-binding proteins target activation of the AIM2 inflammasome by Francisella infection. *Nat Immunol* **16,** 467–475 (2015).

171. Kerur, N. *et al.* cGAS drives noncanonical-inflammasome activation in age-related macular degeneration. *Nature Medicine* **24,** 50–61 (2018).

172. Nassour, J. *et al.* Autophagic cell death restricts chromosomal instability during replicative crisis. *Nature* 1–21 (2019). doi:10.1038/s41586-019-0885-0

173. Diner, B. A., Lum, K. K., Toettcher, J. E. & Cristea, I. M. Viral DNA Sensors IFI16 and Cyclic GMP-AMP Synthase Possess Distinct Functions in Regulating Viral Gene Expression, Immune Defenses, and Apoptotic Responses during Herpesvirus Infection. *mBio* **7,** e01553–16–15 (2016).

174. Wright, P. E. & Dyson, H. J. Intrinsically disordered proteins in cellular signalling and regulation. *Nat Rev Mol Cell Biol* **16,** 18–29 (2015).

175. Gentili, M. *et al.* The N-Terminal Domain of cGAS Determines Preferential Association with Centromeric DNA and Innate Immune Activation in the Nucleus. *Cell Reports* **26,** 2377–2393.e13 (2019).

176. Malumbres, M. Cyclin-dependent kinases. *Genome Biol.* **15,** 122–10 (2014).

177. Wang, Y. *et al.* Inflammasome Activation Triggers Caspase-1- Mediated Cleavage of cGAS to Regulate Responses to DNA Virus Infection. *Immunity* **46,** 393–404 (2017).

178. Brangwynne, C. P. *et al.* Germline P Granules Are Liquid Droplets That Localize by Controlled Dissolution/Condensation. *Science* **324,** 1729–1732 (2009).

179. Brangwynne, C. P., Mitchison, T. J. & Hyman, A. A. Active liquid-like behavior of nucleoli determines their size and shape in Xenopus laevis oocytes. *Proc Natl Acad Sci USA* **108,** 4334–4339 (2011).

180. Li, P. *et al.* Phase transitions in the assembly of multivalent signalling proteins. *Nature* **483,** 336–340 (2012).

181. Lin, Y., Protter, D. S. W., Rosen, M. K. & Parker, R. Formation and Maturation of Phase-Separated Liquid Droplets by RNA-Binding Proteins. *Molecular Cell* **60,** 208–219 (2015).

182. Banani, S. F., Lee, H. O., Hyman, A. A. & Rosen, M. K. Biomolecular condensates: organizers of cellular biochemistry. *Nature Publishing Group* **18,** 285–298 (2017).

183. Shin, Y. & Brangwynne, C. P. Liquid phase condensation in cell physiology and disease. *Science* **357,** (2017).

184. Liu, Z.-S. *et al.* G3BP1 promotes DNA binding and activation of cGAS. *Nat Immunol* 1–17 (2018). doi:10.1038/s41590-018-0262-4

185. Lahaye, X. *et al.* NONO Detects the Nuclear HIV Capsid to Promote cGAS-Mediated Innate Immune Activation. *Cell* **175,** 488–501.e22 (2018).

186. Frattini, A. *et al.* High variability of genomic instability and gene expression profiling in different HeLa clones. *Sci Rep* **5,** 15377 (2015).

187. Liu, Y. *et al.* Multi-omic measurements of heterogeneity in HeLa cells across laboratories. *Nat Biotechnol* 1–15 (2019). doi:10.1038/s41587-019-0037-y

188. Xia, T., Konno, H., Ahn, J. & Barber, G. N. Deregulation of STING Signaling in Colorectal Carcinoma Constrains DNA Damage Responses and Correlates With Tumorigenesis. *Cell Reports* **14,** 282–297 (2016).

189. Xia, T., Konno, H. & Barber, G. N. Recurrent Loss of STING Signaling in Melanoma Correlates with Susceptibility to Viral Oncolysis. *Cancer Res.* **76,** 6747–6759 (2016).

190. Konno, H. *et al.* Suppression of STING signaling through epigenetic silencing and missense mutation impedes DNA damage mediated cytokine production. *Oncogene* 1–15 (2018). doi:10.1038/s41388-017-0120-0

191. Hanahan, D. & Weinberg, R. A. Hallmarks of Cancer: The Next Generation. *Cell* **144,** 646–674 (2011).

192. Posor, Y., Eichhorn-Grünig, M. & Haucke, V. Phosphoinositides in endocytosis. *BBA - Molecular and Cell Biology of Lipids* **1851,** 794–804 (2015).

193. Tsujita, K. & Itoh, T. Phosphoinositides in the regulation of actin cortex and cell migration. *BBA - Molecular and Cell Biology of Lipids* **1851,** 824–831 (2015).

194. Watson, R. O. *et al.* The Cytosolic Sensor cGAS Detects Mycobacterium tuberculosis DNA to Induce Type I Interferons and Activate Autophagy. *Cell Host and Microbe* **17,** 811–819 (2015).

195. Chan, Y. K. & Gack, M. U. Viral evasion of intracellular DNA and RNA sensing. *Nature Reviews Microbiology* **14,** 360–373 (2016).

196. Wu, J.-J. *et al.* Inhibition of cGAS DNA Sensing by a Herpesvirus Virion Protein. *Cell Host and Microbe* **18,** 333–344 (2015).

197. Deng, L. *et al.* STING-Dependent Cytosolic DNA Sensing Promotes Radiation-Induced Type I Interferon-Dependent Antitumor Immunity in Immunogenic Tumors. *Immunity* **41,** 843–852 (2014).

198. Erdal, E., Haider, S., Rehwinkel, J., Harris, A. L. & McHugh, P. J. A prosurvival DNA damage-induced cytoplasmic interferon response is mediated by end resection factors and is limited by Trex1. *Genes Dev.* **31,** 353–369 (2017).

199. Heijink, A. M. *et al.* BRCA2 deficiency instigates cGAS-mediated inflammatory signaling and confers sensitivity to tumor necrosis factor-alpha-mediated cytotoxicity. *Nature Communications* **10,** 1071–14 (2019).

200. Chabanon, R. M. *et al.* PARP inhibition enhances tumor cell–intrinsic immunity in ERCC1-deficient non–small cell lung cancer. *Journal of Clinical Investigation* **129,** 1211–1228 (2019).

201. Dunn, J. D., Alvarez, L. A., Zhang, X. & Soldati, T. Reactive oxygen species and mitochondria: A nexus of cellular homeostasis. *Redox Biology* **6,** 472–485 (2015).

202. Murphy, M. P. How mitochondria produce reactive oxygen species. *Biochem. J.* **417,** 1–13 (2009).

203. Panday, A., Sahoo, M. K., Osorio, D. & Batra, S. NADPH oxidases: an overview from structure to innate immunity-associated pathologies. *Cellular and Molecular Immunology* **12,** 5–23 (2015).

204. Zierhut, C. *et al.* The Cytoplasmic DNA Sensor cGAS Promotes Mitotic Cell Death. *Cell* **178,** 302–315.e23 (2019).

205. Wei, W. E. A. Differentiation between Senescence (M1) and Crisis (M2) in Human Fibroblast Cultures. *Experimental Cell Research* 1–4 (1999).

206. Maciejowski, J. & de Lange, T. Telomeres in cancer: tumour suppression and genome instability. *Nat Rev Mol Cell Biol* **18,** 175–186 (2017).

207. Hornung, V. *et al.* AIM2 recognizes cytosolic dsDNA and forms a caspase-1-activating inflammasome with ASC. *Nature* **458,** 514–518 (2009).

Appendix 2: Supplemental Figures

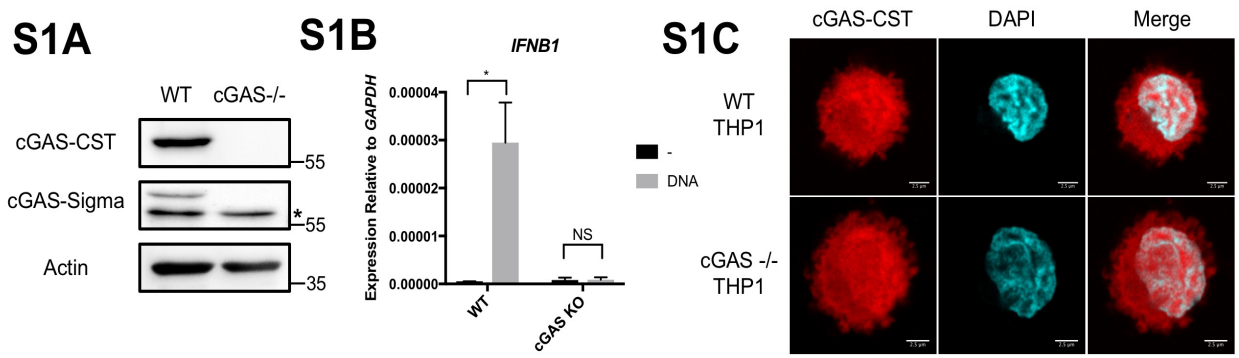
S1A
WT
cGAS-/-
cGAS-CST
cGAS-Sigma
Actin
55
55
35
S1B
IFNB1
Expression Relative to GAPDH
0.00004
0.00003
0.00002
0.00001
0.00000
*
NS
WT
cGAS KO
-
DNA
S1C
cGAS-CST
DAPI
Merge
WT THP1
cGAS -/- THP1

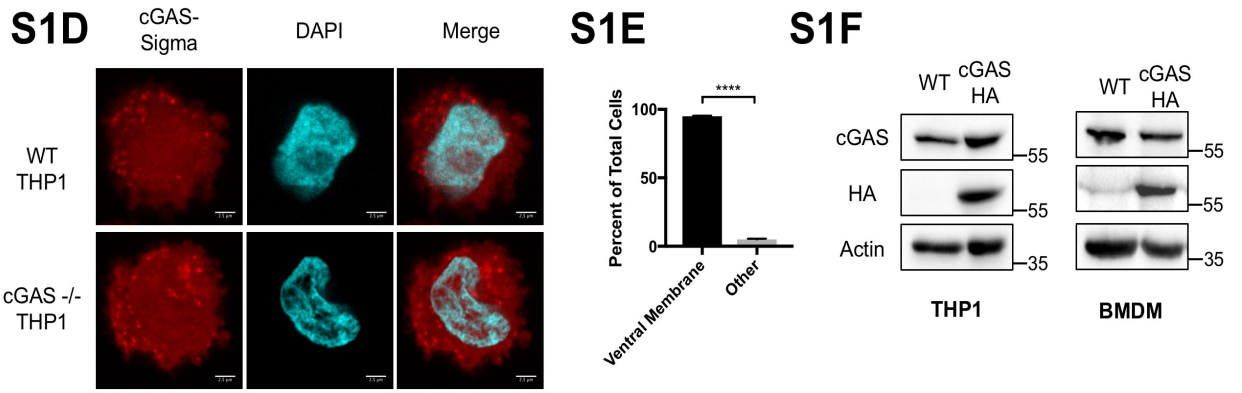
S1D
cGAS-Sigma
DAPI
Merge
WT THP1
cGAS -/- THP1
S1E
Percent of Total Cells
100
50
0
****
Ventral Membrane
Other
S1F
WT
cGAS HA
cGAS
HA
Actin
55
55
35
THP1
BMDM

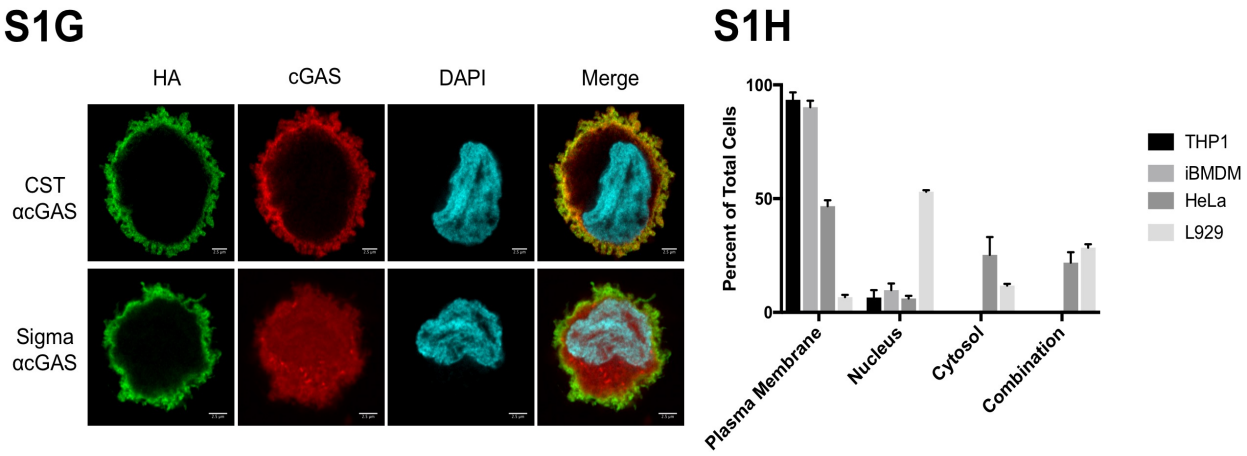
S1G
HA
cGAS
DAPI
Merge
CST αcGAS
Sigma αcGAS
S1H
Percent of Total Cells
100
50
0
THP1
iBMDM
HeLa
L929
Plasma Membrane
Nucleus
Cytosol
Combination

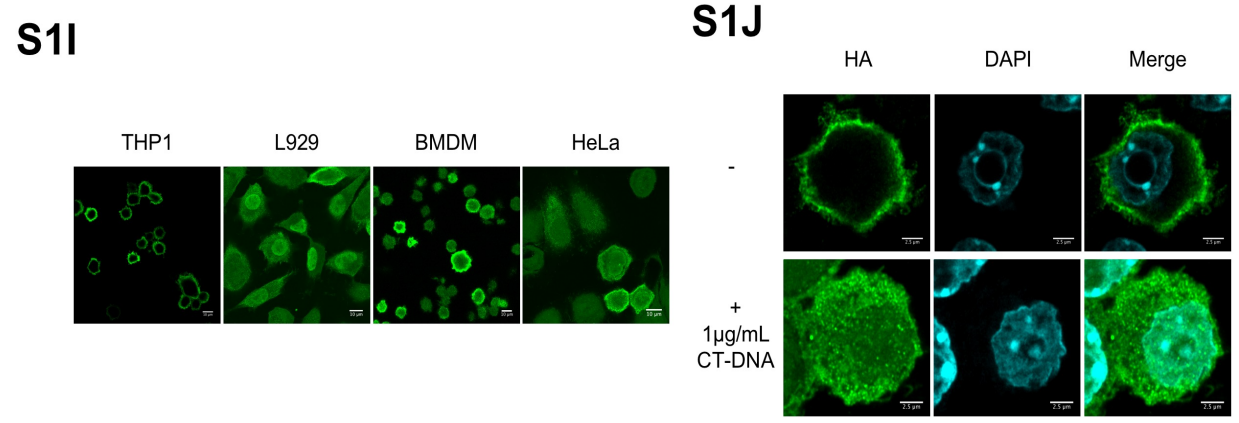
S1I
THP1
L929
BMDM
HeLa
S1J
HA
DAPI
Merge
-
+ 1µg/mL CT-DNA

Supplemental Figure 1: Related to Figure 2.1

S1A) Validation of a two cGAS antibodies by western blot analysis with cGAS +/+ and cGAS -/- THP1 lysates. Actin was used as a loading control. The cGAS-CST antibody was used for all other western blots. **S1B)** Validation of cGAS +/+ and cGAS -/- THP1 cells through measurement of *IFNβ1* expression via qRT-PCR at 3 hours CT-DNA transfection (1μg/mL). **S1C)** Confocal micrograph of cGAS +/+ and cGAS -/- THP1 cells using the cGAS-CST antibody. **S1D)** Confocal micrograph of cGAS +/+ and cGAS -/- THP1 cells using the cGAS-Sigma antibody. **S1E)** Quantification of endogenous cGAS localization site. Ventral membrane indicates the plasma membrane-coverslip contact site. **S1F)** Western blot analysis to compare total cGAS expression in WT THP1 or WT BMDM as compared to cGAS-HA expressing THP1 or BMDM, respectively. **S1G)** Confocal micrographs of CST and Sigma cGAS antibodies detecting C-terminally tagged cGAS-HA in THP1 cells. **S1H)** Quantification of cGAS-HA localization in various cell lines. **S1I)** Wide field views of cGAS-HA in various cell lines. **S1J)** cGAS-HA localization in iBMMs before or 30 minutes after transfection with 1μg/mL CT-DNA. Experiments shown are representative of or averages of n=3 biological replicates, and statistical analysis was preformed using a student's T test. Data with error bars represent the mean with SEM. Asterisk coding is as follows: * p<= 0.05; ** p<=0.01; *** p<=0.001; **** p<=0.0001

S2A

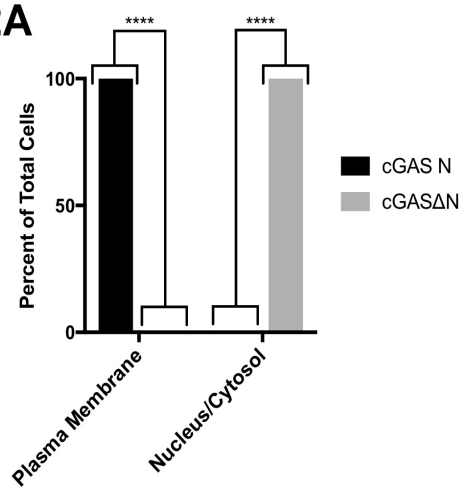
****
****
100
50
0
Percent of Total Cells
cGAS N
cGASΔN
Plasma Membrane
Nucleus/Cytosol

S2B

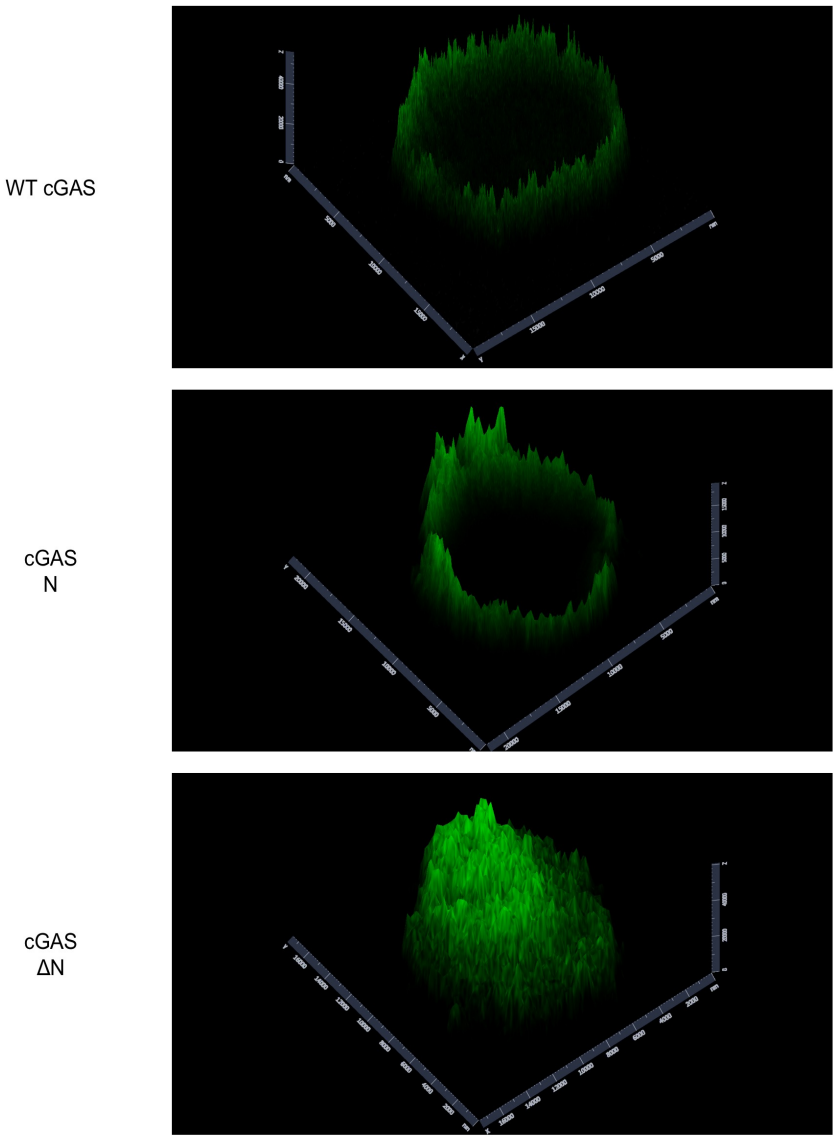
WT cGAS
cGAS
N
cGAS
ΔN

Supplemental Figure 2: Related to Figure 2.2

S2A) Quantification of cGAS-N-HA and cGASΔN-HA localization in stably expressed in iBMMs. Visualized by confocal microscopy. **S2B)** Pseudo-3D renderings of cGAS, cGAS N, and cGASΔN expressed in iBMDMs. A 2D confocal micrograph of each construct is on the x and y axes, while the pixel intensity is plotted on the z axis. Images were created using Zen software. Experiments shown are representative of or averages of n=3 biological replicates, and statistical analysis was preformed using a student's T test. Data with error bars represent the mean with SEM. Asterisk coding is as follows: * p<= 0.05; ** p<=0.01; *** p<=0.001; **** p<=0.0001.

S3A

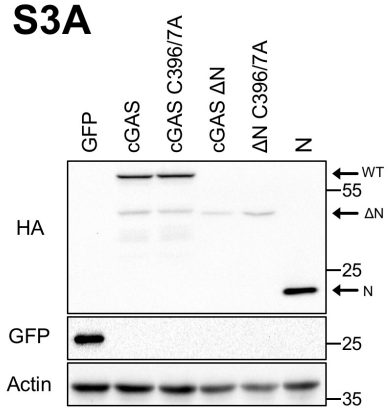
GFP
cGAS
cGAS C396/7A
cGAS ΔN
ΔN C396/7A
N
HA
WT
55
ΔN
25
N
GFP
25
Actin
35

S3B

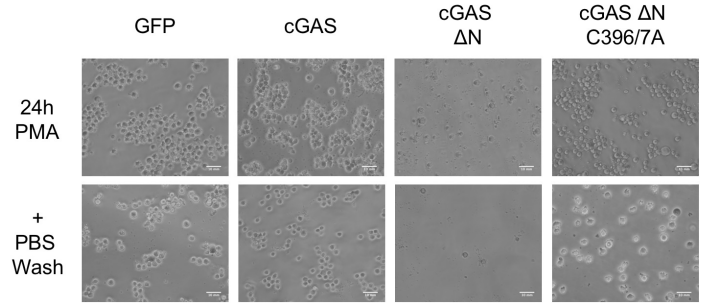
GFP
cGAS
cGAS ΔN
cGAS ΔN C396/7A
24h PMA
+ PBS Wash

Supplemental Figure 3: Related to Figure 2.4

S3A) Western blot analysis of expression of cGAS mutant panel stable expression in THP1 cells. **S3B)** Phase contrast microscopy of THP1 cell lines treated overnight with 50ng/mL PMA before and after a gentle PBS wash. Experiments shown are representative of n=3 biological